AMP-Activated Protein Kinase α1 Dependent Signaling in Renal Tissue Fibrosis

Dissertation

der Mathematisch-Naturwissenschaftlichen Fakultät

der Eberhard Karls Universität Tübingen

zur Erlangung des Grades eines

Doktors der Naturwissenschaften

(Dr. rer. nat.)

vorgelegt von

Md. Sobuj Mia

aus Jhenidah, Bangladesch

Tübingen

2015

Tag der mündlichen Qualifikation:	17.11.2015
Dekan:	Prof. Dr. Wolfgang Rosenstiel
1. Berichterstatter:	Prof. Dr. Florian Lang
2. Berichterstatter:	Prof. Dr. Friedrich Goetz

"Science is not only a disciple of reason but, also, one of romance and passion."

Stephen Hawking

ACKNOWLEDGEMENTS

I would like to express my grateful acknowledgement and heartfelt gratitude to the following people who have helped and supported me for the completion of my PhD study.

First and foremost, I record my grateful acknowledgement to my first supervisor Professor Dr. Florian Lang, Chair of the Institute of Physiology I, for his enthusiastic supervision, endless support, cordial behaviour, critical review and providing all necessary facilities throughout my work at the Institute of Physiology I, University of Tübingen, Germany.

I would like to lay my humble gratitude towards my group leaders Dr. Ioana Alesutan and Dr. Jakob Voelkl for their timely help, valuable input, suggestions, advice and inspiration to make my PhD experience productive and stimulating.

Furthermore, I would also like to convey my deep gratitude towards my second supervisor Prof. Dr. Friedrich Goetz, for giving me an opportunity to present the dissertation at the faculty of Biology, University of Tübingen, Germany.

There are many colleagues that I would like to give special thanks in the Physiology laboratory especially Ms. Martina Feger, Ms. Tatsiana Castor, Ms. Sabina Honisch, Britta Walker, Bernat Elvira, Goxing Liu, Abul Fajol, Uwe Schueler, Kousi Alzoubi, Lejla Subasic, Mrs. Tanja Loch, Mrs. Sari Rübi, Mr. Faruk Subasic, Efi Feber and all other colleagues for their suggestion, help, friendship and supports during my Study.

My special thanks are extended towards Giuseppina Federico and professor Hermann-Josef Groene from Department of Cellular and Molecular Pathology, German Cancer Research Center, Heidelberg, Germany, for their experimental supports and intellectuality.

Special thanks go to my Bangladeshi friends Muhammad Muniruzzaman and Shabab Bin Hannan, at Tübingen who made my life very enjoyable here.

Last, but certainly not least, I would like to thank my parents, sisters and brothers for their love, support and constant inspiration. I dedicate this thesis to the memory of my father whose role in my life was, and remains, immense.

ZUSAMMENFASSUNG

Tubulointerstitielle Fibrose ist ein gemeinsames Kennzeichen der chronischen Nierenerkrankung hervorgerufen durch Diabetes, Bluthochdruck, Ischämie, obstruktive Uropathie und andere Nierenschäden. Die heterotrimere AMP-aktivierte Kinase (AMPK) besteht aus drei Untereinheiten (α, β, γ) und fungiert als zellulärer Energiesensor. Die Aktivierung der AMPK trägt zur Umwandlung von Monozyten zu Fibroblasten bei und fördert die Ablagerung von extrazellulärer Matrix. Dennoch kann die Aktivierung der AMPK auch antifibrotische Effekte vermitteln. Diese Diskrepanz könnte durch Isoform-spezifische Effekte der AMPK zustande kommen. Diese Studie untersuchte daher die Rolle der AMPKα1-Isoform bei renaler Fibrosierung. Zu diesem Zweck wurden genetisch veränderte Mäuse mit einer AMPKα1-Defizienz ($AMPK\alpha1^{-/-}$) und korrespondierende Wildtyp-Mäuse ($AMPK\alpha1^{+/+}$) einer unilateralen ureteralen Obstruktion (UUO) über 3 Tage, 7 Tage und 3 Wochen oder einer Angiotensin II (ANG II)-Infusion für 2 Wochen unterzogen. Quantitative RT-PCR, Western-Blotting und Immunohistochemie wurden verwendet, um mRNA-Transkriptionsspiegel bzw. Proteinmenge zu untersuchen. Sowohl UUO als auch ANG II-Behandlung führten zur erhöhten Proteinexpression von AMPKα1 im renalen Gewebe von $AMPK\alpha1^{+/+}$-Mäusen. Im Gegensatz wurde die AMPKα2-Protein expression in der Niere dieser Tiere durch UUO, aber nicht durch ANG II herunterreguliert. Die α-smooth muscle actin (α-SMA)-Expression wurde sowohl durch UUO als auch ANG II-Behandlung erhöht, ein Effekt, der durch die AMPKα1-Defizienz signifikant reduziert wurde. Die Phosphorylierung der TGF-β-aktivierten Kinase 1 (TAK1) wurde ebenso durch UUO und ANG II in den Nieren von $AMPK\alpha1^{+/+}$-Mäusen erhöht, was wiederum durch die AMPKα1-Defizienz gemindert wurde. Die UUO-induzierte erhöhte mRNA-Expression von *Col1a1* und *Col3a1* war in $AMPK\alpha1^{-/-}$-Mäusen reduziert. Allerdings wurde keine Veränderung der Kollagenablagerung festgestellt. Die erhöhte mRNA-Expression von proinflammatorischen und profibrotischen Zytokinen war in $AMPK\alpha1^{-/-}$-Mäusen nach ANG II oder UUO vermindert. Eine reduzierte Expression von *Cd206* und *Cxcl16* in $AMPK\alpha1^{-/-}$-Nieren nach UUO lässt auf eine reduzierte Einwanderung inflammatorischer Zellen schließen. Dennoch zeigten $AMPK\alpha1^{-/-}$-Mäuse einen vermehrten tubulären Schaden und eine erhöhte Apoptose in der Niere nach UUO. In *Xenopus*-Oozyten reduzierte die Koexpression einer Wildtyp und einer konstitutiv aktiven AMPK, aber nicht einer inaktiverten AMPK den Kv1.5-vermittelten Strom. Sowohl die konstitutiv aktive AMPK als auch Nedd4-2 reduzierten Kv1.5 K^+-Kanal-Membranbesatz der Zelle. Zusammenfassend, eine Isoform-Verschiebung bei renaler Fibrose von AMPKα2 zu AMPKα1 kann die Bildung von Myofibroblasten verstärken und trägt zu den Signalereignissen in der fibrotischen Niere bei. AMPK beeinflusst die TAK1-Phosphorylierung und reguliert den Zellmembranbesatz von Kv1.5, was die Effekte von AMPK bei renaler Fibrose vermitteln könnte.

SUMMARY

Tubulointerstitial fibrosis is a common hallmark of chronic kidney disease caused by diabetes, hypertension, ischemia, renal injury and obstructive uropathy. The hetereotrimeric AMP-activated protein kinase (AMPK) consists of three subunits (α, β, γ) and is a master sensor of cellular energy status. Activation of AMPK contributes to monocyte-fibroblast transition and production of matrix protein even though accumulating evidence suggests that activated AMPK inhibits tissue fibrosis, which may be due to isoform specific effects of AMPK. Therefore, the isoform specific function of AMPKα1 in renal fibrosis was investigated. To this end, gene-targeted mice lacking functional AMPKα1 (AMPKα1$^{-/-}$) and corresponding wild-type mice (AMPK α1$^{+/+}$) were subjected to unilateral ureteral obstruction (UUO) for 3 days, 7 days and 3 weeks or angiotensin II infusion (ANG II) for 2 weeks. Quantitative RT-PCR, western blotting and immunostaining were used to determine transcript levels and protein abundance respectively. Both, UUO and ANG II treatment increased the protein abundance of AMPKα1 in kidney tissues of AMPKα1$^{+/+}$ mice. In contrast, AMPKα2 protein in UUO treated renal tissue of AMPKα1$^{+/+}$ mice was down-regulated, but not in ANG II infused mice. Importantly, α-smooth muscle actin (α-SMA) was upregulated in renal tissue by both UUO and ANG II treatment, an effect significantly blunted by AMPKα1 deficiency. TGF-β activated kinase 1 (TAK1) phosphorylation was increased by UUO and ANG II treatment in renal tissue of AMPKα1$^{+/+}$ mice, an effect significantly blunted by AMPKα1 deficiency. The UUO induced elevated transcript levels of *Col1a1* and *Col3a1* was reduced in AMPKα1$^{-/-}$ mice, although collagen deposition remained unchanged following UUO. The increased mRNA expression of pro-inflammatory and pro-fibrotic cytokines was attenuated in AMPKα1$^{-/-}$ mice following both, UUO or ANG II treatment. Furthermore, infiltration of inflammatory cells was impaired in AMPKα1$^{-/-}$ mice indicated by lower mRNA expression of *Cd206* and *Cxcl16* after UUO. Nonetheless, AMPKα1$^{-/-}$ mice displayed aggravated tubular injury and apoptosis induced by UUO. In *Xenopus* oocytes, co-expression of wild-type and a mutated constitutively active AMPK, but not a mutated inactive AMPK reduced Kv1.5-mediated currents. Constitutively active AMPK and Nedd4-2 reduced Kv1.5 K^+ channel protein abundance in the cell membrane. In conclusion, the isoform shift from AMPKα2 towards AMPKα1 potentiates myofibroblast formation and contributes to signaling involved in renal fibrosis. AMPK affects TAK1 phosphorylation and regulates Kv1.5 abundance, which may mediate the effects of AMPK during renal fibrosis.

TABLE OF CONTENTS

LIST OF FIGURES

LIST OF TABLES

ABBREVIATIONS

ACC	Acetyl Co-A carboxylase
ACE	Angiotensin converting enzyme
ANG II	Angiotensin II
AICAR	5-Aminoimidazole-4-carboxamide ribonucleotide
AID	Auto inhibitory domain
AMP	Adenosine monophosphate
AMPK	AMP-activated protein kinase
AP-1	Activator protein-1
CaMKKβ	Ca^{2+}/calmodulin-dependent protein kinase kinase β
CKD	Chronic kidney disease
Col1a1	Collagen type 1
Col3a1	Collagen type 3
Cox2	Cyclooxygenase-2
CTGF	Connective tissue growth factor
ECM	Extracellular matrix
EMT	Epithelial to mesenchymal transition
ERK	Extracellular signal regulated kinase
ESRD	End stage renal disease (ESRD)
GPCRs	G-protein coupled receptors
15-HETE	15-hydroxyeicosatetraenoate
HK-2	Human proximal tubular cells
HSCs	Hepatic stellate cells
ICAM-1	Intracellular adhesion molecule-1
IL-6	Interleukin-6
JNK	Jenus-N-terminal kinase

LPS	Lipopolysaccharide
LKB1	Liver kinase B1
MAPK	Mitogen activated protein kinase
MCP-1	Macrophage chemoattractant protein
Nedd4-2	Neuronal cell expressed developmentally downregulated 4-2
Nox4	NADPH oxidase 4
NF-kB	NFkappa B
PAI-1	Plasminogen activator-1
PBS	Phosphate buffer saline
PCR	Polymerase chain reaction
PKC	Protein kinase C
PVDF	Polyvinylidene difluoride
SDS	Sodium dodecyl sulfate
SDS-PAGE	Sodium dodecyl sulfate-poly acrylamide gel electrophoresis
SGLT1	Na^+ coupled glucose transporter
TAK1	TGF-β activated kinase 1
TBST	Tris-buffered saline-tween20
TGF-β	Transforming growth factor-β
TLR	Toll like receptor
TNFα	Tumor necrosis factor α
UUO	Unilateral ureteral obstruction
α-SMA	Alpha smooth muscle actin

1. INTRODUCTION

1.1 Fibrotic disease

Fibrosis is defined by excessive accumulation of fibrous connective tissues in response to various pathological stimuli, which can lead to permanent scarring and distortion the normal architecture of organs, and may ultimately lead to organ failure [1, 2]. Fibrosis is a common pathologic feature of all chronic inflammatory diseases and shows features of an inadequate wound healing response [3]. The deposition of collagen in response to tissue injury is part of the host defensive mechanism, but chronic stimulation of this process can lead to fibrotic disease [4]. Fibrotic organ remodelling is encountered in a variety of pathological conditions, e.g. during repeated exposure to toxins, chronic autoimmune inflammation, chronic smoking, myocardial infarction and cardiac remodelling, untreated diabetes and hypertension [5]. Although fibrotic disease has become a serious threat to human health and mortality, the treatment option that specifically targets the pathogenesis of fibrosis are still very limited. Irrespective of the aetiology of fibrotic organ remodelling, the accumulation and persistent activation of myofibroblasts is a hallmark of fibrotic diseases [6]. Importantly, the origin of the myofibroblast is a matter of extensive debate. Myofibroblasts may derive from resident fibroblasts, infiltration of bone-marrow born cells or from epithelial to mesenchymal transition (EMT) [3, 7]. However, irrespective of their origins, myofibroblasts are crucial mediators of tissue fibrosis [3].

1.2 Renal tissue fibrosis

Renal tissue fibrosis is the hallmark of chronic kidney disease (CKD), regardless of its aetiology [8, 9]. Chronic kidney disease is characterized by progressive renal impairment, loss of glomerular and peritubular capillary architecture, proliferation of tubular and interstitial cells, tubular epithelial to mesenchymal transition (EMT), infiltration of inflammatory cells, apoptosis and deposition of extracellular matrix (ECM) [10].

Chronic kidney disease thereby ultimately leads to renal tissue fibrosis, which is characterized by excessive accumulation of extracellular matrix (ECM) by activated fibroblasts [11]. Renal

fibrosis is considered as a failed wound healing response that occurs after chronic or sustained injurious insults. The renal tissue undergoes a series of attempts to repair and recover from injurious damage as a part of wound-healing response to injury [12]. These events include activation of resident cells to stimulate the production and secretion of pro-inflammatory cytokines [13]. Glomerular or interstitial infiltrated inflammatory cells become activated and produce several transmitter molecules such as reactive oxygen species, fibrogenic and inflammatory cytokines [14, 15]. This in turn sets the stage to activate mesangial cells, fibroblasts and tubular epithelial cells to undergo phenotypic conversion and eventually produce α smooth muscle actin (α-SMA) and an excessive amount of ECM including collagen type I, collagen type III, and fibronectin [16].

1.3 Mechanisms of renal fibrosis

1.3.1 Interstitial inflammation

Inflammation is a physiological response to tissue injury caused by pathogens or trauma [17]. The inflammation needs to be resolved in a timely manner, otherwise sustained, non-resolving inflammation can lead to fibrosis and tissue scarring which disrupts the tissue structure and can cause organ dysfunction [18]. Inflammatory processes are promoted by the expression of local chemokines, cytokines and membrane adhesion molecules [19]. These can be produced by kidney parenchymal and endothelial cells which thereby provide a directional signal for the recruitment of leukocytes towards the site of injury [19]. The recruited leukocytes are the major source of soluble mediators that promote inflammation and tubular cell injury, and may further amplify the secretion of other inflammatory and pro-fibrotic signaling molecules [20]. The inflammatory cells orchestrating the fibrotic processes include lymphocytes, monocytes/macrophages and dendritic cells [9]. A crucial role in this process is attributed to macrophages [9]. Chemokines (for instance macrophage chemoattractant protein MCP-1, CXCL16) and adhesion molecules (such as intracellular and vascular cell adhesion molecules ICAM-1, VCAM-1) aid in the recruitment of macrophages through chemotaxis (**Fig. 1**) [21, 22]. Macrophages exert a pivotal role in both the promotion and resolution of inflammation: Inflammatory monocytes can differentiate into two different and distinct subsets of

macrophages: inflammatory macrophages (M1) and anti-inflammatory macrophages (M2) [23, 24]. Pro-inflammatory macrophages (M1) secrete pro-inflammatory compounds at the onset of inflammation while anti-inflammatory macrophages (M2) contribute to the resolution of inflammation [25].

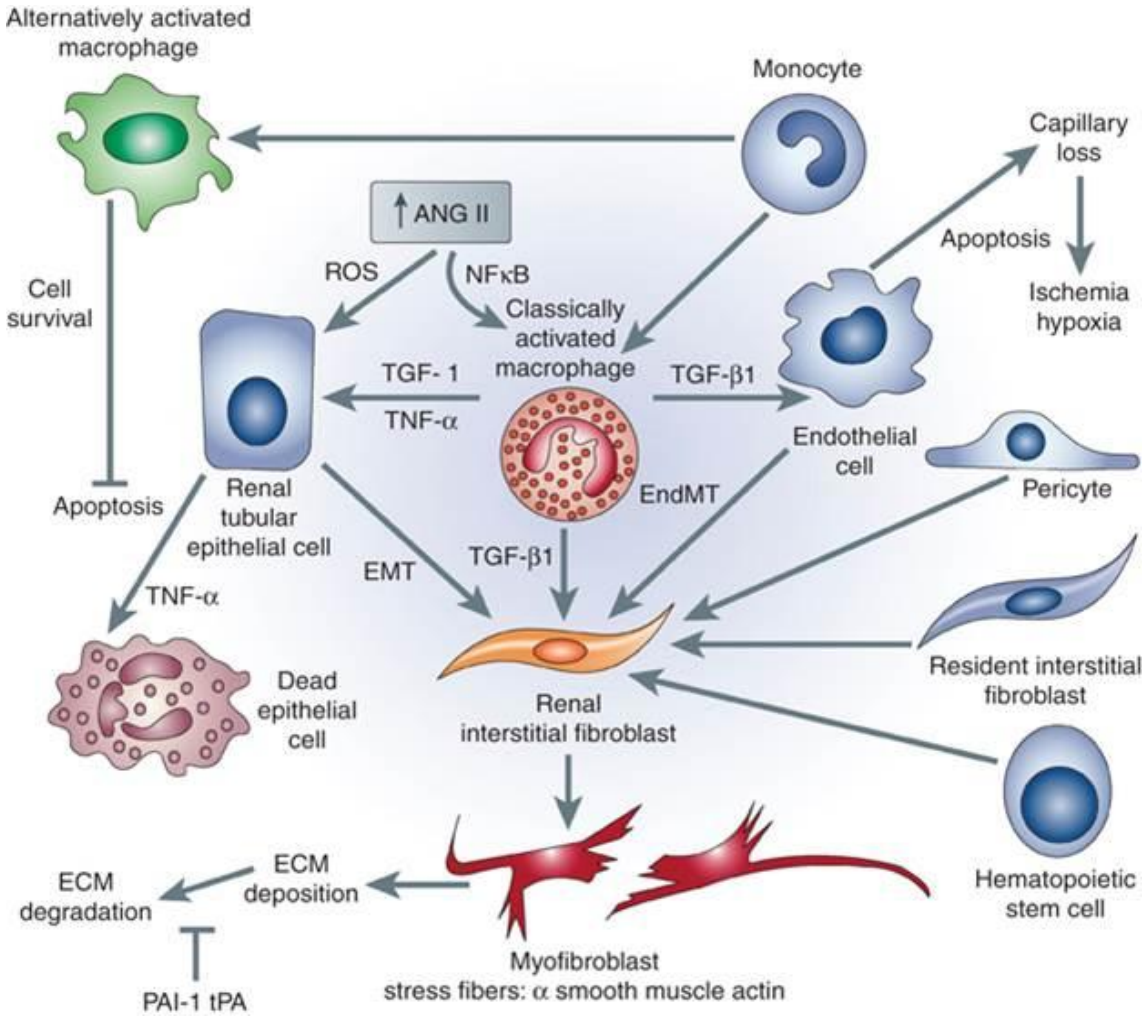

Figure 1. Schematic illustration of cellular interaction in the kidney subjected to unilateral ureteral obstruction, taken from Robert L *et al, Kidney Int*. 2009. Infiltrated monocytes are classically activated into macrophages and produce cytokines such as TGF-β1 and tumor necrosis factorα (TNFα). The secreted cytokines may either trigger the phenotypic conversion of tubular epithelial cells into a mesenchymal phenotype (epithelial to mesenchymal transition (EMT)) or trigger apoptosis. ANG II further promotes activation of macrophages via NF-kB and affects renal tubular cell fate by increasing reactive oxygen species (ROS). TGF-β1, either produced by macrophages or other cells, stimulates the formation of myofibroblasts which are the effectors in the deposition of excessive ECM [26].

However, M2 macrophages may promote fibrotic tissue remodeling [27]. Macrophages skew from M1 to M2 stage during inflammation [28]. M2 macrophages induce the expression of TGF-β1 [28]. A crucial role in this process is attributed to tumor necrosis factor alpha (TNFα) whose pro-inflammatory and cytotoxic effects are exerted at least partly by activation of NFkappaB (NFκB) to induce the production of cytokines, chemokines and growth factors during renal inflammation (**Fig. 1**) [29]. NFκB activity and inflammatory cell activity may be further increased by angiotensin II [29].

1.3.2 Fibroblast activation

The inflammatory processes and pro-fibrotic cytokines create a fibrogenic pressure in the kidney resulting in the activation of matrix producing fibroblasts [30]. Many different types of cells in the kidney, such as fibroblasts, tubular epithelial cells, vascular smooth muscle cells and macrophages are capable of producing ECM protein [31]. Activated fibroblasts or myofibroblasts are the major source of the production and deposition of ECM components such as collagen type I, collagen type III, and fibronectin (**Fig. 2**) [32].

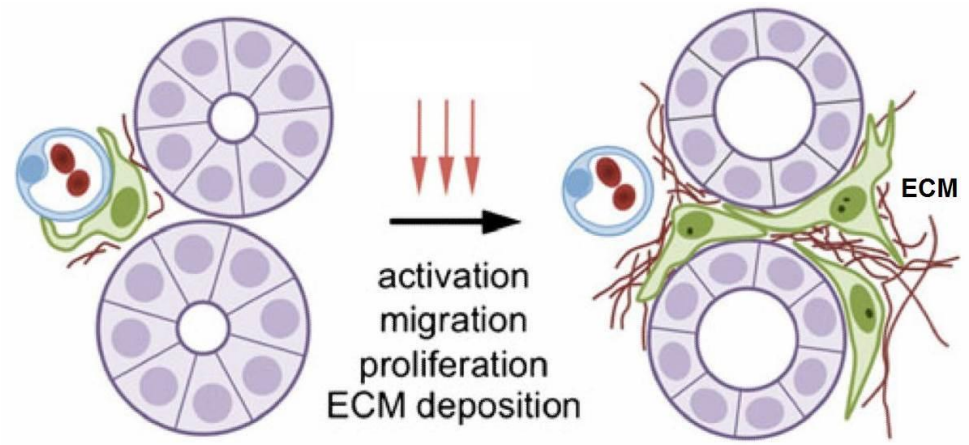

Figure 2. Activation of fibroblast in chronic kidney disease, modified from *Grgic I et al. pediatr. Nephrol. 2012*. Myofibroblasts are activated under the influence of persistent irritation and injury. The chronic stimuli lead to the activation of fibroblasts into myofibroblasts along with migration, proliferation and extracellular matrix accumulation. This ECM accumulation causes renal tissue scarring and results in a progressive loss of renal function [3].

The myofibroblasts are characterized by high expression of α smooth muscle actin (α-SMA), which serves as a marker of fibrotic activity [9, 32]. Matrix accumulation and activation of matrix-producing effector cells are generally considered as a central event in renal fibrogenesis [9]. However, the origins of the myofibroblasts are still controversial, whether they mostly originate from resident fibroblasts, infiltration of bone-marrow born cells or from epithelial to mesenchymal transition (EMT) (Fig. 1) [3, 7].

1.3.3 Tubular injury and apoptosis

In renal disease, renal tubular injury may lead to cellular activation, dedifferentiation, cell cycle entry, abnormal cell cycle progression or cell death [20]. Injured tubular cells may undergo necrosis, apoptosis or necro-apoptosis [33]. Necrosis is not frequently observed in chronic kidney disease but may also happen following intense stimulation of the cells [20]. Apoptosis is the most frequently encountered cell death in the progressive form of CKD [34]. Apoptosis may be triggered by activation of intracellular lethal molecules and suppression of pro-survival factors [35]. Under normal conditions, the cells maintain homeostasis by keeping a fine balance between cell death and proliferation. An imbalance of an excessive rate of tubular cell death over the rate of tubular proliferation contributes to the development of tubular cell depletion and tubular atrophy in the course of CKD. EMT may contribute to reduce the epithelial cell numbers although this concept is still controversial [36]. In injured cells the cell cycle arrests in the G2/M phase, which precedes apoptotic cell death and may also contribute to reduce number of epithelial cells. In addition G2/M phase arrest promotes fibrosis through the secretion of TGF-β1, which is a strong activator of fibroblasts [37]. ANG II, TGF-β1, TNFα, oxidative stress as well as mechanical stress are the main driving forces to stimulate the tubular cells to undergo apoptosis [38].

1.3.4 Deposition of ECM

Irrespective of their origin, activated fibroblasts ultimately produce an excessive amount of ECM. Deposition of ECM and its decreased degradation then cause renal fibrosis [39]. The normal architecture of kidney is disturbed by the excessive accumulation of ECM, which may eventually lead to the loss of normal kidney function [40]. This process may also be triggered

in acute injury or transient renal injury. The tissue damage is eventually repaired via tubular regeneration and matrix remodeling and the normal renal structure restored after an acute renal injury [41]. Conversely, prolonged injury causes the tissue to react with overproduction of ECM and renal fibrosis [17]. The fibrosis of the kidney is frequently encountered in renal disease, leads to progressive loss of renal function and has been recognized as a serious health concern [40].

1.4 Signaling pathways involved in renal fibrosis

1.4.1 Smad signaling in renal fibrosis

Increasing evidence suggests that TGF-β and its downstream receptor-regulated Smad transcriptional effectors molecule is a key pathway leading to fibrogenic cell activation in various organs [42]. Studies from both human and experimental models reported that TGF-β is up-regulated in virtually every type of chronic renal injury [43]. The activation of mesangial cells, fibroblasts and phenotypic conversion of epithelial to mesenchymal cells, driving these cells to become matrix-producing fibrogenic cells is crucially mediated by TGF-β [44]. EMT mediated formation of mesenchymal cells from trans-differentiation of epithelial cells is associated with loss of E-cadherin expression (a marker of epithelial cells) [45]. The down-regulation of E-cadherin expression is at least in part mediated by the transcription factor Snail [46]. Snail is required for TGF-β induced EMT conversion [47]. Furthermore, TNFα dependent NF-κB activation protects Snail from ubiquitin mediated degradation [48]. Therefore, Snail is regarded as an important transcription factor that is required for EMT, fibroblast migration and renal fibrosis and links renal inflammation and fibrosis [49]. Up-regulation of TGF-β appears to be a convergent pathway that integrates many other fibrogenic factors such as angiotensin II or glucose overload [50]. TGF-β transmits its signal through type I and type II receptor serine/threonine kinase membrane receptors [51]. Upon binding of TGF-β to its receptor the phosphorylation of its downstream effectors Smad2/3 is triggered (**Fig 3**) [51]. Phosphorylated Smad2/3 recruits Smad4 and subsequently translocate into the nucleus where they recognize regulatory Smad binding elements and transcriptionally activate or repress TGF-β dependent target genes (**Fig 3**) [52].

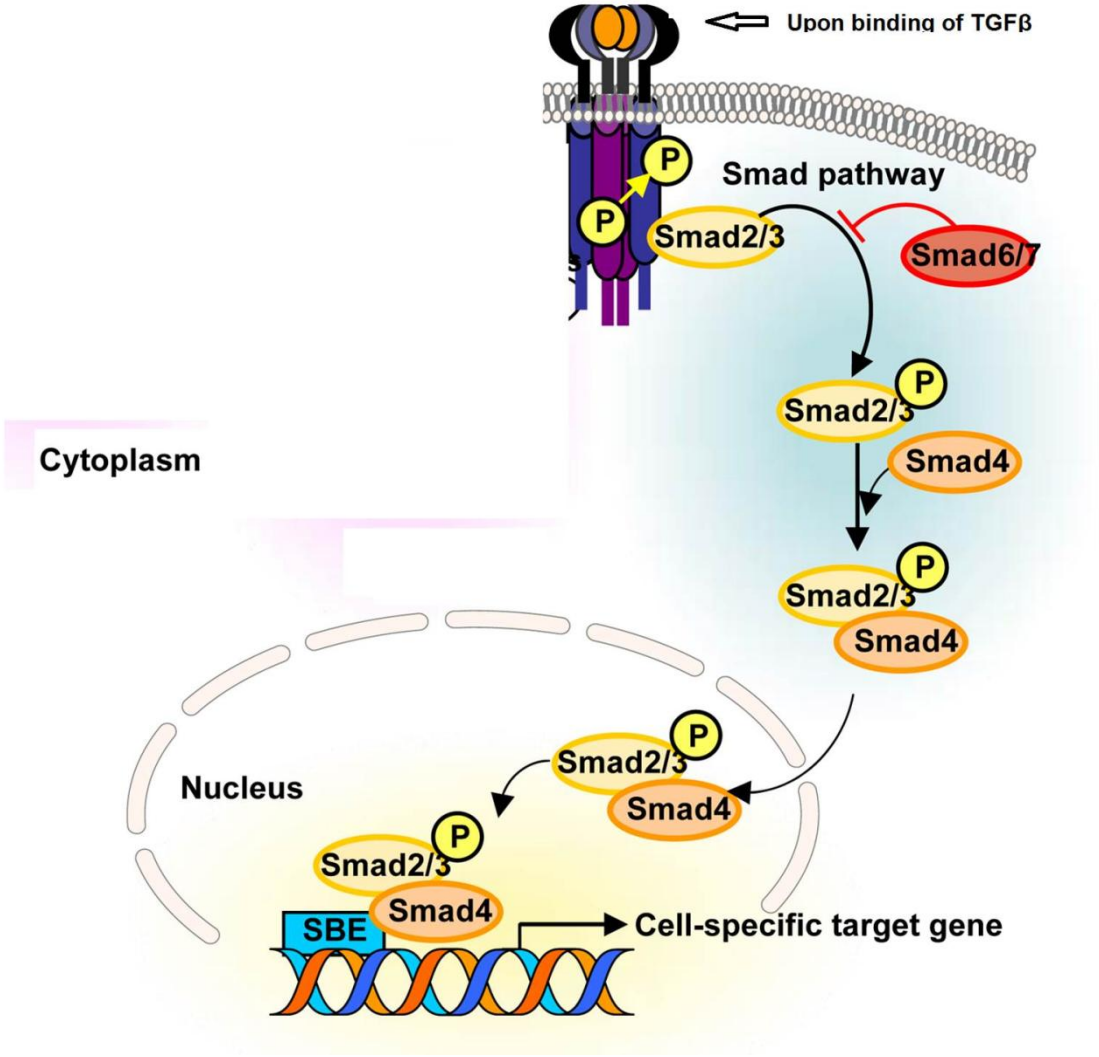

Figure 3. Schematic diagram of SMAD signaling, modified from Choi ME *et al, Semin nephrol.* 2012. Upon binding of TGF-β to its receptor Smad2/3 is phosphorylated. Phosphorylated Smad2/3 binds with Smad4 and translocates to the nucleus to bind with specific DNA regions of target genes to effect on proliferation, migration, differentiation, stress response and apoptosis [53] .

In various renal diseases, TGF-β/Smad signaling is hyper-activated [54]. Induction of TGF-β and its effectors is also observed in the fibrotic kidney [54]. Smad transcriptional corepressors limit Smad-signaling in healthy kidneys and protects the tissue from an unwanted TGF-β response [55]. The long term inhibition of TGF-β might not be a feasible therapeutic option for renal fibrosis, as TGF-β may also act as an anti-inflammatory cytokine [56]. This suggests that TGF-β1 may play a dual role in the tissue response to injury. However several

studies have demonstrated that the Smad signaling pathway is not able to solely explain the diverse functions of TGF-β1. In addition to Smad signaling, TGF-β1 exerts effects via Smad independent pathways with or without crosstalk with Smad [57].

1.4.2 Non-Smad signaling in renal fibrosis

Accumulating evidence suggests that other pathways besides Smad are important in the effects of TGF-β. The TGF-β activated kinase 1 (TAK1) is a key signaling molecule through which TGF-β may exert its fibrotic action independent of Smad. A variety of triggers besides TGF-β may also activate TAK1, including environmental stimuli, pro-inflammatory cytokines such as tumor necrosis factor (TNF) α, interleukin 1 (IL)-1, and lipopolysaccharides (LPS) [58-60]. The upstream effects of TAK1 activation are however still insufficiently defined [58-60]. Activation of TAK1 can transduce signals towards several downstream targets including p38, JNK and the transcription factor AP-1, as well as NFκB (**Fig. 4**) [60]. TAK1 activation is therefore a key event in the signaling pathways leading to tissue fibrosis [60]. In cultured mesangial cells, TAK1 is required for the TGF-β-induced expression of collagen type I and IV as well as fibronectin [61].

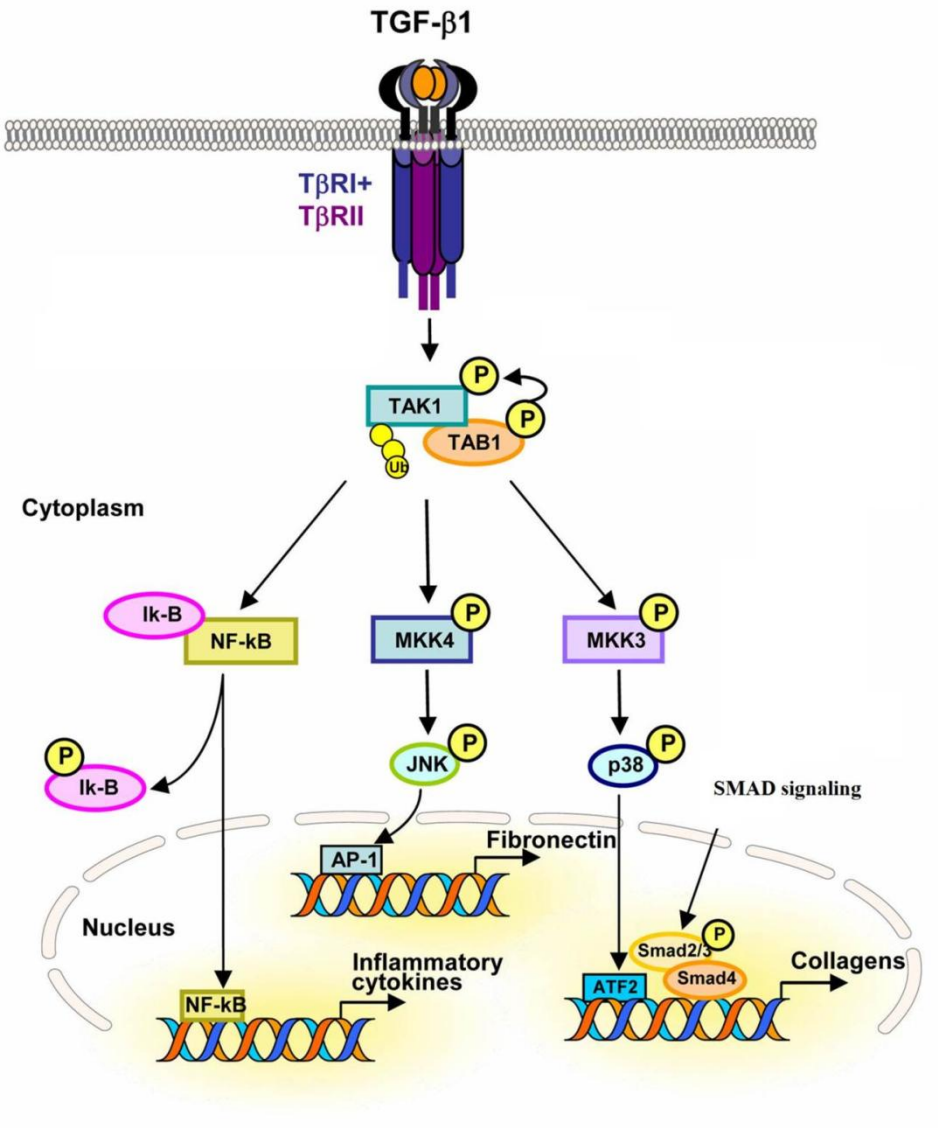

Figure 4. TGF-β activates TAK1 signaling in fibrosis, modified from Choi ME *et al, Semin nephrol.* 2012. TGF-β1-induced TAK1 activation facilitates activation of downstream signaling pathways including JNK-AP-1, p38-ATF2, and NF-kB. Activated transcription factors modulate the fibrotic response. TAK1 signaling may show also a crosstalk with Smad signaling [53].

TAK1 has therefore been widely recognized as a key factor promoting tissue fibrosis [62]. However, hepatocyte specific deletion of TAK1 causes spontaneous hepatocyte death, inflammation, fibrosis and carcinogenesis in mice [63]. This seemingly opposite effect indicates that TAK1 may inherit a complex role, which may be dependent on tissue/cell type and type of activation. Nonetheless, compelling evidence supports a critical role of TAK1 as a major factor of TGF-β induced pro-fibrotic signaling [62, 64, 65].

1.5 Angiotensin II

The renin-angiotensin-aldosterone system (RAAS) is involved in the regulation of sodium balance, body fluid volume and arterial pressure [66]. Angiotensinogen, a glycoprotein, released from the liver, is cleaved by the plasma enzyme renin, secreted by juxtaglomerular cells in the kidney, to form the decapeptide angiotensinogen I (ANG I) (**Fig. 5**) [67].

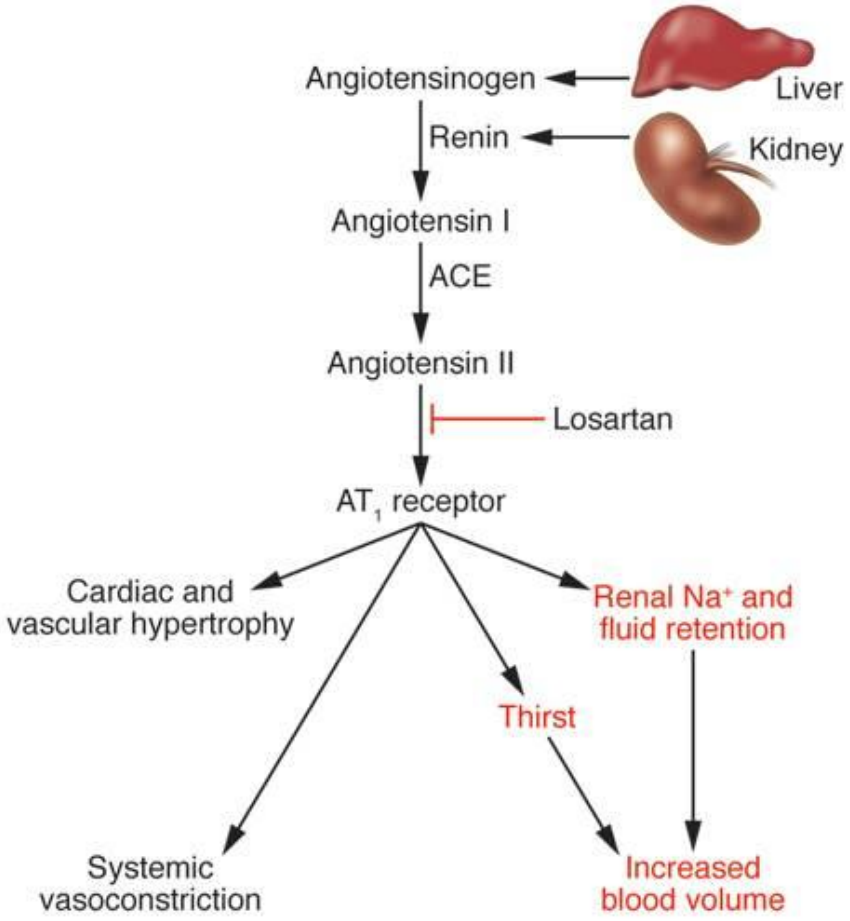

Figure 5. Classical view of Renin-Angiotensin system, modified from Parsons KK and Coffman TM, *J clin. Invest*, 2007. The liver releases angiotensinogen which is converted into the major effector angiotensin II through sequential enzymatic cleavage by renin and angiotensinogen converting enzyme. Circulating angiotensin II binds with the AT1 receptor to induce water and sodium reabsorption, an increase of blood pressure and can directly stimulate cardiac hypertrophy [68].

Angiotensin I is subsequently converted into its active form angiotensin II (ANG II) by the angiotensin converting enzyme (ACE), which is predominantly expressed on the surface of the pulmonary endothelial cells [69, 70]. Angiotensin II is a powerful vasoconstrictor and causes an increase of blood pressure [39]. Furthermore, it stimulates the secretion of aldosterone in the adrenal glands, which increases the reabsorption of sodium and water by the kidney and thereby causes an increased blood pressure (Fig. 5) [71]. Besides its classical role as vasoconstrictor, ANG II has various other important effects [72-74].

1.5.1 Angiotensin II in inflammation

ANG II modulates inflammatory processes [75]. ANG II can stimulate the recruitment of inflammatory cells into renal parenchymal issue. ANG II contributes to the adhesion of circulating cells to endothelial cells in renal disease and can thus induce structural change of the kidney [76-78]. This entire process is mediated by the up-regulation of certain chemokines, cytokines and adhesion molecules. ANG II up-regulates several pro-inflammatory genes such as vascular cell adhesion molecule-1 (VCAM-1), intercellular adhesion molecule-1 (ICAM-1), interleukin-6 (IL-6), cyclooxygenases (COX2) and monocyte chemoattractant factor protein -1 (MCP-1), through activation of various intracellular signaling pathways, including NFκB, MAPK as well as Rho and redox signaling cascades (**Fig. 6**) [79]. ANG II may therefore facilitate progressive inflammation, further enhance the migration of mononuclear cells into the interstitium and the progression of fibrosis (**Fig. 1**) [80, 81]. ANG II was therefore attributed a role in the events leading to renal fibrosis [82].

1.5.2 Angiotensin II in fibrosis

ANG II participates in the pathogenesis of chronic diseases such as hypertension, atherosclerosis, cardiac hypertrophy and renal injury at least in part through regulation of inflammation and fibrosis [78]. ANG II is considered as a common pathogenic stimulus in end stage renal disease, glomerulosclerosis and interstitial fibrosis [83]. ANG II mediates pathologic phenomena partly by stimulating the release of transforming growth factor (TGF-

β) and plasminogen activator inhibitor type 1 (PAI-1) [79]. ANG II promotes fibrogenesis furthermore by upregulation of monocyte chemoattractant factor protein -1 (MCP-1) (**Fig. 6**) [84]. In several models of renal disease, ACE inhibitors or AT1 receptor antagonists confer protective effects against disease progression, and thus ameliorate proteinuria, infiltration of inflammatory cells and fibrosis in the mouse kidney [79, 85]. Systemic infusion of TGF-β in turn causes elevated tissue levels of ANG II, hypoxia and renal fibrosis, indicating a complex and close relationship between TGF-β and ANG II [86]. ANG II induces fibronectin, CTGF and collagen 1 upregulation via Smad2/3/4 dependent pathways (**Fig. 1**), which can be attenuated by transient transfection of Smad7 [87]. Unilateral ureteral obstruction induced renal injury, myocardial infraction and ANG II-infused mediated Smad activation is diminished by Smad7 overexpression [88, 89]. Therefore, suppression of Smad activation in cardiac and renal fibrosis could be an important anti-fibrotic target.

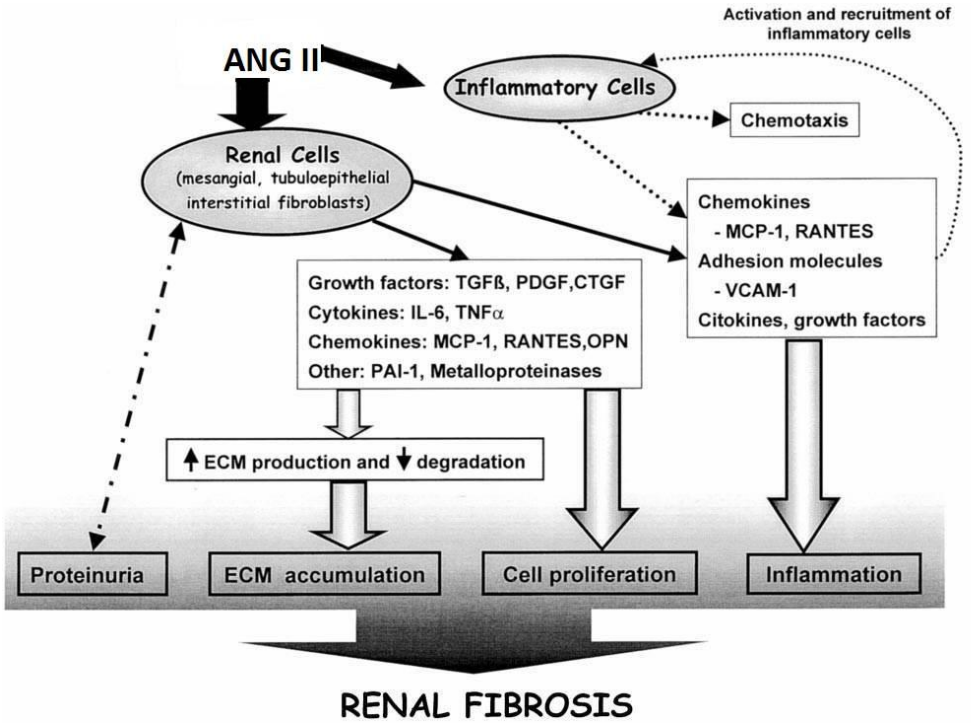

Figure 6. Cellular events involved in ANG II-induced renal fibrosis, modified from Mezzano SA *et al, hypertension.* 2001. ANG II activates inflammatory cells by increasing chemokines and adhesion molecules both in resident and infiltrating cells. This response at least partly relies on chemotaxis and production of MCP-1 and TGF-β or indirectly activating resident cells which eventually contributes to the progression of fibrosis. Several proteins are increased by ANG II through which it regulates cell growth and matrix regulation in renal cells [39].

Nevertheless, as previously discussed, TGF-β can also transduce fibrogenic signals by Smad independent pathways (**Fig. 4**). Effects of ANG II are intracellularly transmitted via TAK-1 [90]. ANG II promotes cardiac hypertrophy in a TAK1 dependent and Smad2/3 independent manner [91]. Angiotensin has therefore a crucial role in fibrotic diseases, which are mediated by various intracellular pathways.

1.6 Kv1.5

Recent evidence indicates a role for ion channels in fibroblast activation [92, 93]. The voltage-gated potassium K^+ channel Kv1.5, encoded by *KCNA5* gene, contributes to the regulation of cell membrane potential and cell volume [94]. The Kv1.5 channel is considered as a delayed rectifier potassium channel and is involved in the regulation of cell membrane potential in a wide variety of tissues including pancreatic β-cells, brain, macrophages, dendritic cells, and heart [95, 96]. Kv1.5 causes the repolarization of cardiac action potential in the heart [97]. Kv1.5 channel is abundantly expressed at uniform level in atrial myocytes [98]. The Kv1.5 channel is expressed in immune system, kidney, skeletal, smooth muscle and brain [99-101]. Mutation induced loss of function of Kv1.5 channel is implicated in several human diseases such as atrial fibrillation [102]. Several studies indicate that Kv1.5 has a putative functional pathophysiological role [103-105]. Kv1.5 is expressed in several human tumor cells and the expression of this channel is altered in prostate cancer, colon cancer, breast cancer and lung cancer [106-109]. Kv1.5 channels appear to contribute to the development of cancer through their involvement in proliferation, adhesion, migration and invasion [110].

1.6.1 Fibrosis regulated by Kv1.5

Angiotensin II upregulates Kv1.5 channel expression through ROS dependent TGF-β1 - ERK1/2 signaling cascade in rat atrial myocytes, which contributes to the development of atrial fibrillation [105]. The activity and expression of Kv1.5 is suppressed in response to ischemia, an effect, at least partially explained by 15-hydroxyeicosatetraenoate (15-HETE) formation [111]. The suppression or inhibition of Kv1.5 leads to impairment of cellular apoptosis and thus may exacerbate the progression of cancer [112]. KV1.5 is expressed in fibroblasts and may modulate the activity of these cells [113]. Thus, dysregulation of Kv1.5 might impact on cardiac fibrosis [113]. Along those lines, Kv1.5 might be involved in fibroblast activations in other organs. Down-regulation of Kv1.5 may theoretically affect renal fibrosis.

1.7 Models of fibrotic disease

The molecular events and ECM deposition in renal fibrosis may be simulated by preclinical animal models [114]. The hallmarks of renal fibrosis as an end-stage of various kidney disease may be mimicked by unilateral ureteral obstruction (UUO) [114]. UUO induced renal tissue changes resembles human-ureteral-tract-obstruction induced kidney injury but the fibrogenic processes involve also several key cellular events in the course of CKD including kidney fibrosis [20]. Furthermore, angiotensin II exposure triggers renal fibrosis [115]. The angiotensin II induced renal fibrosis relies on TGF-β dependent and independent effects and resembles human pathophysiology [115]. These animals allow the study of mechanisms contributing to and resulting in fibrosis [114, 115].

1.8 AMPK as a master sensor of energy balance

The AMP-activated protein kinase (AMPK) is an evolutionary conserved Ser/Thr protein kinase and acts as a master sensor of cellular energy balance. AMPK is activated by changes in the cytosolic AMP/ATP concentration ratio and therefore is activated following hypoxia, starvation, glucose deprivation and muscle contraction. AMPK is a heterotrimeric complex consisting of a catalytic alpha (α) subunit (63 KDa), regulatory beta (β) (30 KDa) and gamma (γ) subunits (38-63 KDa) [116]. AMPK contains a conventional kinase domain at the N terminal region and auto inhibitory domain (AID) which is immediately followed by a linker (**Fig. 7**).

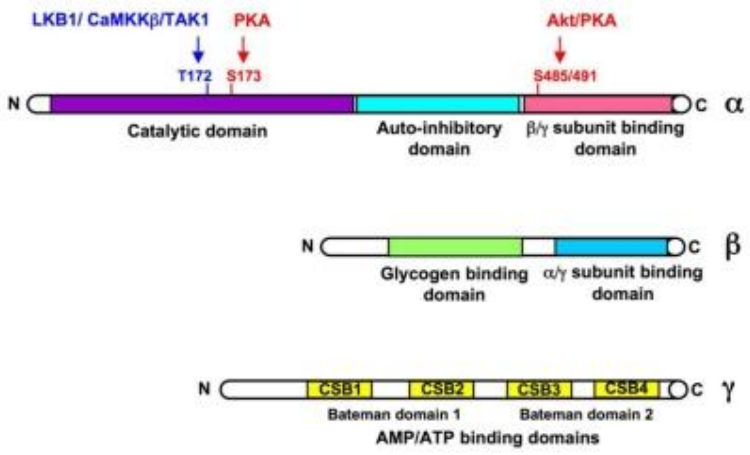

Figure 7. Structural organization of AMPK, obtained from Viollet B *et al, Crit Rev Biochem Mol Biol,* 2010. AMPK is a heterotrimeric protein consists of an α catalytic, β and γ subunit. [117].

Each subunit has multiple isoforms (α1, α2, β1, β2, γ1, γ2, γ3), which are encoded by different genes. Different expression patterns and tissue distribution of the isoforms have been reported, but the isoform specific functions remain insufficiently defined [118]. AMPKα1 and AMPKα2 subunits are expressed almost by all cell types, although the ratio may vary [119]. The ubiquitously expressed AMPKα1 is mostly found in the non-nuclear fraction while AMPKα2 may be localized in both non-nuclear fraction as well as the nucleus [117, 120]. The

two catalytic AMPKα isoforms may modulate different downstream targets and facilitate thereby different effects [121]. Cardiac muscle and skeletal muscle express the AMPKα2 subunit at a higher abundance than the AMPKα1 subunit [122]. AMPKα1 phosphorylates cytosolic and plasma membrane proteins while AMPKα2 has been more associated with transcriptional effects induced by metabolic signals [123, 124].

Hormonal and nutritional signals targeted to maintain cellular energy balance and metabolic functions can activate AMPK [125]. Furthermore, AMPK is activated by an increased AMP/ATP ratio, which then results in a shutdown of energy consuming pathways and stimulation of energy producing pathways [126]. AMPK effects on lipid metabolism by phosphorylating Acetyl-CoA carboxylase (ACC) at Thr-79 which controls the limiting step for lipid biosynthesis [127]. AMPK also governs transcription of some specific genes involved in metabolic regulation through which long term metabolic regulation can be maintained [123]. Control over food intake and energy expenditure can also be regulated by AMPK in response to hormonal signals, including leptin, ghrelin and adiponectin (**Fig. 8**) [128].

1.8.1 Ion channels and transporters regulated by AMPK

AMPK fosters cell survival during energy depletion by regulating a wide variety of ion channels, carriers and transporters [129]. Cellular depolarization by inhibition of K^+ channels may reduce the electrical driving force for the electrogenic Na^+ coupled HCO_3^- transport, which causes alkalinization of cell [129]. An alkalinization of the cell would further promote glycolytic flux and thereby generate ATP from glucose without the requirement of an energy consuming transport in the cell [129]. AMPK foster the degradation of plasma membrane proteins at least partly by activating Nedd4-2 and promote ubiquitination of plasma membrane proteins [129]. AMPK is a powerful regulator of several channels and carriers, as described in table 1, to initiate their removal from the plasma membrane by ubiquitination (**Table 1**) [130].

Table 1 A short list of channels or transporter regulated by AMPK.

Channels and Transporters	Effects of AMPK	Mechanism of Action	References
BKCa	down-regulation	Direct-channel phosphorylation	[131]
ENaC	down-regulation	Nedd4-2-mediated Degradation	[132]
KCa3.1	down-regulation		[133]
KCNQ1	down-regulation	Nedd4-2	[134]
Kv7.1	down-regulation	Nedd4-2	[135]
Nav1.5	up-regulation		[136]
NHE	up-regulation		[137]

1.8.2 Regulation of AMPK by different kinases

AMPK is activated allosterically by AMP [138]. However, in addition to its allosteric regulation, AMPK can also be regulated by reversible phosphorylation [139]. The phosphorylation of the subunit at Thr-172 site is crucial for AMPK activation [140]. There are three different upstream AMPK kinases identified until now. The liver kinase, LKB1 is a primary AMPK kinase which is constitutively active and is not regulated by AMP (**Fig. 8**) [141]. Upon binding of AMP to AMPK, AMPK may be phosphorylated by LKB1 at Thr-172 (**Fig. 8**) [142]. Another AMPK kinase is the Ca^{2+}/calmodulin-dependent protein kinase kinase β (CaMKKβ), which phosphorylates and activates AMPK in response to elevated levels of intracellular Ca^{2+}, independent of the cellular AMP/ATP ratio (**Fig. 8**) [143]. The third putative upstream AMPK kinase is the TGF-β activated kinase 1 (TAK1) which is implicated in the regulation of AMPK in different physiological and pathophysiological conditions (**Fig. 8**) [144].

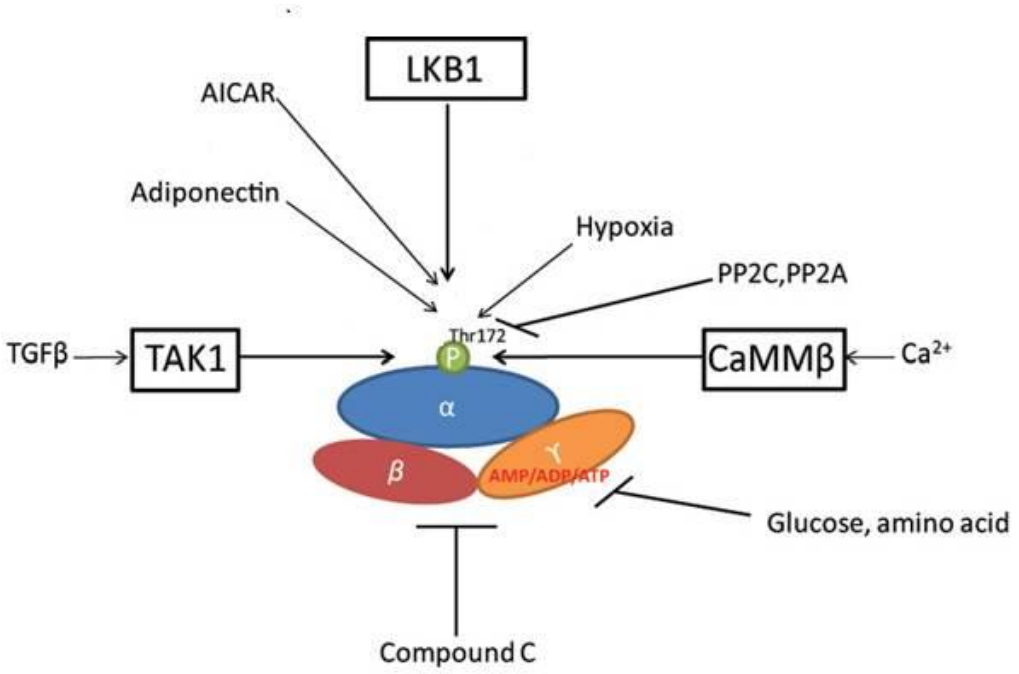

Figure 8. Regulation of AMPK activity through different kinases, modified from Wang S *et al.*, *Clin Sci (Lond)*, 2012. AMPK is activated by phosphorylation at Thr-172 through different upstream kinases: CaMKK, LKB1 and TAK1. Phosphorylation of AMPK by CaMKK and LKB1 depends upon the concentration of intracellular Ca^{2+} and the AMP/ATP ratio respectively. The mechanism and relevance of TAK1 dependent phosphorylation of AMPK is still insufficiently defined [145].

1.8.3 Regulation of AMPK in the kidney

The activation and functions of the AMPK signaling pathway have been extensively studied over the last decade in various organs including liver, skeletal muscle and heart. The role of AMPK in renal physiology and disease is still ill defined, although AMPK is abundantly expressed in kidney. Both catalytic subunits α1 and α2 are expressed in kidney [146]. The AMPK upstream kinase LKB1 is abundantly expressed in the kidney whereas CaMKKβ is not detectable in physiological conditions [147]. AMPK may play an important role in ion transport, may regulate Na^+ and electrolyte balance [148-150]. AMPK may be especially

important during pathological processes in the kidney. Adiponectin, a hormone produced by adipocytes, activates AMPK thereby mediates reduction of oxidative stress by reducing NADPH oxidase 4 (Nox4) expression in podocytes [151]. AMPK activation is reduced in the diabetic kidney [152]. AICAR and metformin, two pharmacological activators of AMPK, inhibit EMT and fibrogenic processes in obstructive renal injury [153, 154]. However, the effects of AICAR and metformin may be via pathways independent of AMPK [155]. Accordingly, activation of AMPK in the heart during ischemic conditions is considered to be beneficial [156]. Along these lines, AMPK has been implied in renoprotection following ischemic injury [157, 158]. Nonetheless, the exact role of AMPK and the isoform specific effects of AMPK in renal tissue remain to be elucidated.

1.8.4 Role of AMPK in inflammation

In the case of injury, activated fibroblasts produce ECM and cause apoptosis [16]. An increasing body of evidence indicates that AMPK plays a pivotal role in the transduction of inflammatory signals [159-162]. AMPK activity is reduced by pro-inflammatory stimuli such as lipopolysaccharides (LPS) and increased by several anti-inflammatory cytokines [163]. Upon a pro-inflammatory stimulus, AMPK inhibition may enhance the production and secretion of TNFα, IL-6 and IL-1 while overexpression of AMPK can stimulate the production of IL-10 [163]. LPS induced lung injury can be attenuated by activation of AMPK [164]. Isoform specific effects of AMPK may be of crucial importance during inflammatory processes: Other than AMPKα2, the AMPKα1 isoform plays a key role in pro-inflammatory signals triggered by the toll-like receptor 4 (TLR4) through molecular interaction with TAK1 [162]. TAK1 has therein been described as a downstream effector of AMPKα1, which mediates the pro-inflammatory effects of AMPK [162]. Constitutive activation of AMPKα1 in endothelial cells causes inflammation by abnormal expression of COX2, E-selectin, intercellular adhesion molecule (ICAM), the chemokine CCL2, and TNFα [161]. Elevated levels of COX2 may be associated with obesity related renal damage, cardiac abnormalities and fatty liver injuries [165, 166]. Therefore, AMPK may mediate either pro-inflammatory or anti-inflammatory signals, and these may depend on isoform specific effects.

1.8.5 Role of AMPK in fibrosis

AMPK activity is modified in different metabolic stress condition such as diabetes and obesity [159, 167]. Several studies therefore investigated the effects of AMPK on renal fibrosis: AMPK activation with AICAR blunts the fibrotic response following obstructive injury [154]. Similarly Metformin reduces the renal fibrosis after unilateral ureteral obstruction [168]. TGF-β, high glucose, angiotensin II and aldosterone induced EMT is reduced by AMPK activation in human proximal tubular cells (HK-2 cells) [153].

Paradoxically, genetic deletion of adiponectin inhibits the bone-marrow derived fibroblast accumulation in the kidney, which is crucial in the induction of renal fibrosis following obstructive injury [32]. Adiponectin is a multifunctional cytokine that plays an important role in inflammation and metabolic processes, and mediates its effects at least partly via AMPK activation [169]. Accordingly, AMPK inhibition or dominant negative AMPKα1 transfection suppressed the adiponectin induced α-SMA expression and ECM accumulation [32]. These findings may be further supported by the observation, that ANG II induced fibroblast proliferation and collagen accumulation is enhanced by AMPKα1 activation [170]. Therefore, the role of AMPK during fibrosis is rather controversial. In theory, AMPK might promote the survival of energy depleted cells by the replacement of less energy demanding fibrous tissue in response to metabolic or other stressors. The effects of AMPK may however be dependent on its isoform.

2. AIM OF THE STUDY

AMPK might promote the replacement of functional tissue by fibrous tissue to support the survival of energy depleted cells in ischemic condition. Based on this hypothesis, this study investigated the isoform specific functional significance of AMPKα1 in renal inflammation and fibrosis following unilateral ureteral obstruction and angiotensin II infusion. TAK1 and Kv1.5 were investigated as possible mechanisms of AMPKα1 downstream effects.

3. MATERIALS AND METHODS

3.1 Animal experiments

All animal experiments were carried out according to the German law and the recommendation of the guide for care and use of laboratory animals of the National Institutes of Health for the Welfare of Animals. Animal surgery was approved by the respective government authority of the state Baden-Württemberg (Regierungspräsidium). Experiments were performed in gene-targeted mice lacking functional AMPKα1 (AMPKα1$^{-/-}$) and in corresponding wild-type mice (AMPKα1$^{+/+}$) [171, 172]. The AMPKα1$^{-/-}$ mice were described in detail by Viollet *et. al* [173].

3.1.1 Unilateral Ureteral Obstruction

Renal fibrosis was triggered by the unilateral ureteral obstruction (UUO) procedure [174-176]. UUO treatment was performed for three days, seven days and three weeks respectively. Following anesthesia of the mouse, the skin and the abdominal wall was opened by surgical incision. The left ureter was identified followed by and dual ligation with a non-resorbable 7-0 filament. The surgical opening was closed by suturing. Metamizole treatment was used for analgesia (200 mg/kg BW) after the procedure and was maintained by metamizole addition to the drinking water for the duration of the UUO experiment. Mice were sacrificed three days, seven days and three weeks after the UUO procedure. The obstructed as well as non-obstructed kidneys were immediately removed. One kidney portion was fixed by 4% paraformaldehyde/PBS for subsequent immunostaining. Another kidney portion was snap-frozen in liquid nitrogen and stored at −80°C for RNA and protein isolation, respectively [176]. Blood was collected after 7 days of UUO treatment. Blood was analysed by using a pocH-100iv automatic hematology analyzer (Sysmex) to measure the blood count.

3.1.2 Angiotensin II infusion

Angiotensin II was infused in mice by surgical subcutaneous implantation of osmotic minipumps (Alzet) at a dosage of 1.46mg/kgBW/day or saline for two weeks. After two weeks of treatment, mice were then sacrificed, and the kidneys were rapidly removed and snap frozen in liquid nitrogen and stored at −80°C for RNA and protein isolation, respectively.

3.2 Analysis of protein expression in renal tissue

3.2.1 Protein isolation from murine renal tissues

After weighing of the kidney tissue samples, ice-cold lysis buffer **(**Thermo Fisher Scientific) supplemented with complete protease and phosphatase inhibitor cocktail (Thermo Fisher Scientific, USA) was added to the renal tissue (20µl lysis buffer/mg kidney tissue). Tissues were homogenized with IKA T10 basic homogenizer (IKA –Werke, GmbH) for 5 seconds. The homogenized samples were kept on the ice for 20 minutes for the complete lysis of the tissues. Next, the samples were centrifuged at 10.000 rpm for 5 minutes and the supernatant was transferred into a new tube. Protein concentrations were estimated with Bradford protein assay reagent (Biorad, Munchen, Germany).

3.2.2 SDS-PAGE electrophoresis

The proteins were separated using 8%, 10% or 12 % SDS-polyacrylamide gels (**Table 2, 3**) depending on the molecular weight of the target proteins.

Table 2. 5% stacking gel for Tris-Glycine SDS polyacrylamide gel electrophoresis

Chemicals	**Total volume (8 ml)**
dH20	5.5 ml
Acrylamide mix (30%)	1.3 ml
Tris-HCl (1.0 M, pH 6.8)	1.3 ml
SDS (10%)	80 µl
Ammonium persulphate (10%)	80 µl
TEMED	8 µl

Table 3. Resolving gels for Tris-Glycine SDS polyacrylamide gel electrophoresis

Chemicals	**8% Gel (20 ml)**	**10% Gel (20 ml)**	**12% Gel (20 ml)**
dH20	9.3 ml	7.9 ml	6.6 ml
Acrylamide mix (30%)	5.3 ml	6.7 ml	8.0 ml
Tris-HCl (1.5 M, pH 8.8)	5.0 ml	5.0 ml	5.0 ml
SDS (10%)	200 µl	200 µl	200 µl
Ammonium persulphate (10%)	200 µl	200 µl	200 µl
TEMED	12 µl	8 µl	8 µl

The proteins (30 µg/ sample) were boiled in Roti-Load1 Buffer (Carl Roth, GmbH) at 100ºC for 5 min. Before and after heating, the samples were vortexed and centrifuged for best dissolving. The peqGOLD Protein-Marker V (Peqlab, Erlangen, Germany) was used as a molecular weight marker. Murine tendon tissues were used as positive control for Collagen I Western blot. Prepared protein samples were loaded into the gel wells by using special gel loading tips (VWR, international). Electrophoresis was performed for about 2.5 hours, at 80/120 mV, at room temperature by using electrophoresis power supply (Pharmacia Biotech) (**Table 4**).

Table 4. 10X Running Buffer

Tris base	250 mM
Glycine	1.9 M
SDS	1 %

3.2.3 Immunobloting

After separation on SDS-PAGE gels, proteins were transferred to PVDF membranes (Roche, Germany). The protein transfer was made for 1 hour at 100 mV using ice blocks (**Table 5, 6**).

Table 5. 10X Transfer Buffer

Tris base	198 mM
Glycine	1.5 M

Table 6. 1X Transfer Buffer

10X Transfer buffer	100 ml
Methanol	100 ml
dH20	800 ml

The PVDF membranes containing the transferred proteins were blocked with 5% non-fat dry milk in Tris-buffered saline / 0.1 % Tween 20 (TBST) (**Table 7, 8**) for one hour at room temperature to avoid any unspecific binding of the antibodies to the membranes.

Table 7. 10X TBS

Tris base	200 mM
NaCl	1.3 M
Adjust pH	7.6

Table 8. 1X TBS

10X TBS	100 ml
dH20	900 ml
Tween-20	1 ml

After blocking, the membranes were incubated overnight at 4°C with the following primary antibodies: rabbit anti-pAMPK Thr^{172}, rabbit anti-AMPKα, rabbit anti- pTAK1 Ser^{412}, rabbit anti- TAK1, rabbit anti- pSmad2 $Ser^{465/467}$, rabbit anti- Smad2, rabbit anti- pACC Ser^{79}, rabbit anti-ACC, rabbit anti-TGF-β, rabbit anti-GAPDH (Cell Signaling, Danvers, MA, USA) (used at a 1:1000 dilution), rabbit anti-Collagen 1 (Abcam, Germany) (used at a 1:1000 dilution), goat anti-AMPKα2 (Santa Cruz, USA) (used at a 1:2000 dilution), rabbit anti-AMPKα1 (Novus Biology, Germany) (used at a 1:1000 dilution) or rabbit anti-α-smooth muscle actin (Abcam, Germany) (used at a 1:2000 dilution). The antibodies were diluted in 5% BSA/TBST or in 5% non-fat dry milk/TBST (for Collagen 1 Western blotting).

The following day, the membranes were washed three times for 10 minutes with TBST and then incubated with secondary goat anti-rabbit HRP-conjugated antibody (diluted 1:1000, Cell Signaling) or donkey anti-goat HRP-conjugated antibody (diluted 1:2000, Santa Cruz, USA)

for 1 hour at room temperature. Secondary antibodies were diluted in 5% non-fat dry milk/TBST. Next, the membranes were washed three times for 10 minutes with TBST.

Antibody binding was detected with the ECL detection reagent (Thermo Fisher Scientific, USA) or homemade ECL solution (**Table 9-11**). Membranes were exposed to X-ray film (GE Healthcare, Europe, GmbH) and developed with developing and fixing solution (Sigma Aldrich, Germany) in the dark room. For loading controls, the membranes were stripped with stripping buffer (Carl Roth, GmbH) at 60°C for 5 min. Bands were quantified with Quantity One Software (Bio-Rad Laboratories) and results were normalized to the protein expression in the obstructed kidney tissues of wild-type mice for the UUO experiments. For the results following angiotensin II infusion, protein expression in the kidney tissues of control treated wild-type mice was used for the normalization of data.

Table 9. Solution A for ECL (200 ml)

Tris-HCl (0.1 M)	2.42 g
Luminol	50 mg
dH20	200 ml
Adjust pH	8.6

Table 10. Solution B for ECL (10 ml)

P-hydroxy cumaric acid	11 mg
DMSO	10 ml

Table 11. Working Solution for ECL

Solution A	1 ml
Solution B	100 µl
Hydrogen peroxide	0.3 µl

3.2.4 Histology and immunostaining

For immunohistochemistry, paraffin-embedded kidney tissue samples were sectioned at 3 μm thickness. Sections were incubated with rabbit anti-Collagen I/III (1:20, Biotrend, Köln, Germany), mouse monoclonal α-smooth muscle actin (α-SMA) primary antibody (1:200, Sigma, Schnelldorf, Germany), followed by biotinylated anti-rabbit secondary antibody (1:150, Dianova, Hamburg, Germany) and biotinylated anti-mouse Ig secondary antibody (1:200, Dianova, Hamburg, Germany). For negative controls, sections were incubated without primary antibody. Signals were visualized by using substrate AEC kit (BioGenex, Milmont Drive Fremont, CA, United States) according to the manufacturer protocol. The evaluation of the CollagenI/III staining has been performed as follows:

0- no staining detectable,
1- mild staining detectable,
2-moderate staining detectable,
3- intense staining detectable.

A degree-specific staining index has been defined as the percentage of fields with the respective degree of injury. The total staining score index has been calculated as the sum of specific damage indices (the index with degree 1 was multiplied by 1, the index with degree 2 was multiplied by 2, the index with degree 3 was multiplied by 3).

PAS staining sections were used for morphometric analysis performed by using a semiautomatic image analyzing system (Leica Q600 Qwin; Leica Microsystems, Cambridge, UK). Examination of at least 15 fields of cortex and inner medulla obtained after exclusion of glomeruli (20X magnification) was made for evaluation of the percentage of differentiated proximal tubules.

3.3 Analysis of apoptosis in renal tissue

To visualize the apoptotic cells in paraffin-embedded 3 μm kidney tissue sections, In Situ Cell Death Detection kit, POD (Tunel technology) (Roche, Mannheim, Germany) has been used according to the manufacturer's protocol. The number of Tunel-positive cells has been counted in 10 random fields (40X magnification).

3.4 Analysis of gene expression in renal tissue

3.4.1 RNA isolation

Total RNA was extracted from mouse kidney tissues using Trifast Reagent (Peqlab, GmbH) according to the manufacturer's instructions. Using IKA T10 basic homogenizer (IKA – Werke GmbH), tissue samples were lysed in Trifast reagent. Chloroform is added after homogenising the samples and centrifuged at 12000 rpm for 15 minutes at 4°C. The RNA containing aqueous phase was precipitated by mixing isopropanol followed by centrifugation at 12000 rpm for 10 minutes at 4°C. After washing with 75% ethanol, the RNA pellets were allowed to dry at room temperature. RNA is re-suspended by addition of RNase free water and concentration of RNA was measured by optical density measurement using Biophotometer Plus (Eppendorf, Germany).

3.4.2 cDNA synthesis

Reverse transcription of 2 µg RNA was performed using oligo$(dT)_{12\text{-}18}$ primers (Invitrogen) and SuperScript III Reverse Transcriptase (Invitrogen). First strand cDNA synthesis was performed at 50°C for 1 hour, using a thermal heat-block PCR machine (Peqlab, GmbH). The reaction was stopped by heating to 70°C for 10 minutes.

3.4.3 Quantitative RT-PCR

In order to amplify the target genes in quantitative real-time PCR, reactions were set up in a total volume of 20 µl using 2 µg of cDNA, 100 nM forward and reverse primers (Invitrogen, **Table 12**) and iQ™ Sybr Green Supermix (Bio-Rad Laboratories) according to the manufacturer's protocols. Quantitative real-time PCR was performed with the CFX96 iCycler iQ™ Real-Time PCR Detection System (Bio-Rad Laboratories) according to the manufacturer's instructions. The cycling conditions were as follows:

95°C -2 min

95°C – 15 sec

55-60°C – 45 sec (40 cycles)

The melt curve analysis: 55-95°C (0.5°C increment) – 2 sec/step.

Table 12. Primers sequences (5'→3' orientation) (Invitrogen, Darmstadt, Germany)

a-Sma	fw: CCCAGACATCAGGGAGTAATGG rev: CTATCGGATACTTCAGCGTCA
c-Fos	fw: CGGCATCATCTAGGCCCAG rev: TCTGCTGCATAGAAGGAACCG
Col1a1	fw: ACCCGAGGTATGCTTGATCTG rev: CATTGCACGTCATCGCACAC
Col3a1	fw: ACCCGAGGTATGCTTGATCTG rev: GGACATGATTCACAGATTCCAGG
Il6	fw: TCTATACCACTTCACAAGTCGGA rev: GAATTGCCATTGCACAACTCTTT
Gapdh	fw: AGGTCGGTGTGAACGGATTTG rev: TGTAGACCATGTAGTTGAGGTCA
Pai-1	fw: TTCAGCCCTTGCTTGCCTC rev: ACACTTTTACTCCGAAGTCGGT
Snai1	fw: CACACGCTGCCTTGTGTCT rev: GGTCAGCAAAAGCACGGTT

Cxcl16	fw: ATACCGCAGGGTACTTTGGAT rev: CTGCAACTGGAACCTGATAAAGA
Cd206	fw: GAGGGAAGCGAGAGATTATGGA rev: GCCTGATGCCAGGTTAAAGCA
Cox2	fw: TGCACTATGGTTACAAAAGCTGG rev: TCAGGAAGCTCCTTATTTCCCTT

The specificity of the PCR product was verified by analysis of the melting curves. All PCRs were performed in duplicate, and mRNA fold changes were calculated by the $2^{-\Delta\Delta Ct}$ method. Amplification of the house-keeping gene Gapdh was employed to normalize the amplification of targeted genes.

3.5 Xenopus laevis oocyte expression system

3.5.1 Constructs

The constructs which were used for generation of cRNA are presented in the **Table 13**. The methodology for cRNA generation was described previously [177].

Table 13. List of constructs

Name of constructs	**References**
wild-type human Kv1.5	[178]
Kv1.5-HA containing an extracellular hemagglutinin epitope	[104]
wild-type human AMPKα1-HA	[179]
AMPKβ1-Flag	[179]
AMPKγ1-HA	[179]
constitutively active AMPK$^{\gamma 1R70Q}$-HA	[180]
kinase dead mutant AMPKα1^{K45R}-HA	[181]
wild-type human Nedd4-2	[182]

3.5.2 Voltage clamp in *Xenopus* oocytes

Xenopus oocytes were isolated from adult *Xenopus laevis* females. *Xenopus laevis* frogs were anesthesized by bathing in a solution containing 3- aminobenzoic acid ethyl ester (0.1%, Sigma, Aldrich, Germany). A small abdominal incision was made and oocytes were removed, followed by closure of the skin by sutures. cRNA encoding Kv1.5 (2.5 ng) was injected with or without 4.6 ng of cRNA encoding either AMPKα1-HA + AMPKβ1-Flag + AMPKγ1-HA (AMPK^{WT}), or AMPKα1-HA + AMPKβ1-Flag + AMPKγ1R70Q-HA (AMPK $^{\gamma R70Q}$) or AMPKα1K45R-HA + AMPKβ1- Flag +AMPKγ1-HA (AMPK$^{\alpha K45R}$) and with or without 10 ng cRNA encoding Nedd4-2 on the day of preparation of the *Xenopus* oocytes. The oocytes were incubated at 18°C in ND96 solution supplemented with antibiotics (**Table 14**).

Table 14. Recipes for ND96 solution

Chemicals	**Concentration**
NaCl	88.5 mM
KCl	2 mM
$MgCl_2$	1 mM
$CaCl_2$	1.8 mM
NaOH	2.5 mM
HEPES	5 mM (pH 7.4)
sodium pyruvate	100 mg/l
Gentamycin	100 mg/l
Tetracycline	50 mg/l
Ciprofloxacin	1.6 mg/l
Theophiline	90 mg/l

Three/four days after the injection, two electrode voltage-clamp measurements were performed at room temperature. In two electrode voltage-clamp experiments, the Kv1.5 channel currents were elicited every 20 s with 2 s pulses from -80 mV to +50 mV applied from a holding potential of -100 mV. Pulses were applied in 10 mV increments. The data were filtered at 1 kHz and recorded with a Digidata 1322A A/D-D/A converter and Chart V.4.2 software for data acquisition and analysis (Axon Instruments). The analysis of the data was performed with Clampfit 9.01 (Axon Instruments) software.

3.5.3 Detection of Kv1.5 cell surface expression by chemiluminescence

To determine Kv1.5-HA cell surface expression, oocytes were injected with 15 ng of cRNA encoding HA-tagged Kv1.5 with or without 4.6 ng of cRNA encoding either AMPKα1-HA + AMPKβ1-Flag + AMPKγ1-HA ($AMPK^{WT}$), or AMPKα1-HA + AMPKβ1-Flag + AMPKγ1R70Q-HA ($AMPK^{\gamma R70Q}$) or AMPKα1K45R-HA + AMPKβ1- Flag +AMPKγ1-HA ($AMPK^{\alpha K45R}$). After the incubation period of 3 days, the oocytes were blocked in 5%

BSA/ND96 solution on ice on a shaker for 1 hour. Next, the oocytes were incubated with 1 µg/ml primary rat monoclonal anti-HA antibody (clone 3 F10; Boehringer, Biberach, Germany) for 1 hour on ice, on a shaker. After washing the oocytes for 3 times 10 minutes with ND96 solution, the *Xenopus* oocytes were further incubated in 2 µg/ml secondary HRP-conjugated goat anti-rat antibody (Cell Signaling, Danvers, MA, USA). The oocytes were washed for five times 10 minutes in ND96 solution. Individual oocytes were put in 96-well plates with 20 µl of SuperSignal ELISA Femto Maximum Sensitivity Substrate (Pierce, Rockford, IL) and chemiluminescence of single oocytes was quantified in a luminometer (WalterWallac2 plate reader; Perkin Elmer, Jügesheim, Germany) by integrating the signal over a period of 1s. Results show normalized arbitrary light units which are proportional to the detector voltage.

3.5.4 Immunocytochemistry and confocal microscopy

The *Xenopus* oocytes were fixed in 4% paraformaldehyde/PBS for 12 hours followed by cryoprotection in 30% sucrose for another 12 hours and frozen in mounting medium. For immunostaining, 8 µm sections were dehydrated at room temperature and fixed in acetone/methanol (1:1) for 15 minutes at room temperature. The sections were blocked for 1 hour in 1% BSA/PBS at room temperature followed by overnight incubation with primary rat monoclonal anti-HA antibody (diluted 1:100; clone3 F10; Boehringer, Biberach, Germany) in a moist chamber at 4°C. The binding of primary antibody was visualized by incubation with secondary anti-rat Alexa 488-conjugated antibody (diluted 1: 200; Invitrogen) for 1 hour at room temperature, in the dark. Next, oocytes were analyzed by a fluorescence laser scanning microscope (LSM 510; carlzeiss MicroImaging, Gottingen, Germany) with a plan 40x/1.2WDICIII. Brightness and contrast settings were kept constant during imaging of all oocytes in each injection series.

3.6 Statistical analysis

Results are presented as arithmetic means ± SEM, where *n* shows the number of independent experiments. For the UUO model, data were tested for significance between genotypes using Student t-test (normal distributed data) or Mann-Whitney test (non-normal distributed data) according to Shapiro-Wilk test. Paired t-test or Wilcoxon test were applied for statistical testing between non-obstructed control kidneys and obstructed kidneys. Bonferoni correction was used for multiple comparisons. For the results in the angiotensin II infusion model and the *Xenopus* oocytes expression system, statistical testing was performed by one-way Anova followed by posthoc analysis. Only results with $p<0.05$ were considered statistically significant.

4. RESULTS

4.1 Renal AMPKα1 and Unilateral Ureteral Obstruction

The experiments were performed in gene-targeted mice lacking functional AMPKα1 ($AMPK\alpha1^{-/-}$) and corresponding wild-type mice ($AMPK\alpha1^{+/+}$) to explore the impact of AMPKα1 isoform in the development of renal tissue fibrosis induced by unilateral ureteral obstruction (UUO). The obstructive nephropathy was induced for 3 days, 7 days and 3 weeks respectively.

As a result, the $Ampk\alpha1^{-/-}$ mice had significantly lower red blood cell count and significantly increased spleen weight to body weight ratio as compared to $AMPK\alpha1^{+/+}$ mice (**Table 15**). Accordingly, the AMPKα1-deficient mice develop anemia and splenomegaly.

Table 15. Anemia and splenomegaly in $AMPK\alpha1^{-/-}$ mice

Arithmetic means ± SEM (n=6-7) of blood parameters (red blood cell count (RBC), white blood cell count (WBC), hemoglobin concentration (HGB), hematocrit (HCT), mean corpuscular volume, (MCV), mean corpuscular hemoglobin (MCH), mean corpuscular hemoglobin concentration (MCHC) and platelet count (PLT)) and spleen weight to body weight ratio of AMPKα1 knockout mice ($AMPK\alpha1^{-/-}$) and respective wild-type mice ($AMPK\alpha1^{+/+}$) following 7 days of UUO. *($p<0.05$), **($p<0.01$), ***($p<0.001$) indicates statistically significant differences from respective wild-type mice.

	$AMPK\alpha1^{+/+}$	$AMPK\alpha1^{-/-}$
RBC* 10^6 /µl	8.80 ± 0.20	6.93 ± 0.21 ***
WBC *10^3 /µl	11.71 ± 1.59	9.65 ± 1.17
HGB [g/dl]	15.30 ± 0.26	11.30 ± 0.26 ***
HCT [%]	49.07 ± 1.20	37.70 ± 0.89 ***
MCV [fL]	55.76 ± 0.25	54.52 ± 0.65
MCH [pg]	17.39 ± 0.19	16.33 ± 0.16 **
MCHC [g/dl]	31.21 ± 0.36	29.98 ± 0.17 *
PLT*10^3 /µl	1038.9 ± 38.3	1090.7 ± 74.0
Spleen w./ bw. [mg/g]	5.27 ± 0.44	11.99 ± 0.81 **

4.1.1 Renal AMPKα1 and AMPKα2 isoform expression

The expression of the AMPKα isoforms AMPKα1 and AMPKα2 at different time points after UUO was investigated, and expression levels were analyzed by using Western Blotting.

As shown in **Figure 9** (**A** for **3 days**, **B** for **7 days**, and **C** for **3 weeks**), AMPKα1 protein was expressed in kidney tissue of AMPKα1$^{+/+}$ mice but not in kidney tissue of AMPKα1$^{-/-}$ mice. The protein abundance of AMPKα1 isoform was significantly increased in the obstructed kidney tissues as compared to non-obstructed control kidney tissues of AMPKα1$^{+/+}$ mice following 3 days, 7 days and 3 weeks of UUO (**Fig. 9**). Thus, AMPKα1 protein expression was up-regulated at early, middle and late time points of UUO.

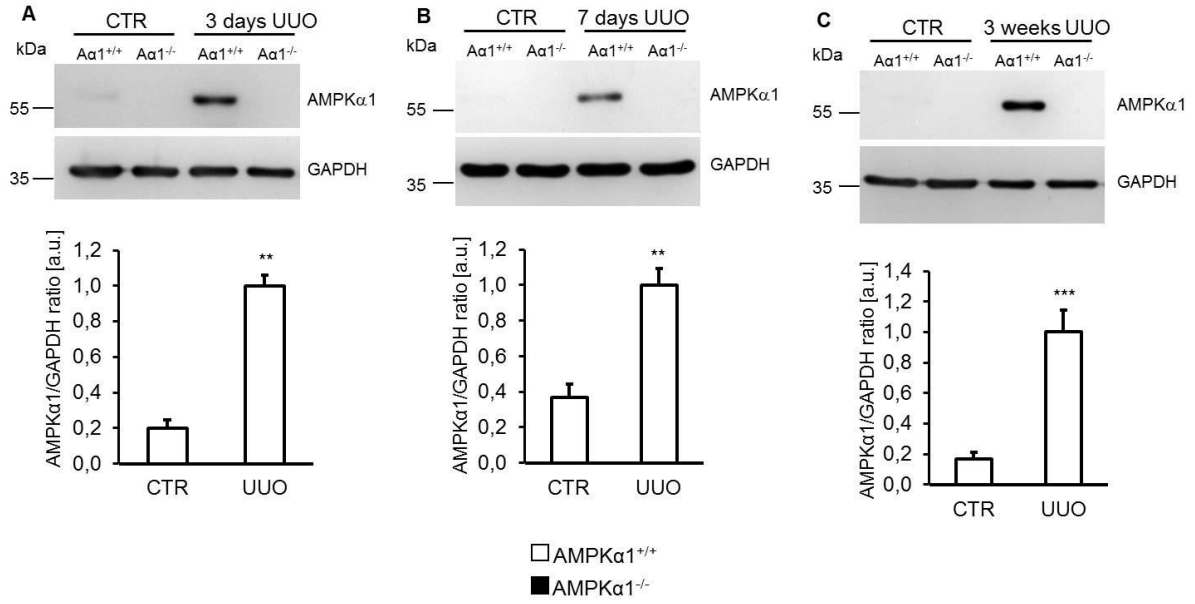

Figure 9: Renal AMPKα1 protein expression in AMPKα1$^{+/+}$ and AMPKα1$^{-/-}$ mice following unilateral ureteral obstruction. Representative original Western blots of expression of AMPKα1 and GAPDH as loading control in renal tissue of non-obstructed control kidney (CTR) and obstructed kidney (UUO) of AMPKα1 knockout mice (Aα1$^{-/-}$) and their corresponding wild-type mice (Aα1$^{+/+}$) after 3 days (**A**), 7 days (**B**) and 3 weeks (**C**) of UUO. Arithmetic means ± SEM (n=7-9) of normalized AMPKα1 to GAPDH protein ratio in renal tissue of non-obstructed control kidney (CTR) and obstructed kidney (UUO) of wild-type mice (Aα1$^{+/+}$, AMPKα1$^{+/+}$) after 3 days, 7 days and 3 weeks of UUO. *($p<0.05$), **($p<0.01$), ***($p<0.001$) indicates statistically significant differences from control kidney tissues of wild-type mice.

In both, the non-obstructed control kidney tissues and the obstructed kidney tissues of AMPKα1$^{-/-}$ mice, the AMPKα2 isoform expression tended to be higher than in respective

kidney tissues of AMPKα1$^{+/+}$ mice. The up-regulation reached statistical significance in the non-obstructed control kidney tissues at 3 days of UUO and in the obstructed kidney tissues at 7 days of UUO respectively (**Fig. 10A and B**).

In contrast to the regulation of the AMPKα1 isoform, AMPKα2 isoform protein expression was not significantly modified in the obstructed kidney tissues as compared to non-obstructed control kidney tissues of both AMPKα1$^{+/+}$ mice and AMPKα1$^{-/-}$ mice following 3 days of UUO (**Fig. 10A**), but was significantly down-regulated following 7 days (**Fig. 10B**) and 3 weeks (**Fig. 10C**) of UUO. Thus, AMPKα2 protein expression was down-regulated at middle and late time points of UUO. Taken together, UUO caused an isoform shift in renal tissue, up-regulating the AMPKα1 isoform and down-regulating the AMPKα2 isoform.

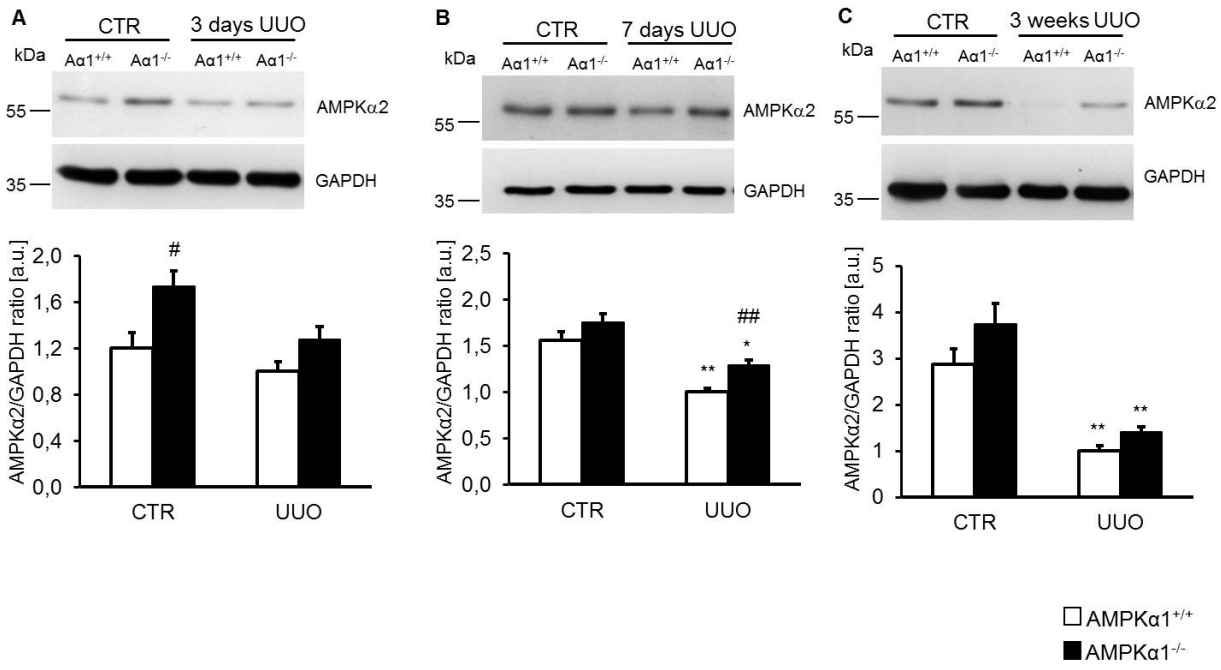

Figure 10: Renal AMPKα2 protein expression in AMPKα1$^{+/+}$ and AMPKα1$^{-/-}$ mice following unilateral ureteral obstruction. Representative original Western blots and arithmetic means ± SEM (n=7-9) of normalized AMPKα2 to GAPDH protein ratio in renal tissue of non-obstructed control kidney (CTR) and obstructed kidney (UUO) of AMPKα1 knockout mice (Aα1$^{-/-}$, AMPKα1$^{-/-}$, black bars) and their corresponding wild-type mice (Aα1$^{+/+}$**,** AMPKα1$^{+/+}$, white bars) after 3 days (**A**), 7 days (**B**) and 3 weeks (**C**) of UUO. *($p<0.05$), **($p<0.01$) indicates statistically significant difference from control kidney tissues of

respective mice; #($p<0.05$), ##($p<0.01$), indicates statistically significant differences from respective kidney tissues of wild-type mice.

4.1.2 Activity of AMPK following obstructive injury

The next experiments determined whether the changes in the catalytic AMPKα isoforms expression affected the total activity of AMPK following UUO. As shown by Western blotting, the abundance of phosphorylated AMPKα at Thr^{172}, an activation site of AMPK, was low in the non-obstructed control kidney tissues of both genotypes. After 3 days and 7 days of UUO, the phosphorylated AMPKα at Thr^{172} was significantly up-regulated in the obstructed kidney tissues as compared to the non-obstructed control kidney tissues of AMPKα$1^{+/+}$ mice (**Fig. 11A** and **B**). The UUO-induced phosphorylation of AMPKα at Thr^{172} was significantly inhibited in the AMPKα$1^{-/-}$ mice (**Fig. 11A** and **B**). After 3 weeks of UUO, the phosphorylation of AMPKα was not significantly modified in the obstructed kidney tissue as compared to the non-obstructed kidney tissue of AMPKα$1^{+/+}$ mice, despite a strong tendency towards down-regulation of the phosphorylation status (**Fig. 11C**).

UUO did not significantly change the expression of total AMPKα protein in the obstructed kidney tissue than in the non-obstructed kidney tissue of AMPKα$1^{+/+}$ mice (**Fig. 11**). However, the total AMPKα protein expression was significantly decreased in the obstructed kidney tissue of AMPKα$1^{-/-}$ mice as compared to AMPKα$1^{+/+}$ mice.

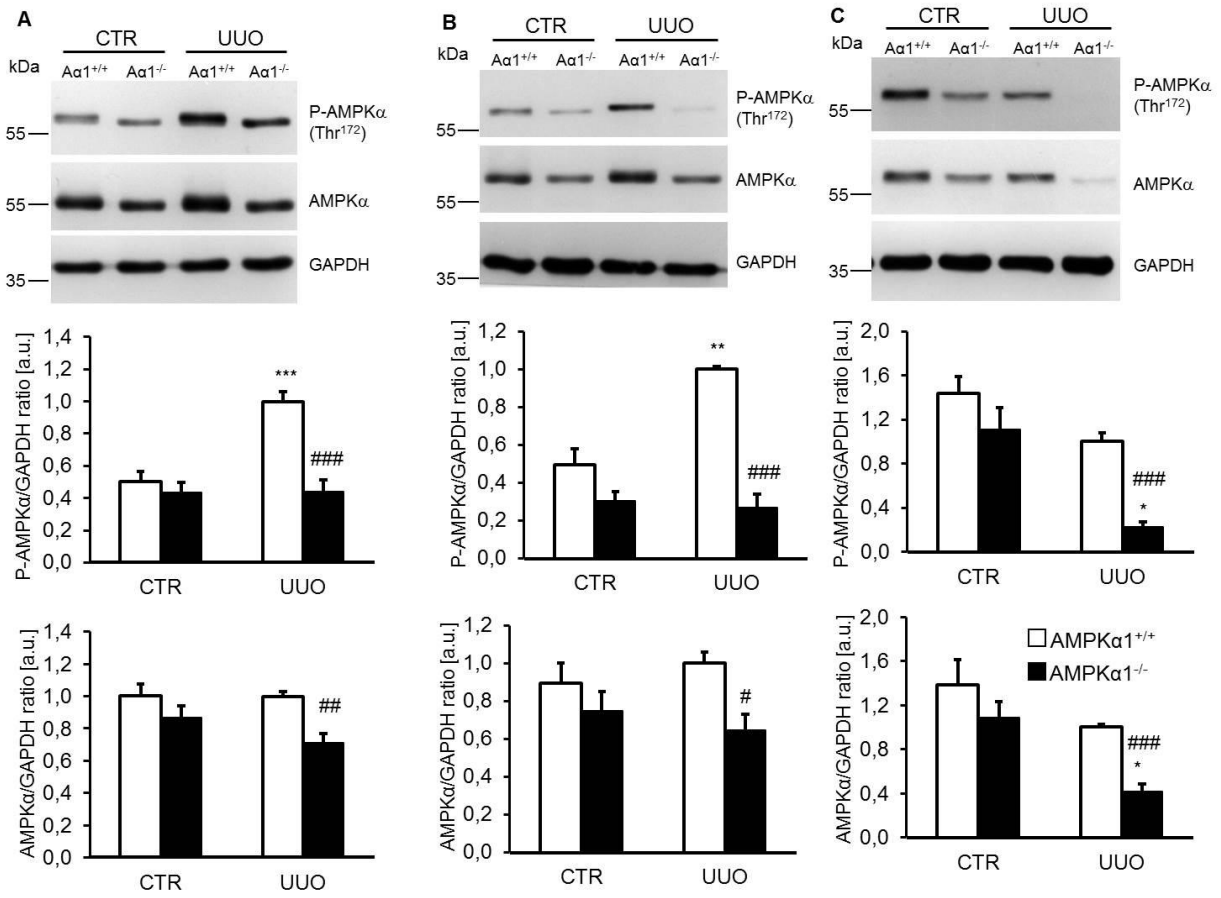

Figure 11: Effects of UUO on the phosphorylation status of AMPKα at Thr^{172}. Representative original Western blots and arithmetic means ± SEM (n=7-9) of normalized phospho-AMPKα (Thr^{172}) to GAPDH and total AMPKα to GAPDH protein ratio in renal tissue of non-obstructed control kidney (CTR) and obstructed kidney (UUO) of AMPKα1 knockout mice (Aα1$^{-/-}$, AMPKα1$^{-/-}$, black bars) and their corresponding wild-type mice (Aα1$^{+/+}$, AMPKα1$^{+/+}$, white bars) after 3 days (A), 7 days (B) and 3 weeks (C) of UUO. *($p<0.05$), **($p<0.01$), ***($p<0.001$) indicates statistically significant differences from control kidney tissues of respective mice; #($p<0.05$), ##($p<0.01$), ###($p<0.001$) indicates statistically significant differences from respective kidney tissues of wild-type mice.

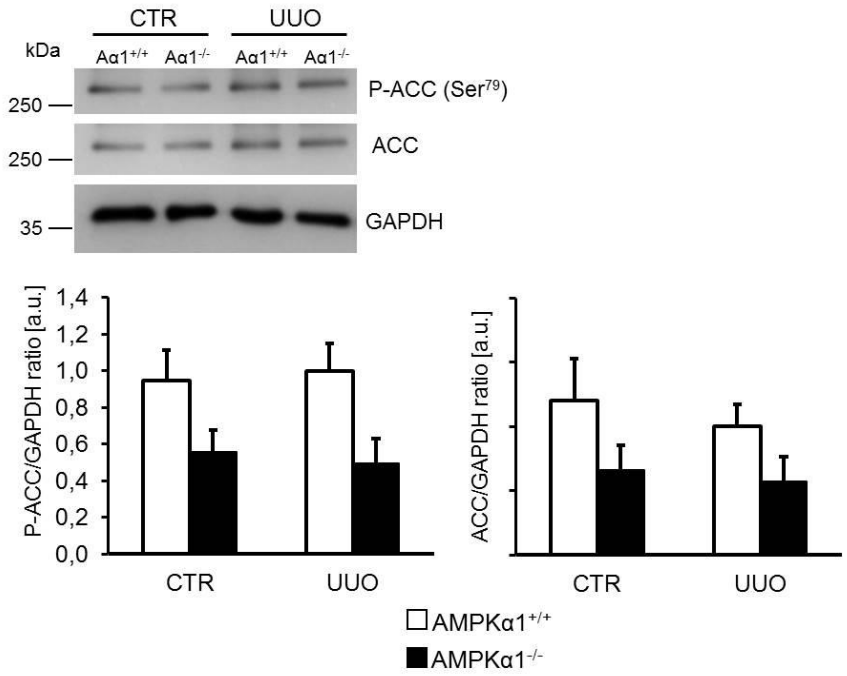

Figure 12: Renal ACC phosphorylation in AMPKα1$^{+/+}$ and AMPKα1$^{-/-}$ mice following unilateral ureteral obstruction. Representative original western blots and arithmetic means ± SEM (n=9) of normalized phospho-ACC (Ser^{79}) to GAPDH and total ACC to GAPDH protein ratio in renal tissue of non-obstructed control kidney (CTR) and obstructed kidney (UUO) of AMPKα1 knockout mice (Aα1$^{-/-}$, AMPKα1$^{-/-}$, black bars) and their corresponding wild-type mice (Aα1$^{+/+}$, AMPKα1$^{+/+}$, white bars,) after 7 days of UUO.

To further explore whether UUO up-regulates AMPKα activity, Western blotting was carried out to verify the phosphorylation status of Acetyl-CoA carboxylase (ACC), a downstream target protein of AMPK. As described in **Figure. 12**, the abundance of phosphorylated ACC and total ACC protein was not significantly changed after 7 days of UUO in the obstructed kidney tissue than in the non-obstructed kidney tissue of both genotypes. Both, phosphorylated and total ACC protein tended to be down-regulated in the AMPKα1$^{-/-}$ kidney tissues than in AMPKα1$^{+/+}$ kidney tissues, but not statistical significance. These data together indicate that UUO increased the phosphorylation of AMPKα without having profound effects on ACC protein phosphorylation.

4.1.3 AMPKα1 promotes myofibroblast activation

A further series of experiments were employed to elucidate whether AMPKα1 isoform regulates the myofibroblast formation following obstructive injury. After UUO, the expression of α-smooth muscle actin (α-SMA) was measured by using quantitative RT-PCR, immunohistochemistry and Western blotting.

As determined by quantitative RT-PCR, the mRNA levels of α-smooth muscle actin (*α-Sma*) at 7 days post-UUO were significantly up-regulated in obstructed kidney tissue as compared to non-obstructed kidney tissue of AMPKα1$^{+/+}$ mice, effects abolished by AMPKα1 deficiency (**Fig. 13**).

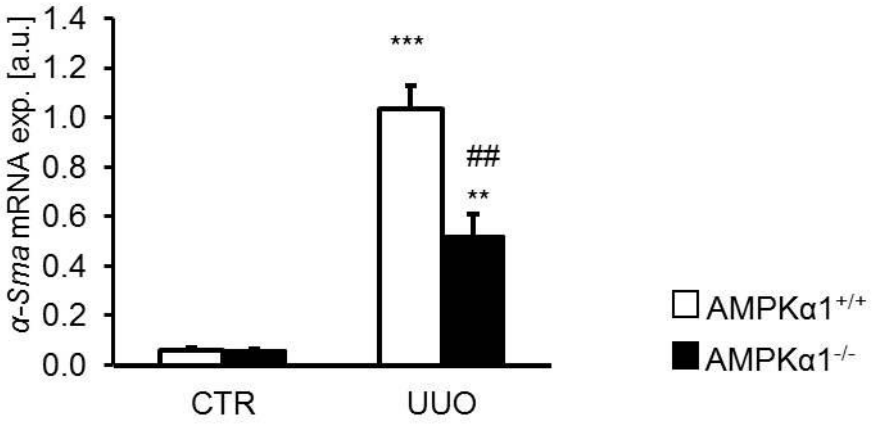

Figure 13: AMPKα1 up-regulates transcript levels of α-smooth muscle actin following unilateral ureteral obstruction. Arithmetic means ± SEM (n=9) of mRNA expression level encoding *α-Sma* in renal tissue of non-obstructed control kidney (CTR) and obstructed kidney (UUO) of AMPKα1 knockout mice (black bars) and their corresponding wild-type mice (white bars) after 7 days of UUO. **($p<0.01$), ***($p<0.001$) indicates statistically significant differences from control kidney tissues of respective mice; ##($p<0.01$) indicates statistically significant differences from respective kidney tissues of wild-type mice.

Moreover, immunohistochemical staining showed that the deposition of α-SMA is markedly lower in the obstructed kidneys of AMPKα1$^{-/-}$ mice than of AMPKα1$^{+/+}$ mice following 7 days of UUO (**Fig. 14**).

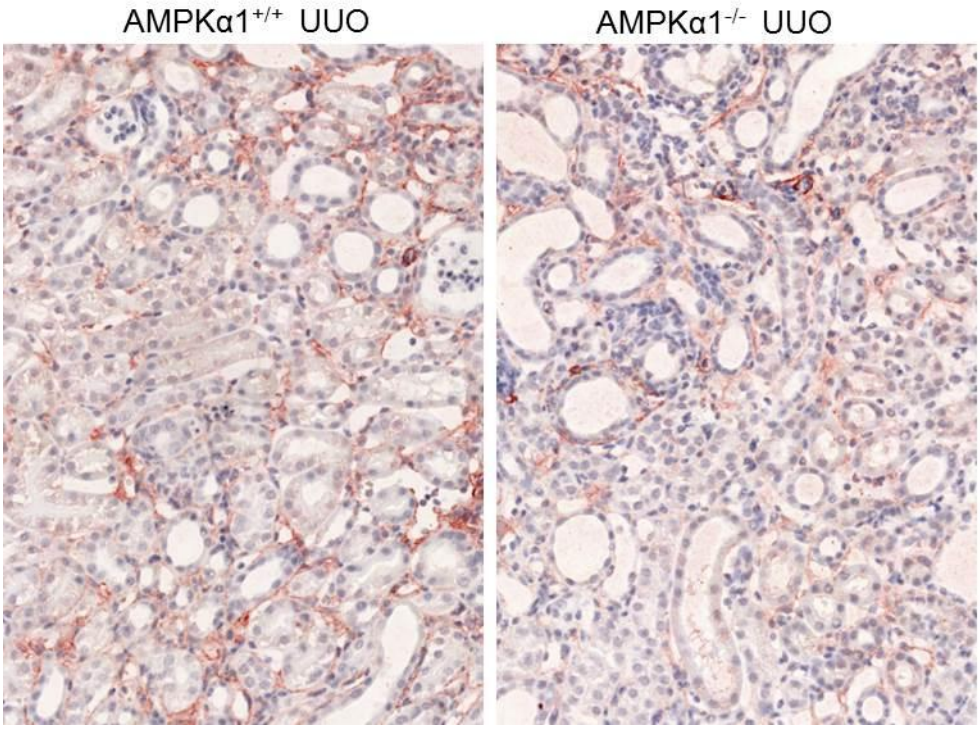

Figure 14: Effects of AMPKα1 deficiency on α-SMA deposition. Representative original histological images of α-smooth muscle actin protein abundance on kidney sections from AMPKα1 knockout mice (AMPKα1$^{-/-}$) and respective wild-type mice (AMPKα1$^{+/+}$) after 7 days of UUO (magnification 200x).

As shown by Western Blotting, UUO induced a significant increase of α-smooth muscle actin (α-SMA) protein expression in the obstructed kidneys than in the non-obstructed control kidneys of the AMPKα1$^{+/+}$ mice. No significant differences on α-SMA protein expression in the obstructed kidney tissues between the AMPKα1$^{-/-}$ mice and the AMPKα1$^{+/+}$ mice were observed following 3 days of UUO (**Fig. 15A**). As illustrated in **Figure.15B and C**, the increased protein expression of α-SMA in the obstructed kidney tissues was significantly blunted by AMPKα1 deficiency following 7 days and 3 weeks of UUO. Taken together, these data suggest that AMPKα1 is responsible for fibroblast activation in response to obstructed injury.

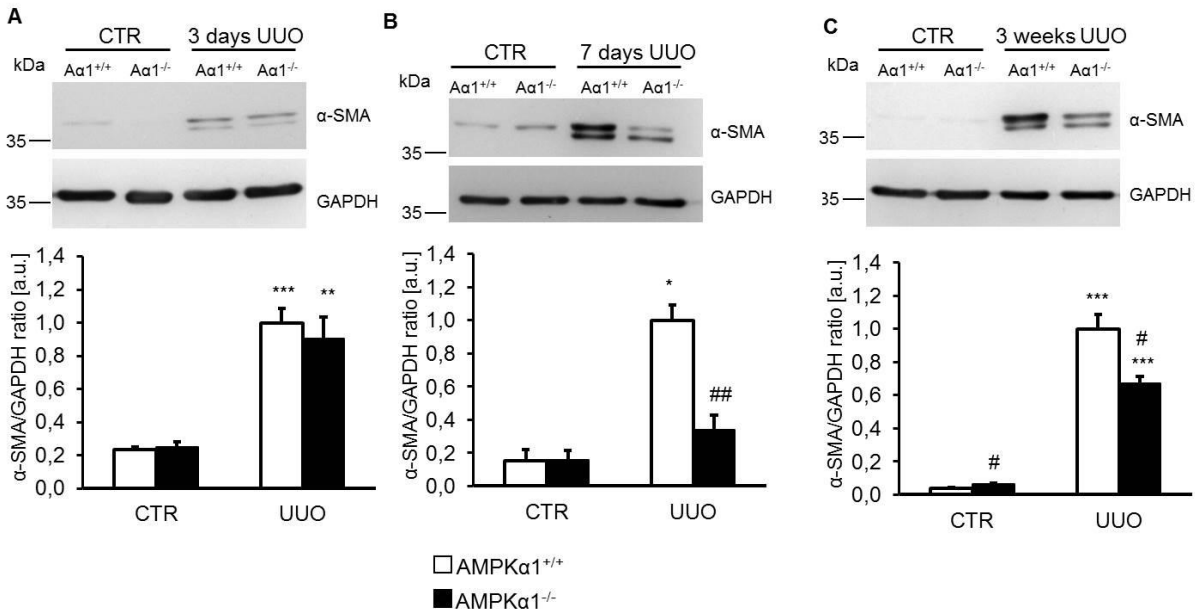

Figure 15: AMPKα1 deficiency inhibits α-smooth muscle actin expression following unilateral ureteral obstruction. Representative original Western blots and arithmetic means ± SEM (n=7-9) of normalized α-smooth muscle actin (α-SMA) to GAPDH protein ratio in renal tissue of non-obstructed control kidney (CTR) and obstructed kidney (UUO) of AMPKα1 knockout mice ($A\alpha1^{-/-}$, $AMPK\alpha1^{-/-}$, black bars) and their corresponding wild-type mice ($A\alpha1^{+/+}$, $AMPK\alpha1^{+/+}$, white bars) after 3 days (**A**) , 7 days (**B**) and 3 weeks (**C**) of UUO.*($p<0.05$), **($p<0.01$), ***($p<0.001$) indicates statistically significant differences from control kidney tissues of respective mice; #($p<0.05$), ##($p<0.01$) indicates statistically significant differences from respective kidney tissues of wild-type mice.

4.1.4 Effects of AMPKα1 deficiency on collagen expression

In the following steps, was examined whether AMPKα1 modifies collagen synthesis. As illustrated in **Figure 16,** following 7 days of UUO, the transcript levels of *Col1a1* and *Col3a1* were significantly increased in obstructed kidney tissues as compared to non-obstructed control kidney tissue of both $AMPK\alpha1^{-/-}$ mice and $AMPK\alpha1^{+/+}$ mice, an effect significantly blunted by AMPKα1 deficiency (**Fig. 16B and C**).

As shown by Western Blotting, Collagen type I protein was significantly less increased in the obstructed kidneys of $AMPK\alpha1^{-/-}$ mice than of $AMPK\alpha1^{+/+}$ mice (**Fig. 16A**). As revealed by

histological analysis, no differences in Collagen type I deposition score were observed in obstructed kidney tissues between AMPKα1$^{-/-}$ mice and AMPKα1$^{+/+}$ mice (**Fig. 17**). These observations suggest that AMPKα1 has moderate effects on collagen deposition following obstructive injury.

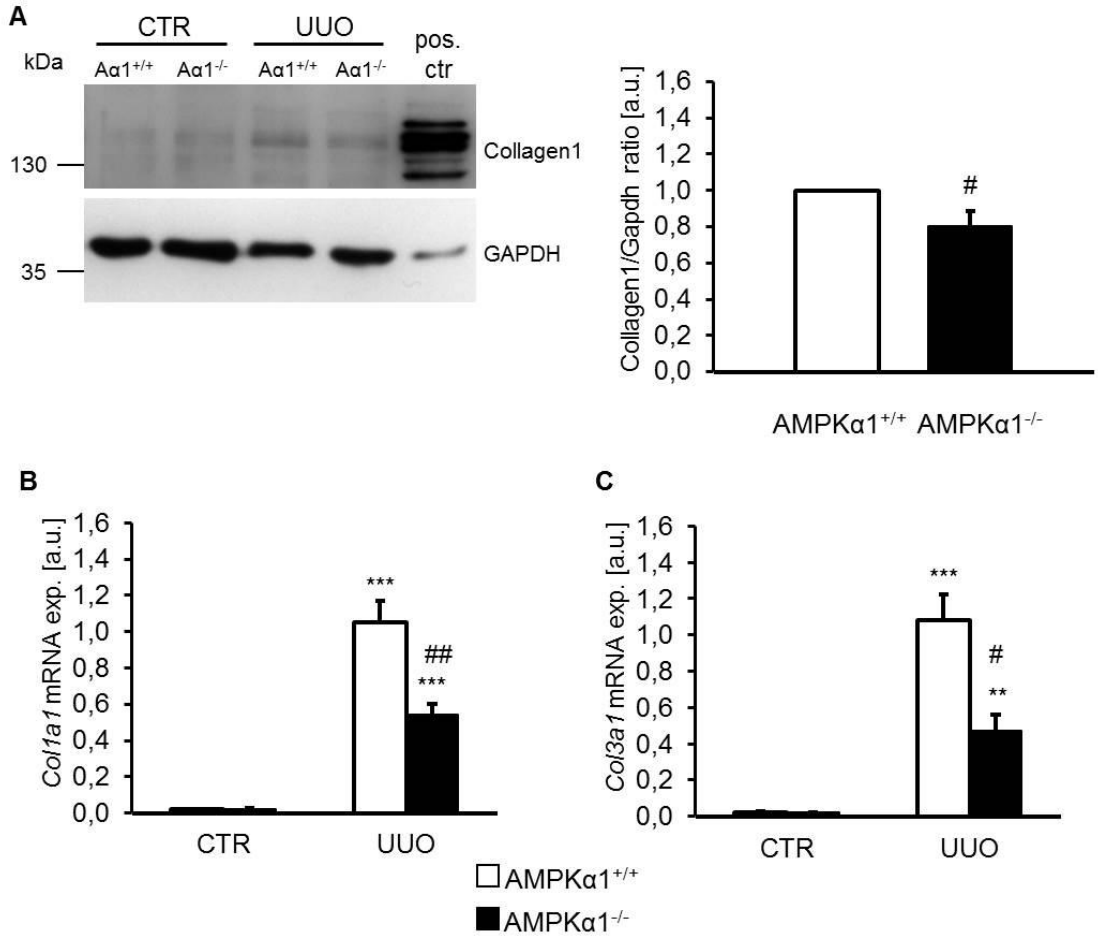

Figure 16: AMPKα1 deficiency impairs collagen expression following unilateral ureteral obstruction. (A) Representative original Western blots and arithmetic means ± SEM (n=9) of normalized Collagen type 1 to GAPDH protein ratio in renal tissue of obstructed kidney of AMPKα1 knockout mice (Aα1$^{-/-}$, AMPKα1$^{-/-}$, black bar) and their corresponding wild-type mice (Aα1$^{+/+}$, AMPKα1$^{+/+}$, white bar) after 7 days UUO. Harvested murine tendon tissues were used as positive controls. Arithmetic means ± SEM (n=9) of mRNA expression level encoding collagen type I (*Col1a1*, **B**) and collagen type III (*Col3a1*, **C**) in renal tissue of non-obstructed control kidney (CTR) and obstructed kidney (UUO) of AMPKα1 knockout mice (black bars) and their corresponding wild-type mice (white bars) after 7 days of UUO. **(p<0.01), ***(p<0.001) indicates statistically significant differences from control kidney tissues of respective mice; #(p<0.05), ##(p<0.01), indicates statistically significant differences from respective kidney tissues of wild-type mice.

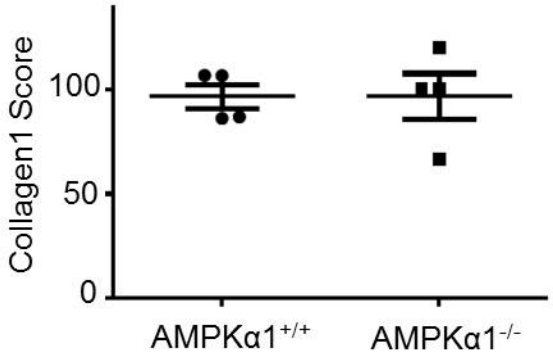

Figure 17. Effects of AMPKα1 deficiency on collagen deposition. Semi-qualitative analysis of kidney sections for Collagen type I/III deposition of obstructed kidneys from AMPKα1 knockout mice ($AMPK\alpha1^{-/-}$) and respective wild-type mice ($AMPK\alpha1^{+/+}$) after 7 days of UUO.

4.1.5 Inhibition of TAK1 expression in AMPKα1 deficiency

A further series of experiments were made to identify downstream mediators of AMPKα1 in the effects following UUO. To this end, the TGF-β expression was examined by Western blotting. The protein abundance of TGF-β precursor was significantly up-regulated in obstructed kidney tissue as compared to non-obstructed kidney tissues of both genotypes (**Fig. 18**). No significant effects of AMPKα1 deficiency were observed.

Furthermore, 7 days of UUO significantly increased the protein abundance of phosphorylated and total Smad2 in the obstructed kidney tissue as compared to non-obstructed kidney tissues of both $AMPK\alpha1^{-/-}$ mice and $AMPK\alpha1^{+/+}$ mice, effects not significantly different between the genotypes (**Fig. 19**).

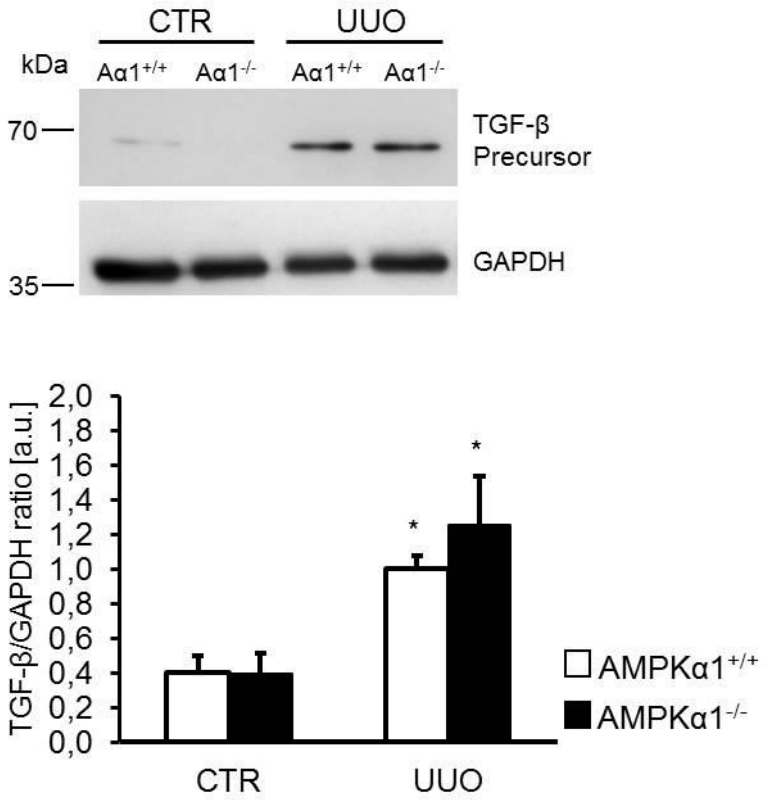

Figure 18: AMPKα1 deficiency does not have profound effect on TGF-β expression following unilateral ureteral obstruction. Representative original Western blots and arithmetic means ± SEM (n= 9) of normalized TGF-β precursor to GAPDH protein ratio in renal tissue of non-obstructed control kidney (CTR) and obstructed kidney (UUO) of AMPKα1 knockout mice ($A\alpha1^{-/-}$, $AMPK\alpha1^{-/-}$, black bars) and their corresponding wild-type mice ($A\alpha1^{+/+}$, $AMPK\alpha1^{+/+}$, white bars) after 7 days of UUO. *($p<0.05$) indicates statistically significant differences from control kidney tissues of respective mice.

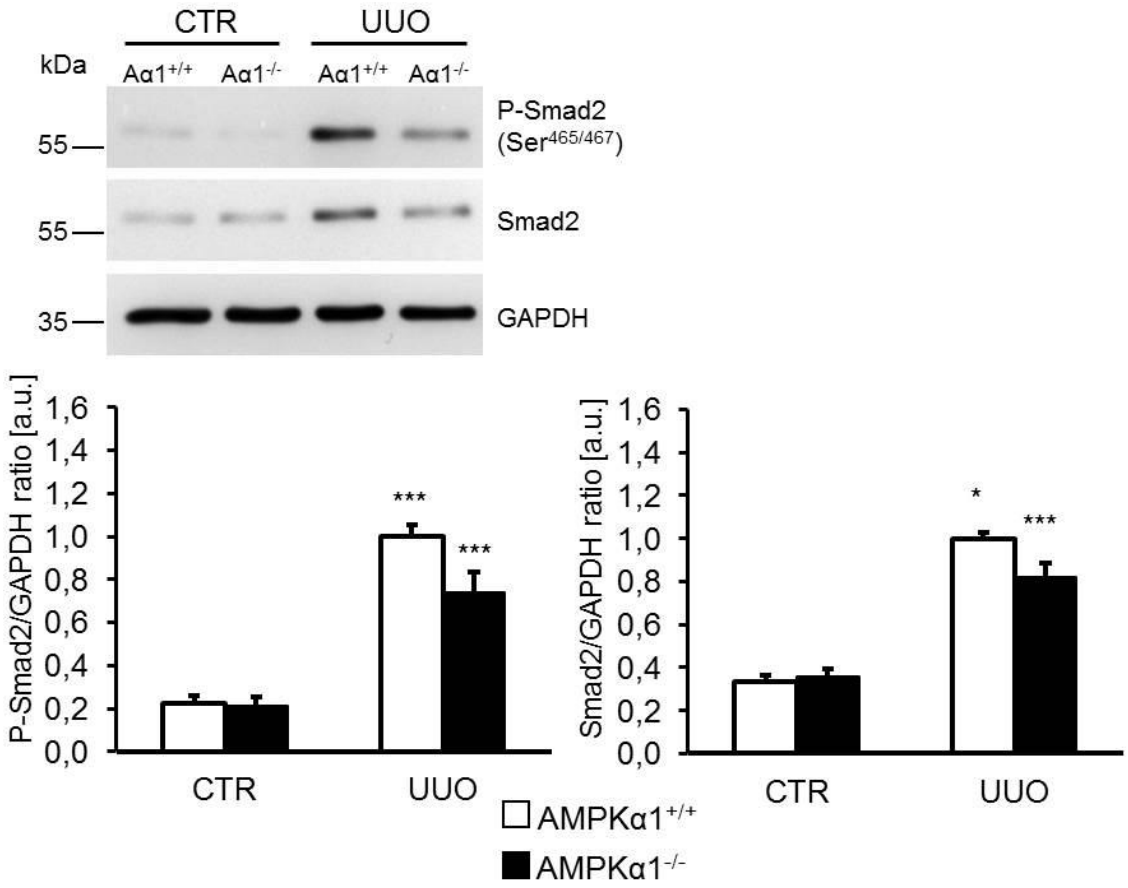

Figure 19: AMPKα1 deficiency does not have profound effect on pSmad2 expression following unilateral ureteral obstruction. Representative original western blots and arithmetic means ± SEM (n= 9) of normalized phospho-Smad2 ($Ser^{465/467}$) to GAPDH protein ratio and total Smad2 to GAPDH protein ratio in renal tissue of non-obstructed control kidney (CTR) and obstructed kidney (UUO) of AMPKα1 knockout mice ($Aα1^{-/-}$, $AMPKα1^{-/-}$, black bars) and their corresponding wild-type mice ($Aα1^{+/+}$, $AMPKα1^{+/+}$, white bars) after 7 days of UUO. *($p<0.05$), ***($p<0.001$) indicates statistically significant differences from control kidney tissues of respective mice.

Next, the expression and phosphorylation of TGF-ß-activated kinase 1 (TAK1) protein was analysed. As shown by Western Blotting, the protein abundance of both phosphorylated and total TAK1 were significantly up-regulated in the obstructed kidney tissues than in non-obstructed control kidney of both $AMPKα1^{-/-}$ mice and $AMPKα1^{+/+}$ mice following 7 days of

UUO, effects significantly blunted by AMPKα1 deficiency (**Fig. 20**). Thus, the results indicate that AMPKα1 regulates renal TAK1 protein in obstructive injury induced by UUO.

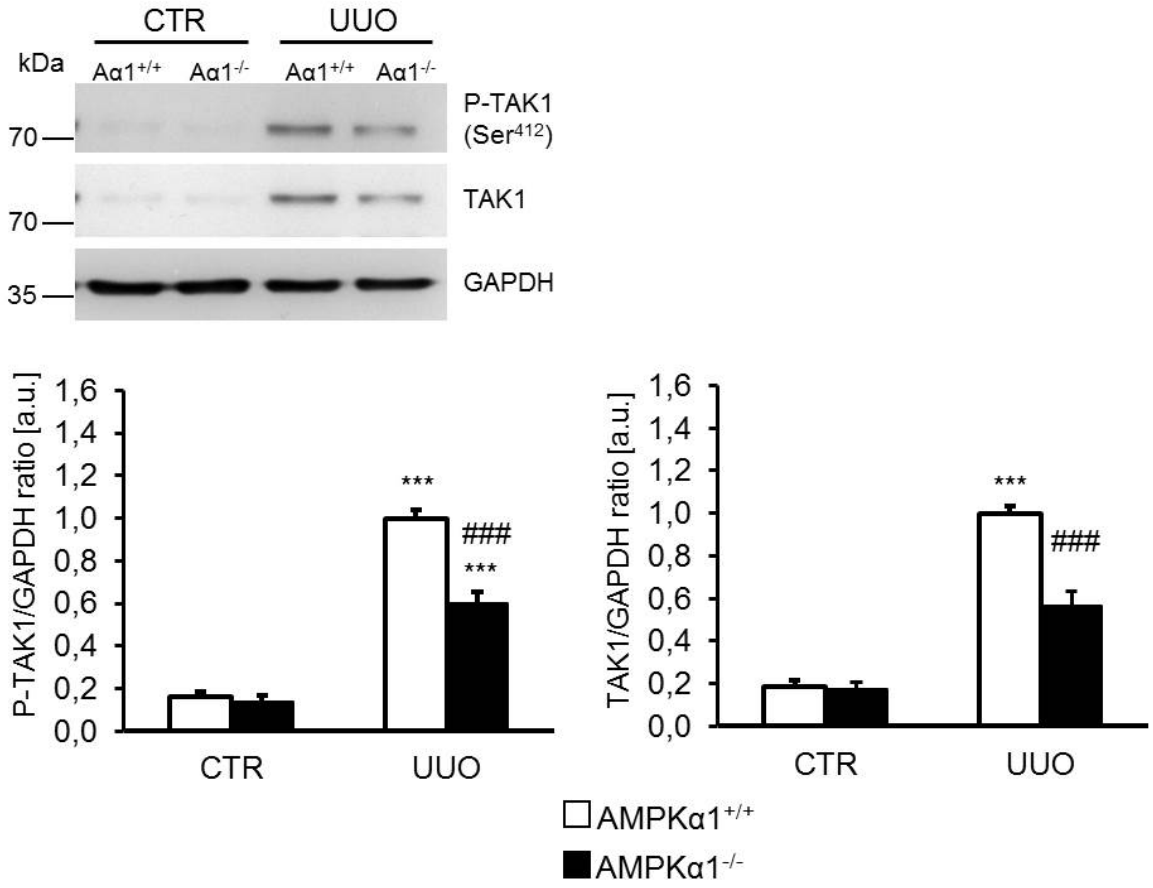

Figure 20: AMPKα1 deficiency inhibits TGF-β-activated protein kinase 1 (TAK1) activation following unilateral ureteral obstruction. Representative original Western blots and arithmetic means ± SEM (n= 9) of normalized phospho-TAK1 (Ser^{412}) to GAPDH protein ratio and total TAK1 to GAPDH protein ratio in renal tissue of non-obstructed control kidney (CTR) and obstructed kidney (UUO) of AMPKα1 knockout mice ($Aα1^{-/-}$, $AMPKα1^{-/-}$, black bars) and their corresponding wild-type mice ($Aα1^{+/+}$, $AMPKα1^{+/+}$, white bars) after 7 days of UUO. *($p<0.05$), **($p<0.01$), ***($p<0.001$) indicates statistically significant differences from control kidney tissues of respective mice; ###($p<0.001$) indicates statistically significant differences from respective kidney tissues of wild-type mice.

4.1.6 AMPKα1 deficiency inhibits TAK1 target gene expression after UUO

TAK1-downstream target genes are: cytokine interleukin 6 (*Il6),* the transcription factor *c-Fos, Snail* and plasminogen activator inhibitor 1 (*Pai-1*). Therefore the renal mRNA expression of these target genes following 7 days of UUO was analysed by quantitative RT-PCR. As a result, UUO increased significantly the mRNA expression of *Il6, c-Fos, Pai1* and *Snai1* in the obstructed renal tissue than in non-obstructed renal tissue from both genotypes, effects significantly blunted in the AMPKα1$^{-/-}$ mice than in AMPKα1$^{+/+}$ mice (**Fig. 21A-D)**.

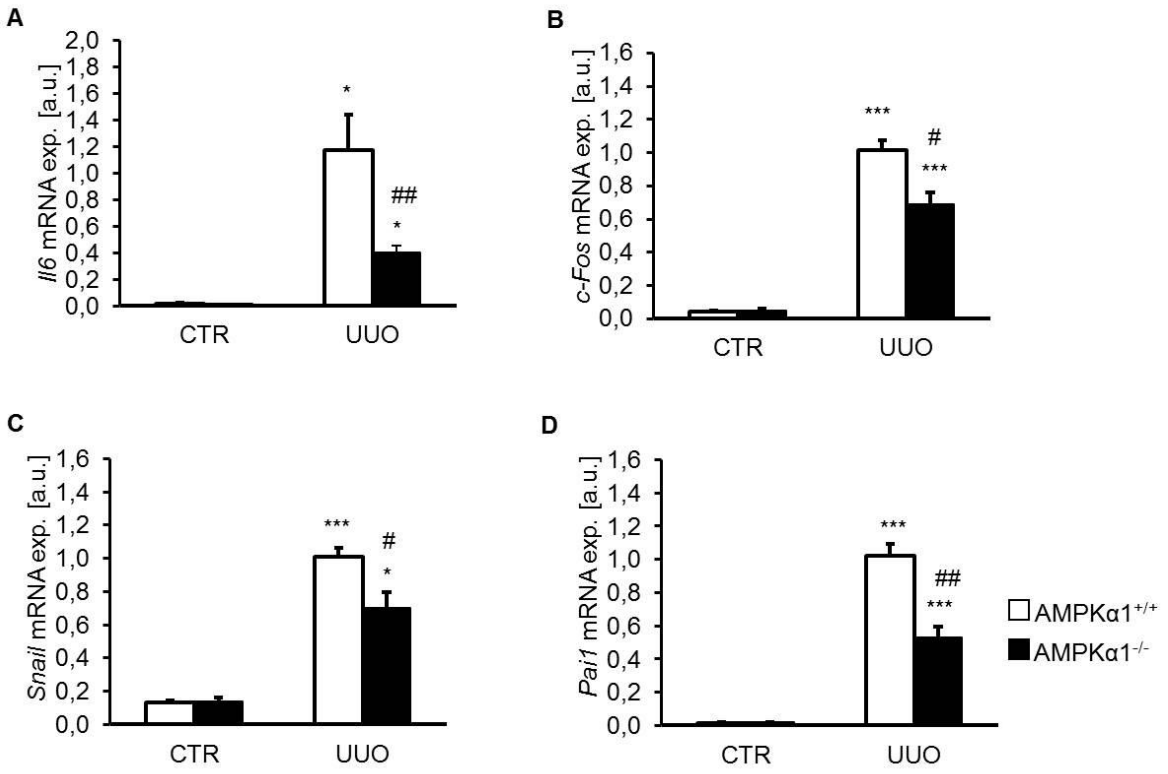

Figure 21: AMPKα1 stimulates TAK1 target genes expression following unilateral ureteral obstruction. Arithmetic means ± SEM (n= 9) of mRNA expression level encoding interleukin 6 (*Il6*, A), *c-Fos* (B), *Snai1* (C) *Pai1* (D) and) in renal tissue of non-obstructed control kidney (CTR) and obstructed kidney (UUO) of AMPKα1 knockout mice (black bars) and their corresponding wild-type mice (white bars) after 7 days of UUO. *($p<0.05$), ***($p<0.001$) indicates statistically significant differences from control kidney tissues of respective mice; #($p<0.05$), ##($p<0.01$) indicates statistically significant differences from respective kidney tissues of wild-type mice.

4.1.7 AMPKα1-sensitive macrophage polarization and pro-fibrotic chemokine production

In the next experiments, it was tested whether AMPKα1 deficiency has any significant role on macrophages polarization and fibrotic chemokine production during obstructive injury. The mRNA expression of *Cd206* (marker for M2 macrophages) and of *Cxcl16* (chemokine associated with myeloid fibroblast formation) was determined by quantitative RT-PCR. As shown in **Figure 22 A and B**, the mRNA levels of *Cd206* and *Cxcl16* were significantly increased in the obstructed kidney tissues as compared to non-obstructed kidney tissues from both AMPKα1$^{+/+}$ mice or AMPKα1$^{-/-}$ mice. The effects were significantly attenuated by AMPKα1 deficiency.

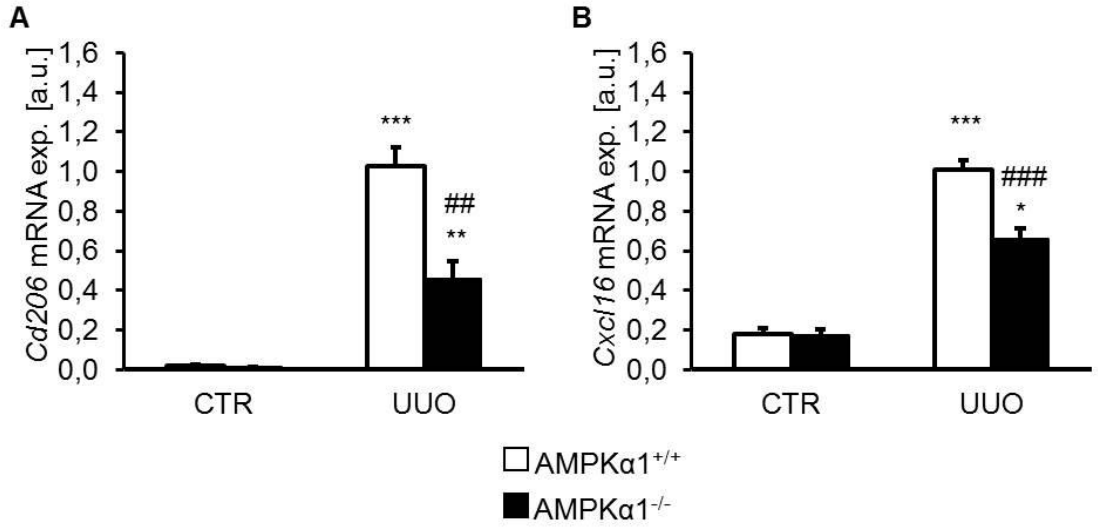

Figure 22: Deficiency of AMPKα1 attenuates M2 macrophage polarization and pro-fibrotic chemokine production following unilateral ureteral obstruction. Arithmetic means ± SEM (n= 9) of mRNA expression level encoding *Cd206* (**A**) and *Cxcl16* (**B**) in renal tissue of non-obstructed control kidney (CTR) and obstructed kidney (UUO) of AMPKα1 knockout mice (black bars) and their corresponding wild-type mice (white bars) after 7 days of UUO. *($p<0.05$), **($p<0.01$), ***($p<0.001$) indicates statistically significant differences from control kidney tissues of respective mice; ##($p<0.01$), ###($p<0.001$) indicates statistically significant differences from respective kidney tissues of wild-type mice.

4.1.8 AMPKα1 deficiency augments apoptosis and tubular dilation after UUO

As shown by PAS staining and morphometric analysis, following 7 days of obstructive injury, the percentage of damaged tubuli was increased in the obstructed kidney tissue of AMPKα1$^{-/-}$ mice as compared to AMPKα1$^{+/+}$ mice **(Fig. 23A)**. Moreover, as shown by TUNEL assay, there was a tendency towards higher number of TUNEL positive cells in the obstructed kidney tissue of AMPKα1$^{-/-}$ mice than of AMPKα1$^{+/+}$ mice (**Fig. 23B**).

This increased apoptosis on day 7 after UUO was further confirmed by determining the ratio of renal *Bax* and *Bcl2* transcript levels, as indicator of apoptosis. Accordingly, the ratio of renal *Bax/Bcl2* mRNA levels was significantly higher in the obstructed kidney tissue of AMPKα1$^{-/-}$ mice as compared to AMPKα1$^{+/+}$ mice (**Fig. 24**). In conclusion, the AMPKα1 deficient mice have higher apoptosis in renal tissue following obstructive injury.

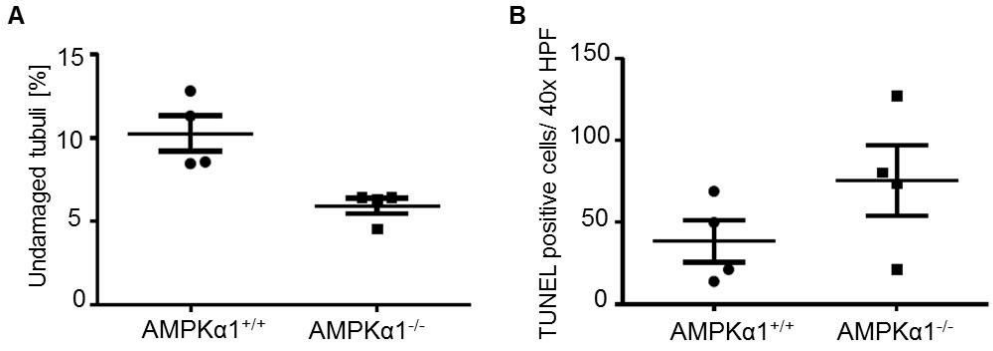

Figure 23: AMPKα1 deficiency aggravates renal tubulointerstitial injury and apoptosis following unilateral ureteral obstruction. **(A)** Percentage of undamaged tubules in sections of obstructed kidneys from AMPKα1 knockout mice (AMPKα1$^{-/-}$) and respective wild-type mice (AMPKα1$^{+/+}$) after 7 days of UUO. (B) TUNEL positive cells number/40x HPF in sections of obstructed kidneys from AMPKα1 knockout mice (AMPKα1$^{-/-}$) and respective wild-type mice (AMPKα1$^{+/+}$) after 7 days of UUO.

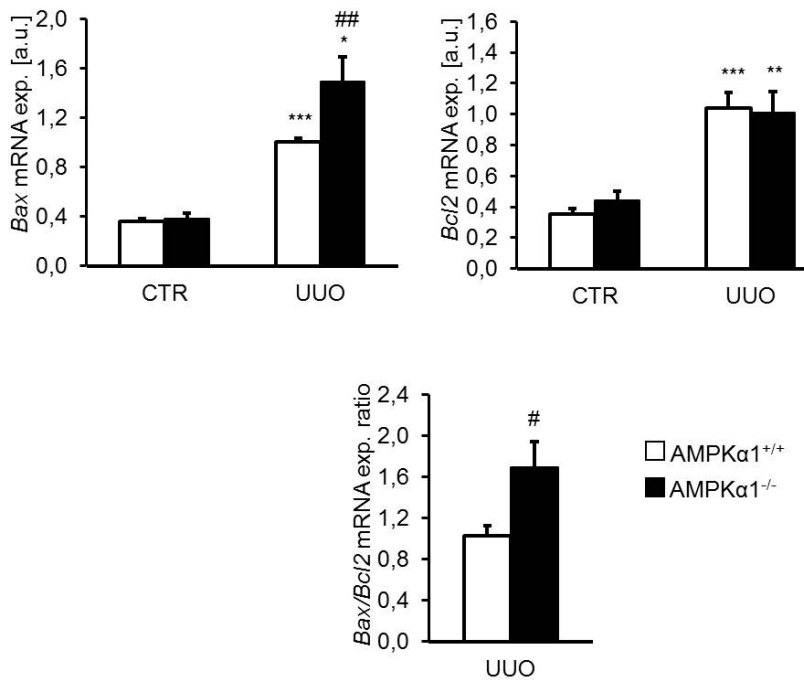

Figure 24. AMPKα1 deficiency increased *Bax/Bcl2* relative mRNA expression ratio following unilateral ureteral obstruction. Arithmetic means ± SEM (n= 9) of mRNA expression level encoding *Bax* and *Bcl2* in renal tissue of non-obstructed control kidney (CTR) and obstructed kidney (UUO) of AMPKα1 knockout mice (black bars) and their corresponding wild-type mice (white bars) after 7 days of UUO. Arithmetic means ± SEM (n= 9) of mRNA expression *Bax/Bcl2* ratio in renal tissue of obstructed kidney (UUO) of AMPKα1 knockout mice ($AMPK\alpha1^{-/-}$, black bar) and their corresponding wild-type mice ($AMPK\alpha1^{+/+}$, white bar) after 7 days of UUO. *($p<0.05$), **($p<0.01$), ***($p<0.001$) indicates statistically significant differences from control kidney tissues of respective mice; #($p<0.05$), ##($p<0.01$) indicates statistically significant differences from respective kidney tissues of wild-type mice.

4.2. AMPKα1-sensitive renal effects of angiotensin II

Angiotensin II (ANG II) regulates inflammatory processes during renal injury. The present study was performed to elucidate the role of AMPKα1 isoform in the pro-inflammatory and pro-fibrotic renal effects of angiotensin II. To this end, ANG II was infused for 2 weeks by subcutaneous implantation of osmotic minipumps in $AMPK\alpha1^{-/-}$ mice and $AMPK\alpha1^{+/+}$ mice. After 2 weeks of treatment, animals were sacrificed for further experiments.

4.2.1 Renal AMPKα isoform expression after angiotensin II treatment

As shown in **Figure 25A,** AMPKα1 isoform was expressed in renal tissue of AMPKα1$^{+/+}$ mice but not of AMPKα1$^{-/-}$ mice. AMPKα1 protein abundance was slightly but significantly increased in kidney tissues of ANG II treated AMPKα1$^{+/+}$ mice as compared to control treated AMPKα1$^{+/+}$ mice (**Fig. 25A**).

Furthermore, following ANG II treatment, the protein expression of AMPKα2 isoform was not significantly modified in renal tissues of both AMPKα1$^{+/+}$ mice and AMPKα1$^{-/-}$ mice (**Fig 25B**). However, the protein expression of AMPKα2 tended to be higher in renal tissue of AMPKα1$^{-/-}$ mice as compared to AMPKα1$^{+/+}$ mice in both ANG II treated and control treated mice, an effect reaching statistical significance following ANG II treatment.

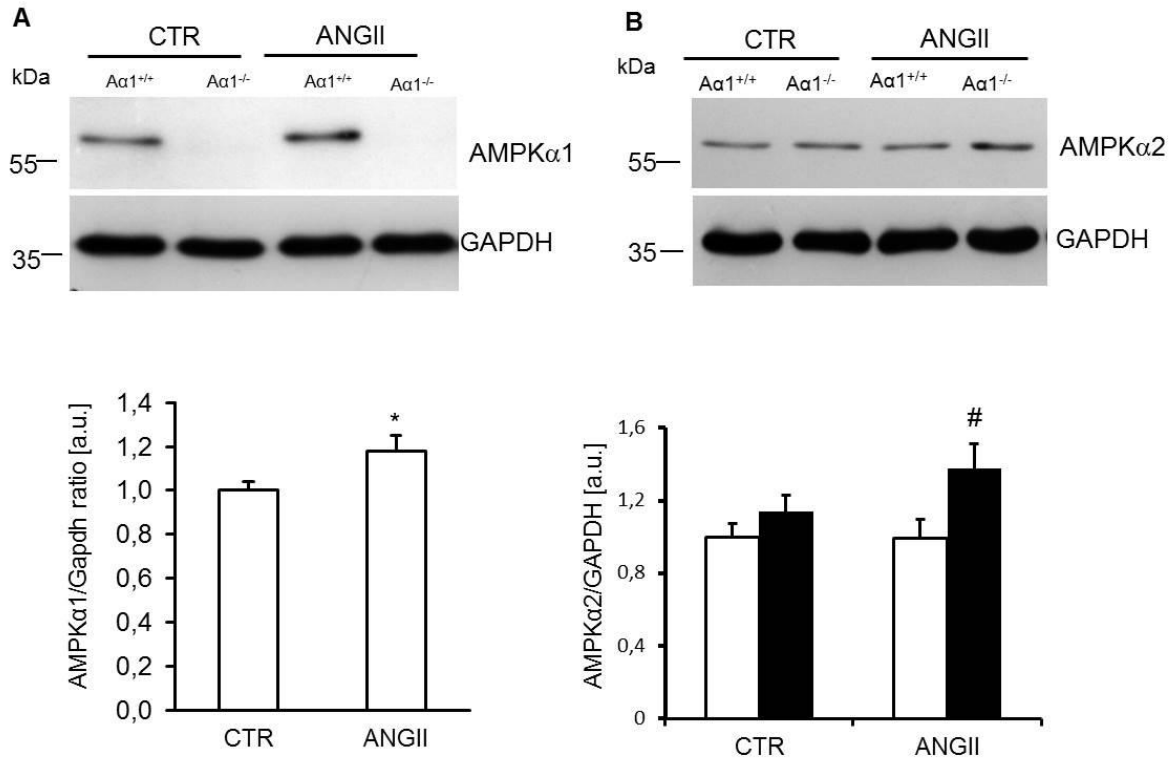

Figure 25: Expression of AMPKα1 and AMPKα2 isoform following angiotensin II infusion. Representative original Western blots and arithmetic means ± SEM (n = 10-12) of normalized AMPKα1 to GAPDH (A), AMPKα2 to GAPDH (B) protein ratio in renal tissue of AMPKα1 knockout mice (Aα1$^{-/-}$, AMPKα1$^{-/-}$, black bars) and their corresponding wild-type mice (Aα1$^{+/+}$, AMPKα1$^{+/+}$, white bars) following control (CTR) or angiotensin II (ANGII) infusion. *($p<0.05$) indicates statistically significant

differences from control kidney tissues (CTR) of wild-type mice, # ($p<0.05$) indicates statistically significant differences from respective wild-type mice.

4.2.2 Phosphorylation of AMPKα after angiotensin II infusion

The protein abundance of phosphorylated AMPKα at Thr^{172} in renal tissues was not significantly modified following ANG II treatment in neither AMPKα1$^{-/-}$ mice and AMPKα1$^{+/+}$ mice (**Fig. 26**). The expression of phosphorylated AMPKα was significantly lower in renal tissues from AMPKα1$^{-/-}$ mice than from AMPKα1$^{+/+}$ mice, in both the control treated and the ANG II treated mice. Similarly, ANG II treatment did not significantly modify total AMPKα protein abundance in renal tissues of both genotypes. A tendency towards reduced total AMPKα protein expression in AMPKα1$^{-/-}$ mice than in AMPKα1$^{+/+}$ mice was observed, an effect not reaching statistical significance (**Fig. 26**).

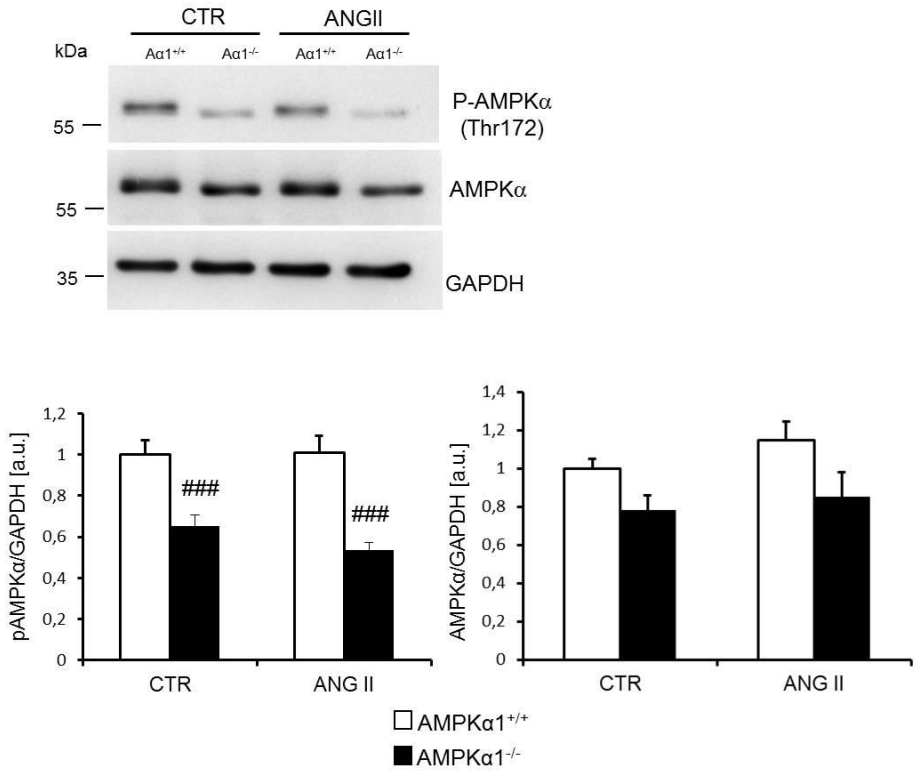

Figure 26: Angiotensin II does not alter the phosphorylation of AMPK. Representative original Western blots and arithmetic means ± SEM (n = 10-12) of normalized pAMPKα to GAPDH, AMPKα to GAPDH protein ratio in renal tissue of AMPKα1 knockout mice (Aα1$^{-/-}$, AMPKα1$^{-/-}$, black bars) and their

corresponding wild-type mice (Aα1$^{+/+}$, AMPKα1$^{+/+}$, white bars) following control (CTR) or angiotensin II (ANGII) infusion. ### ($p<0.001$) indicates statistically significant differences from respective wild-type mice.

4.2.3 Impact of AMPKα1 deficiency on α-SMA expression following angiotensin II

A further series of experiments were performed to elucidate the effects of AMPKα1 isoform deficiency on myofibroblast formation following ANG II treatment. Therefore, the mRNA and protein expression of α-smooth muscle actin (α-SMA) were measured by using quantitative RT-PCR and Western blotting, respectively.

The abundance of mRNA encoding *α-Sma* in renal tissues was not significantly different between control treated AMPKα1$^{+/+}$ mice and AMPKα1$^{-/-}$ mice (**Fig 27B**). ANG II infusion increased significantly the renal *α-Sma* mRNA levels in the AMPKα1$^{+/+}$ mice. This effect was significantly blunted in the AMPKα1$^{-/-}$ mice (**Fig 27B**).

Similar observations were made for α-SMA protein abundance in kidney tissues (**Fig. 27A**). Following angiotensin II treatment, the α-SMA protein abundance was significantly increased in kidney tissues of AMPKα1$^{+/+}$ mice, an effect significantly reduced in the AMPKα1$^{-/-}$ mice.

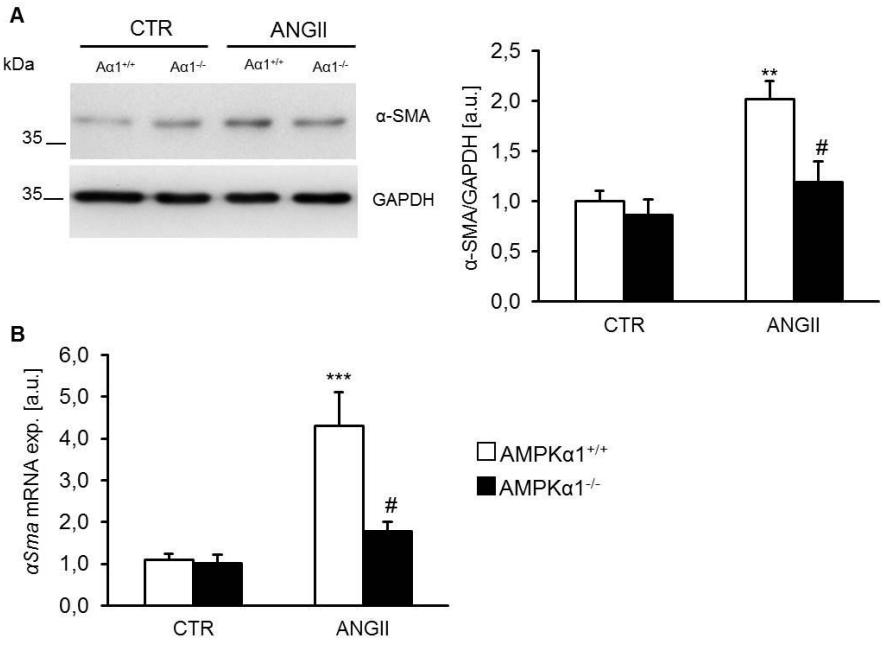

Figure 27: AMPKα1-sensitive up-regulation of transcript levels and protein abundance of α-smooth muscle actin following angiotensin II infusion. (**A**) Representative original Western blots and arithmetic means ± SEM (n = 12) of normalized α-SMA to GAPDH protein ratio in renal tissue of AMPKα1 knockout mice ($A\alpha1^{-/-}$, $AMPK\alpha1^{-/-}$, black bars) and their corresponding wild-type mice ($A\alpha1^{+/+}$, $AMPK\alpha1^{+/+}$, white bars) following control (CTR) or angiotensin II (ANGII) infusion. (**B**) Arithmetic means ± SEM (n = 12) of mRNA expression level encoding α-smooth muscle actin (*α-Sma)* in renal tissue of AMPKα1 knockout mice (black bars) and their corresponding wild-type mice (white bars) following control (CTR) or angiotensin II (ANGII) infusion. ** ($p<0.01$), ***($p<0.001$) indicates statistically significant differences from control, # ($p<0.05$) indicates statistically significant differences from respective wild-type mice.

4.2.4 Lack of AMPKα1 ameliorates TAK1 activation following angiotensin II

In the previous experiments, UUO treatment caused the activation of TGF-ß-activated kinase 1 (TAK1) in an AMPKα1-dependent manner. Therefore, phosphorylated and total TAK1 protein levels were determined in kidney tissues after ANG II treatment. As shown by immunoblotting experiments, the protein abundance of phosphorylated TAK1 at Ser^{412} was not significantly changed between the control treated $AMPK\alpha1^{+/+}$ mice and $AMPK\alpha1^{-/-}$ mice (**Fig. 28**). ANG II treatment caused a significant increase of phosphorylated TAK1 protein in kidney tissues of $AMPK\alpha1^{+/+}$ mice, an effect again significantly blunted in the $AMPK\alpha1^{-/-}$ mice. Accordingly, the protein abundance of phosphorylated TAK1 at Ser412 was significantly higher in $AMPK\alpha1^{+/+}$ mice than in $AMPK\alpha1^{-/-}$ mice following angiotensin II treatment (**Fig. 28**).

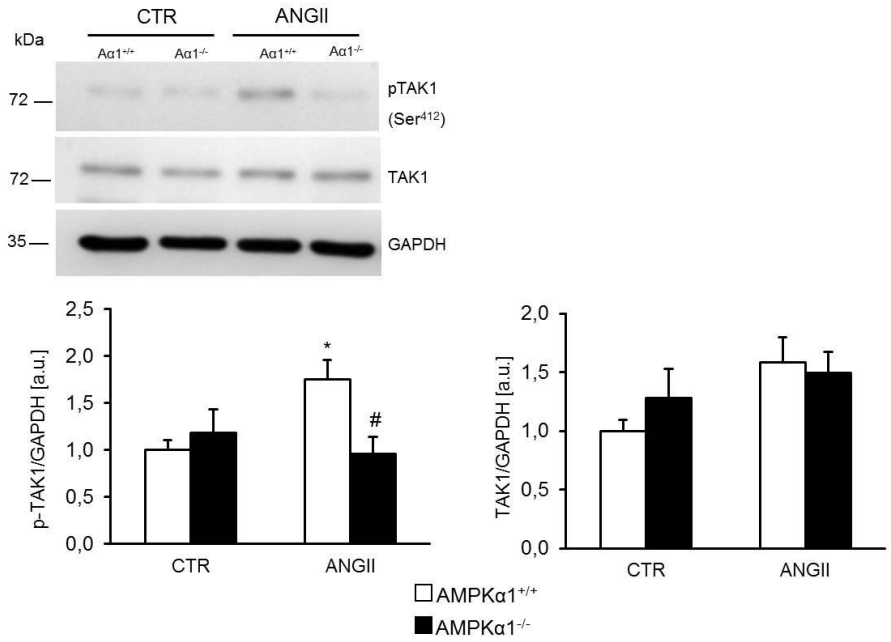

Figure 28: AMPKα1 deficiency inhibits the activation of TGF-ß-activated kinase 1 (TAK1) following angiotensin II infusion. Representative original Western blots and arithmetic means ± SEM (n = 12) of normalized phospho-TAK1 to GAPDH protein ratio and total-TAK1 to GAPDH protein ratio in renal tissue of AMPKα1 knockout mice ($A\alpha1^{-/-}$, $AMPK\alpha1^{-/-}$, black bars) and their corresponding wild-type mice ($A\alpha1^{+/+}$, $AMPK\alpha1^{+/+}$, white bars) following control (CTR) or angiotensin II (ANGII) infusion. *($p<0.05$) indicates statistically significant differences from respective control; #($p<0.05$) indicates significant differences from respective wild-type mice.

In kidney tissues of control treated from both $AMPK\alpha1^{+/+}$ mice and $AMPK\alpha1^{-/-}$ mice, the protein abundance of total TAK1 was not significantly different. Angiotensin II treatment tended to increase total TAK1 protein abundance in renal tissues of both $AMPK\alpha1^{+/+}$ mice and $AMPK\alpha1^{-/-}$ mice, an effect, however, not reaching statistical significant (**Fig. 28**).

4.2.5 AMPKα1-sensitive TAK1 target gene expression following angiotensin II

TAK1 target gene expression is sensitive to AMPKα1 deficiency following obstructive injury. Furthermore, ANG II has a profound role in inflammatory diseases. Therefore, quantitative RT-PCR was performed to evaluate the mRNA levels of TAK1 target genes: *Il6*, *Cox2* and *Pai-1* in renal tissues of AMPKα1$^{+/+}$ mice and AMPKα1$^{-/-}$ mice after 2 weeks of angiotensin II infusion. As a result, the mRNA expression of *Il6*, *Cox2* and *Pai-1* were similar in kidney tissues of control treated AMPKα1$^{+/+}$ mice and AMPKα1$^{-/-}$ mice (**Fig. 29A-C)**. As expected, angiotensin II treatment significantly increased *Il6*, *Cox2* and *Pai-1* mRNA expression in AMPKα1$^{+/+}$ mice, but not in AMPKα1$^{-/-}$ mice. Accordingly, the transcript levels of *Il6*, *Cox2* and *Pai-1* were significantly lower in AMPKα1$^{-/-}$ mice than in AMPKα1$^{+/+}$ mice following angiotensin II infusion.

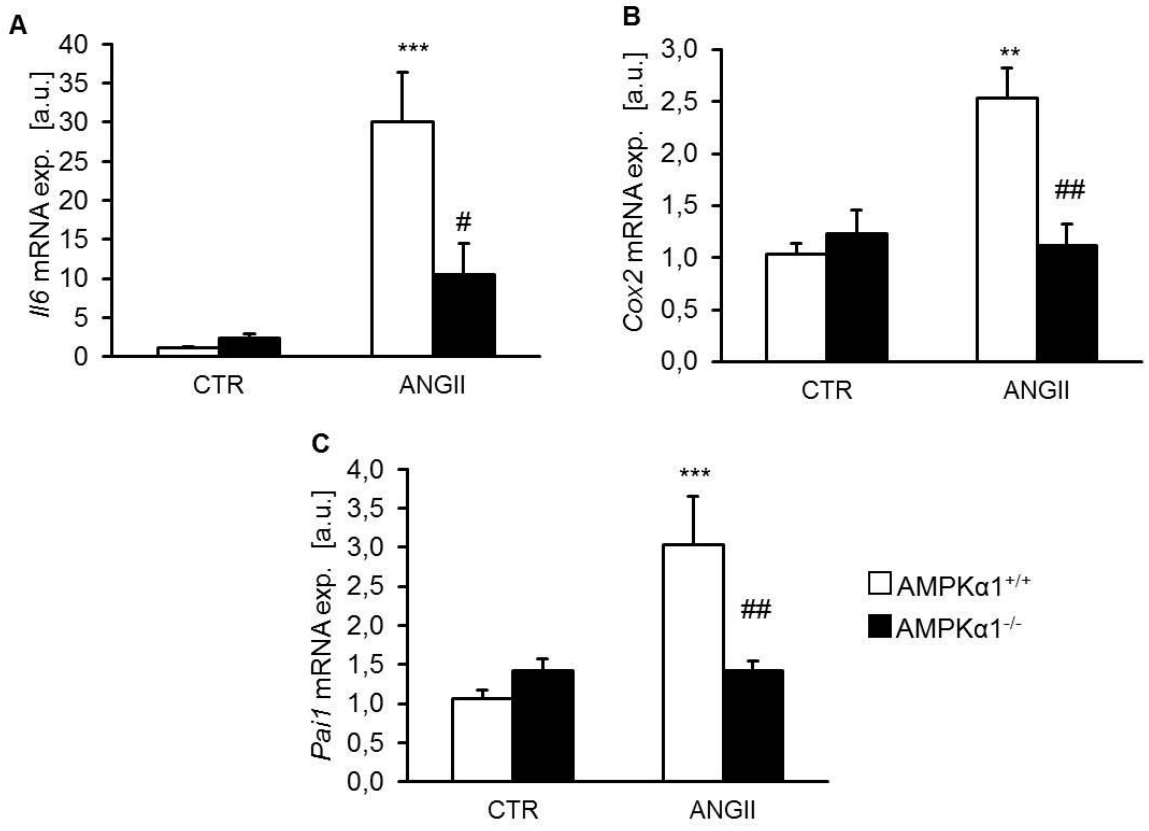

Figure 29: AMPKα1 stimulates TAK1 target genes expression following angiotensin II infusion. Arithmetic means ± SEM (n = 9) of mRNA expression level encoding (**A**) interleukin 6 (Il-6), (**B**) cyclooxygenase 2 (Cox2) and (**C**) plasminogen activator inhibitor 1 (Pai-1) in renal tissue of AMPKα1 knockout mice (Aα1$^{-/-}$, AMPKα1$^{-/-}$, black bars) and their corresponding wild-type mice (Aα1$^{+/+}$, AMPKα1$^{+/+}$, white bars)

following control (CTR) or angiotensin II (ANGII) infusion. **(p<0.01), ***(p<0.001) indicates statistically significant differences from respective control; #(p<0.05), ##(p<0.01) indicates statistically significant differences from respective wild-type mice.

4.3. Regulation of Kv1.5 K^+ channels by AMPK

The present study explored the effects of AMPK on voltage-gated Kv1.5 K^+ channels by using the heterologous *Xenopus laevis* expression system.

In *Xenopus* oocytes, cRNA encoding Kv1.5 was injected with or without additional coexpression of wild-type AMPKα1-HA + AMPKβ1-Flag + AMPKγ1-HA ($AMPK^{WT}$), of constitutively active AMPKα1-HA + AMPKβ1-Flag + AMPKγ1R70Q-HA ($AMPK^{\gamma R70Q}$) or of inactive AMPKα1K45R-HA + AMPKβ1- Flag +AMPKγ1-HA ($AMPK^{\alpha K45R}$).

4.3.1 AMPK decreased K^+ current in Kv1.5-expressing oocytes

In a first series of experiments, the voltage-gated current was determined by two-electrode voltage-clamp in *Xenopus* oocytes. As shown in **Figure 30A-B**, depolarization triggered an outwardly directed current (I_{Kv}) in Kv1.5-expressing *Xenopus* oocytes, but not in water injected oocytes, as control. The K^+ current was significantly down-regulated by co-expression of wild-type $AMPK^{WT}$ in the *Xenopus* oocytes expressing Kv1.5.

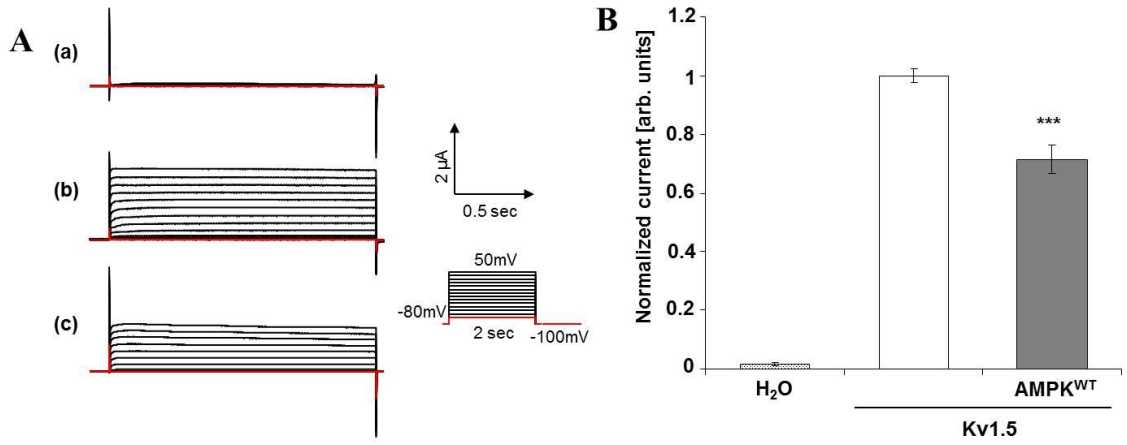

Figure 30. Co-expression of AMPK reduced K^+ current in Kv1.5-expressing oocytes. A. Original tracings of the K^+ current following depolarization from -80 to +50 mV in *Xenopus* oocytes injected with water (a), with cRNA encoding Kv1.5 without (b) or with additional cRNA encoding wild-type AMPK (c). B. Arithmetic means ± SEM (n = 12-15) of K^+ current at +50 mV in *Xenopus* oocytes injected with water, with cRNA encoding Kv1.5 without or with additional cRNA encoding wild-type AMPK. *** ($p<0.001$) indicates statistically significant differences from *Xenopus* oocytes expressing Kv1.5 alone.

The IV curve illustrated in **Figure 31**, shows that at each holding voltage, the K^+ current in *Xenopus* oocytes expressing Kv1.5 together with wild-type AMPK was lower than the K^+ current in *Xenopus* oocytes expressing Kv1.5 alone. No K^+ current was observed in water injected *Xenopus* oocytes at any holding voltage.

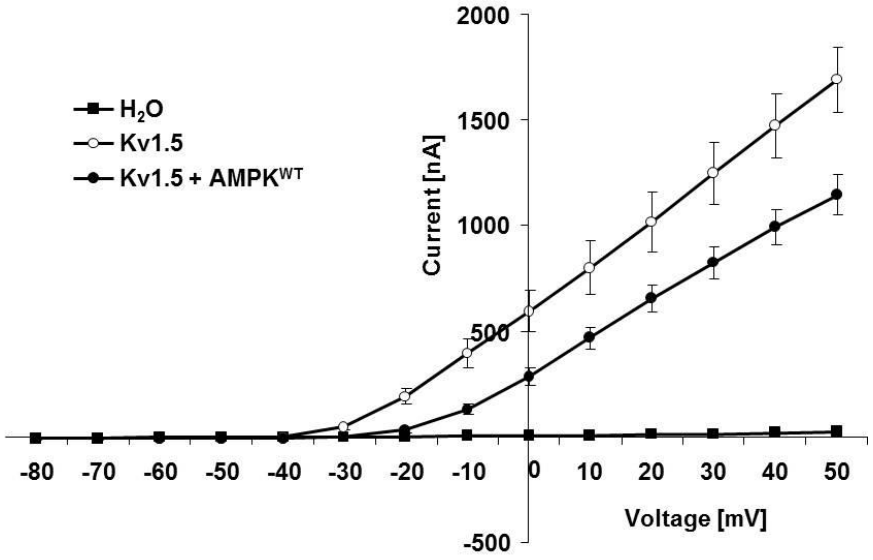

Figure 31. Co-expression of AMPK reduced K+ current in Kv1.5-expressing oocytes at each holding voltage. Current as a function of voltage in *Xenopus* oocytes injected with water, with cRNA encoding Kv1.5 without or with additional cRNA encoding wild-type AMPK.

4.3.2 AMPK activity is necessary for the effects on K^+ current in Kv1.5-expressing oocytes

The test whether AMPK activity is required for the effects on Kv1.5 K^+ channels activity, Kv1.5 was expressed in *Xenopus* oocytes with or without additional coexpression of constitutively active $AMPK^{\gamma R70Q}$ and of inactive mutant $AMPK^{\alpha K45R}$. As shown in **Figure 32A and B**, coexpression of constitutively active $AMPK^{\gamma R70Q}$, but not of inactive mutant $AMPK^{\alpha K45R}$, significantly down-regulated the K^+ current in Kv1.5-expressing *Xenopus* oocytes.

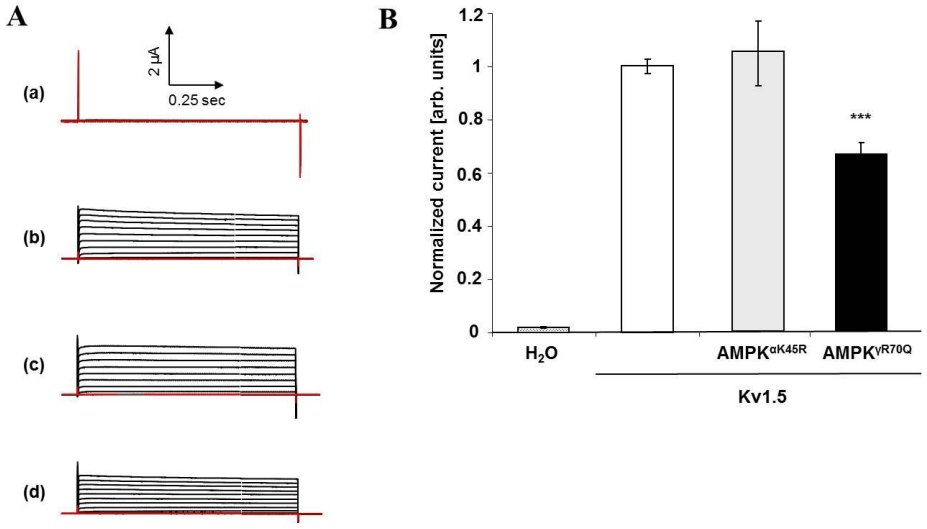

Figure 32: Effects of constitutively active $AMPK^{\gamma R70Q}$ and inactive mutant $AMPK^{\alpha K45R}$ on K^+ current in Kv1.5-expressing oocytes. **A.** Original tracings of the current following depolarization from -80 to +50 mV in *Xenopus* oocytes injected with water (a), with cRNA encoding Kv1.5 without (b) or with additional cRNA encoding inactive mutant $AMPK^{\alpha K45R}$ (c) or constitutively active $AMPK^{\gamma R70Q}$ (d). **B.** Arithmetic means ± SEM (n = 12-19) of the normalized outwardly rectifying K^+ current at +50 mV in *Xenopus* oocytes injected with water, with cRNA encoding Kv1.5 without or with additional cRNA encoding inactive mutant $AMPK^{\alpha K45R}$ or constitutively active $AMPK^{\gamma R70Q}$. ***($p<0.001$) indicates statistically significant differences to *Xenopus* oocytes expressing Kv1.5 alone.

As shown in the IV curve, similar effects of coexpression of constitutively active $AMPK^{\gamma R70Q}$ and of inactive mutant $AMPK^{\alpha K45R}$ were observed at each holding voltage on the K^+ current in Kv-1.5-expressing *Xenopus* oocytes (**Fig. 33**). Therefore, AMPK kinase activity was necessary for the down-regulation of Kv1.5 K^+ currents.

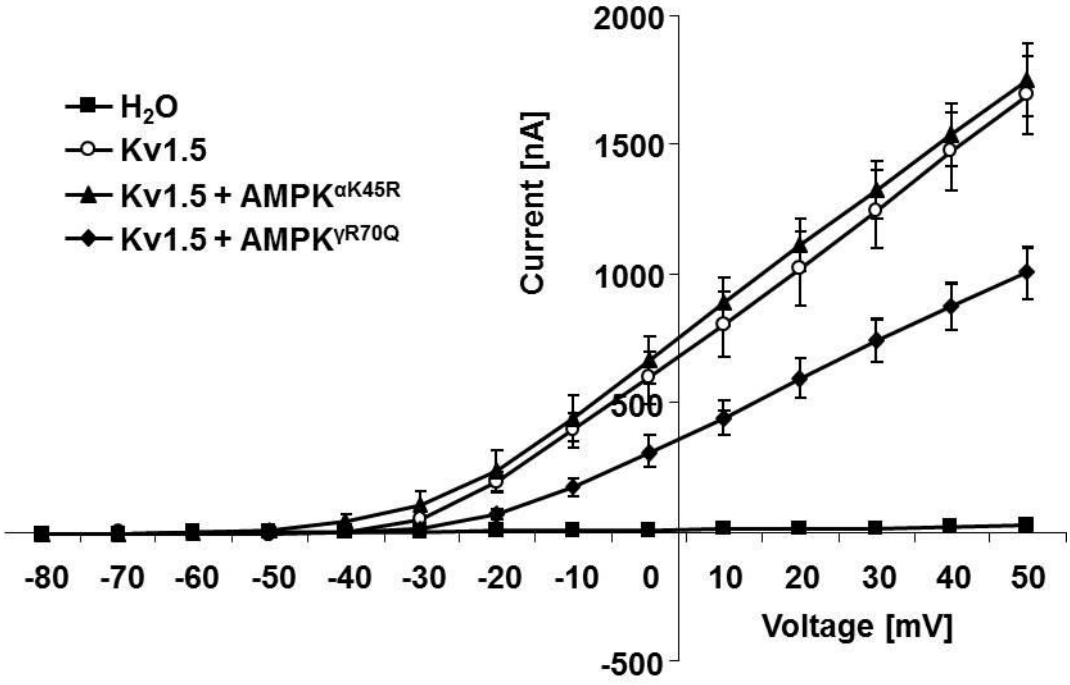

Figure 33. IV curve showing the effects of constitutively active AMPK$^{\gamma R70Q}$ and inactive mutant AMPK$^{\alpha K45R}$ on K^+ current in Kv1.5-expressing oocytes. Current as a function of voltage in *Xenopus* oocytes injected with water, with cRNA encoding Kv1.5 without or with additional cRNA encoding inactive mutant AMPK$^{\alpha K45R}$ or constitutively active AMPK$^{\gamma R70Q}$.

4.3.3 The ubiquitin ligase Nedd4-2 reduced K^+ current in Kv1.5-expressing oocytes

AMPK down-regulates several ion channels by stimulation of the ubiquitin ligase Nedd4-2. To this end, additional experiments were carried out to investigate whether Kv1.5 is regulated by the AMPK-sensitive ubiquitin ligase Nedd4-2. Therefore, Kv1.5 was expressed together with or without wild-type Nedd4-2 in *Xenopus* oocytes. As illustrated in **Figure 34**, coexpression of Nedd4-2 significantly down-regulated K^+ currents in Kv1.5-expressing *Xenopus* oocytes. Thus Kv1.5 activity is sensitive to Nedd4-2.

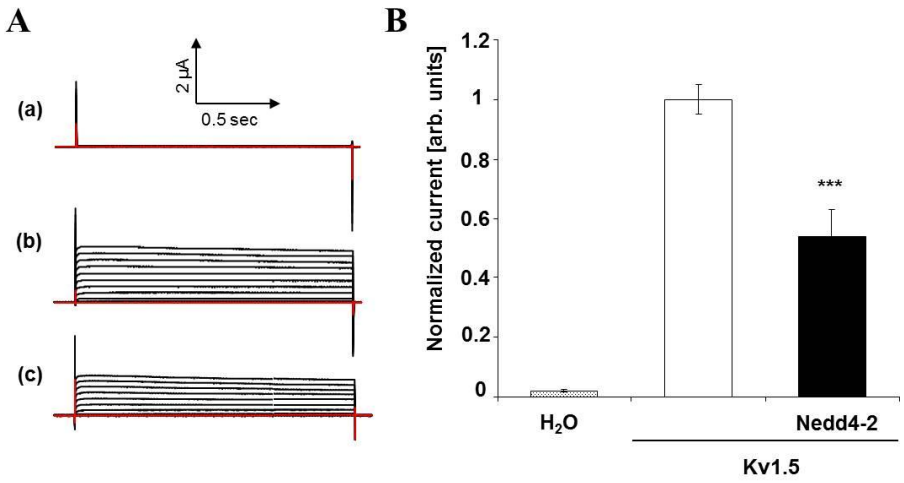

Figure 34: **The ubiquitin ligase Nedd4-2 reduced K^+ current in Kv1.5-expressing oocytes. A.** Original tracings of the current following depolarization from -80 to +50 mV in *Xenopus* oocytes injected with water (a), with cRNA encoding Kv1.5 without (b) or with additional cRNA encoding Nedd4-2 (c). **B.** Arithmetic means ± SEM (n = 12-19) of the normalized K^+ current at +50 mV in *Xenopus* oocytes injected with water, with cRNA encoding Kv1.5 without or with additional cRNA encoding Nedd4-2. *** ($p<0.001$) indicates statistically significant differences from *Xenopus* oocytes expressing Kv1.5 alone.

4.3.4 AMPK decreased Kv1.5–HA plasma membrane protein abundance in Kv1.5-HA-expressing oocytes

The observed inhibitory effect of AMPK on Kv1.5 K^+ currents could be due to reduced K^+ channel activity or down-regulation of the Kv1.5 channel protein abundance in the cell membrane. To answer this question, the protein abundance of Kv1.5 in the plasma membrane of *Xenopus* oocytes was analysed by chemiluminescence experiments by using a HA-tagged Kv1.5 construct. As illustrated in **Figure 35**, *Xenopus* oocytes were injected with water, with cRNA encoding Kv1.5-HA without or with cRNA encoding wild-type $AMPK^{WT}$, inactive mutant AMPK and constitutively active AMPK.

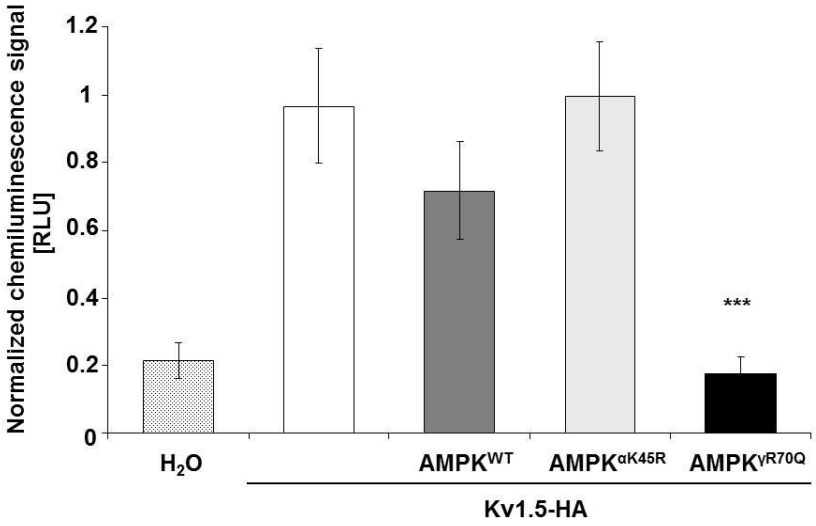

Figure 35: AMPK reduced Kv1.5–HA protein abundance in the plasma membrane of *Xenopus* oocytes. Arithmetic means ± SEM (n = 48-60) of Kv1.5-HA protein abundance in the plasma membrane of *Xenopus* oocytes injected with water, with cRNA encoding Kv1.5-HA without or with additional cRNA encoding wild-type $AMPK^{WT}$, inactive mutant $AMPK^{\alpha K45R}$ or constitutively active $AMPK^{\gamma R70Q}$. *** ($p<0.001$) indicates statistically significant differences from *Xenopus* oocytes expressing Kv1.5-HA alone.

As shown in **Figure 35**, co-expression of constitutively active $AMPK^{\gamma R70Q}$ but not of inactive mutant $AMPK^{\alpha K45R}$ reduced the plasma membrane expression of the Kv1.5-HA channel protein in Kv1.5-HA expressing *Xenopus* oocytes. The Kv1.5-HA protein abundance tended to be reduced following co-expression of wild-type $AMPK^{WT}$, an effect, however, not reaching statistical significance (**Fig. 35**).

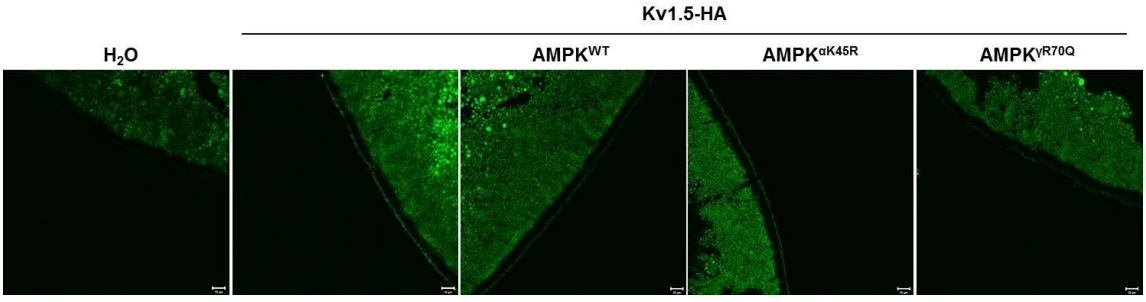

Figure 36. AMPK reduced cell surface Kv1.5–HA protein abundance in Kv1.5-HA-expressing *Xenopus* oocytes. Confocal images showing Kv1.5–HA protein abundance in the *Xenopus* oocytes injected with water, with cRNA encoding Kv1.5-HA without or with additional cRNA encoding wild-type $AMPK^{WT}$, inactive mutant $AMPK^{\alpha K45R}$ or constitutively active $AMPK^{\gamma R70Q}$.

To further test the effect of AMPK on the protein abundance of Kv1.5-HA in the plasma membrane of *Xenopus* oocytes, immunostaining with subsequent confocal microscopy were performed. Similarly as the results in chemiluminescence experiments, coexpression of wild-type $AMPK^{WT}$ and of constitutively active $AMPK^{\gamma R70Q}$ but not of inactive mutant $AMPK^{\alpha K45R}$ reduced the cell surface expression of Kv1.5-HA protein in Kv1.5-HA expressing *Xenopus* oocytes (**Fig. 36**). These results suggest that AMPK down-regulates Kv1.5 K^+ currents at least partly by down-regulation of Kv1.5 protein abundance in the plasma membrane.

5. DISCUSSION

The present study demonstrates that unilateral ureteral obstruction and chronic angiotensin II exposure induces an isoform shift in renal tissue. Both stimuli upregulate the expression of the AMPKα1 isoform. AMPKα1 may act as a pro-fibrotic signalling molecule which contributes to myofibroblast formation and renal pro-fibrotic signalling following unilateral ureteral obstruction (UUO) and angiotensin II infusion. AMPKα1 deficient mice ameliorate expression of markers of inflammation and fibrosis and blunt TAK1 activation. Furthermore, Kv1.5 is downregulated by AMPKα1.

5.1 Role of AMPKα1 in renal fibrosis signaling

AMPKα1 was upregulated in wild-type mice after induction of renal fibrosis by unilateral obstruction or angiotensin II overload. AMPKα1 was strongly upregulated after 3 days of UUO and remains elevated up until 3 weeks of UUO. AMPKα2 levels though declined after 7 days of UUO and were virtually absent in kidneys after 3 weeks of obstructive injury. This demonstrates an isoform shift of AMPKα expression in the injured kidney. A similar isoform shift is observed in the failing heart: heart failure shifts cardiac AMPK activity towards an increased AMPKα1 activity was reported [183]. The isoform shift may however have other causes than changed expression in resident cells: Infiltrating cells in the injured kidney may express high levels of AMPKα1 and therefore account for the increased AMPKα1 protein. The activity of AMPK indicated by phosphorylation of AMPKα Thr^{172} was increased after 3 days and 7 days but not after 3 weeks of UUO. However, after 3 weeks of UUO, AMPKα2 was virtually absent and the remaining activated AMPK may therefore be solely the AMPKα1 isoform. The phosphorylation of ACC, a downstream target of AMPK, was not altered by 7 days of UUO treatment. This may due to a maintained activity of AMPK despite the isoform shift. ANG II treatment did not have any effects on phosphorylation of AMPKα Thr^{172}.

Nonetheless, the isoform shift as indicated by increased AMPKα1 expression appears to have a functional effect: Kidneys from gene targeted mice lacking functional AMPKα1 ($AMPK\alpha1^{-/-}$), but not their wild type littermates ($AMPK\alpha1^{+/+}$) showed a blunted increase of α-smooth

muscle actin expression induced by ureteral obstruction and ANG II infusion. These effects appear to be time course dependent: The expression of α-SMA was not modified at an early time point of UUO by AMPKα1 deficiency, but seems to be important at later stages of UUO. This data nevertheless suggest that AMPKα1 is required for the full effect of unilateral ureteral obstruction and angiotensin II infusion on myofibroblast activation and α-SMA expression. Similarly, two weeks of ANG II treatment also causes α-SMA expression in AMPKα1$^{+/+}$ mice, an effect blunted in AMPKα1$^{-/-}$ mice. However, histological analysis revealed no profound effect of AMPKα1 deficiency on collagen deposition after obstructive renal injury, despite reduced collagen mRNA expression. This finding is in accordance with previous observations: After myocardial infarction, AMPKα1$^{-/-}$ mice show impaired myofibroblast activation but no difference of collagen deposition [184]. According to our observations, AMPKα1may play a permissive role rather than an active role in the activation of fibroblast and α-SMA expression. This indicates a rather complex role in tissue fibrosis as a modulator of pro-fibrotic signaling.

5.2 Possible mediators of the AMPKα1 effects during renal fibrosis

5.2.1 TAK1

The initiation and perpetuation of fibrosis are mediated by effector cells from activated fibroblasts [185]. After UUO treatment, the blunted response of α-smooth muscle actin expression in the AMPKα1$^{-/-}$ mice was paralleled with blunted phosphorylation and expression of TGF-ß-activated kinase 1 (TAK1). Regardless of its origin, TGF-β is a key mediator of fibrotic renal disease [186]. This study revealed elevated TGF-β expression in AMPKα1$^{-/-}$ mice after UUO treatment, which was not significantly different from wild-type mice. Despite a tendency towards a blunted Smad activation in AMPKα1 deficient kidneys after UUO, no significant differences were found between the genotypes. However, previous observations indicate that TGF-ß induced fibrosis could occur independently of Smad [57]. This could be mediated via TAK1, which is a powerful stimulator of the renal fibrotic response [53]. Accordingly, both UUO and angiotensin II induced TAK1 phosphorylation and protein abundance was blunted by AMPKα1 deficiency. Inhibition of TAK1 ameliorates renal

fibrotic response and pro-inflammatory cytokine expression following obstructive injury [187]. Previously it was reported that TAK1-binding protein TAB1 physically binds with AMPK in order to phosphorylate AMPKα Thr^{172} [188]. Therefore, TAK1 is a potential AMPK kinase candidate and may amplify AMPK-dependent functions [144]. On the other hand, AMPKα1 may itself be able to phosphorylate and activate TAK1, and thereby stimulate the expression of pro-inflammatory cytokines [162]. TAK1 up-regulates the expression of c-Fos [189], Il6 [190], Pai1 [191] and Snai1 [191], all of which in turn are important factors in the renal fibrotic response [114, 192-194]. In accordance with the results from this study, AMPK has previously been suggested as a factor in myofibroblast maturation and may be able to augment TGF-ß-induced α-SMA expression via TAK1 [195]. Therefore, AMPKα1 may promote pro-inflammatory and pro-fibrotic changes in the kidney via TAK1.

5.2.2 Inflammatory cells

A variety of cells are recruited following injury to facilitate the wound healing process [196]. Fibrosis has been considered as an abnormal and dysregulated wound healing process, which results in excessive ECM deposition to replace the normal parenchymal structure [197]. IL-6, a downstream target gene of TAK1 [190], acts as a pro-inflammatory and pro-fibrotic mediator in unresolved inflammation [198]. Moreover, IL-6 may compromise tissue repair by shifting acute injury towards a chronic fibrotic remodeling [198]. It may be effective by enhancing macrophage polarization from an M1 to an M2 phenotype [199]. We found the up-regulation of the M2 macrophage marker *Cd206* blunted in AMPKα1-deficient obstructed kidney tissues. This observation is consistent with the report that AMPKα1 promotes macrophage skewing from M1to M2 phase during resolution of inflammation [28]. In renal fibrosis, M2 macrophages contribute to enhanced expression of α-SMA [200]. The chemokine CXCL16 contributes to accumulation of myeloid fibroblasts and macrophages during renal fibrosis [32]. Also UUO induced *Cxcl16* mRNA expression was blunted in renal tissue of AMPKα1 deficient mice. AMPKα1 may therefore stimulate renal myofibroblast activation by enhancing macrophage M2 polarization and infiltration.

Recent observations indicate that UUO is followed by upregulation of adiponectin, which is an activator of AMPK [32]. Genetic ablation of adiponectin is associated reduced fibrotic response

following obstructive injury and with the reduced expression of *Cd206* and *Cxcl16* [32]. The profibrotic effects of adiponectin are mediated by AMPK [32]. Patients suffering from end stage renal disease also show elevated adiponectin levels [201]. The pro-fibrotic action of adiponectin-AMPK axis may thus contribute to increased fibrotic response in end stage renal disease [32, 202]. Consistent with these findings, these studies support the concept that up-regulation of TAK1 contributes to AMPKα1 sensitive pro-inflammatory and pro-fibrotic signaling following UUO and ANG II infusion. Mechanistically, AMPKα1 may promote M2 macrophage infiltration via TAK1-induced IL-6 expression. Nevertheless, it should be considered that the events leading to and governing fibrosis are complex and not attributable to a single pathway. Also, besides the regulation of TAK1, other factors might influence AMPK-dependent effects following obstructive injury. Furthermore, the effects of AMPKα1 deficiency on pro-fibrotic signaling following UUO may be indirect. Increased abundance of suicidal, phosphatidylserine exposing erythrocytes, anemia and/or splenomegaly may modulate the renal fibrotic response [203].

5.3 AMPK and fibrosis in non-renal tissue

The involvement of AMPK in the regulation of fibrotic signaling in other tissues has been suggested by other studies. AMPKα1 is required for angiotensin II-induced proliferation of cardiac fibroblasts [170]. ANG II stimulates cardiac hypertrophy in a TAK1 dependent and Smad independent manner [91]. However, in our study, genetic deletion of AMPKα1 did not have any profound effect on collagen deposition. AMPKα1 deficiency ameliorates α-SMA expression, but not collagen deposition, following myocardial infarction [184]. Impairment of M2 macrophage polarization is similarly associated with an impairment of myofibroblast activation following myocardial infarction [184]. Therefore, AMPKα1 regulation of myofibroblast activation may be not tissue specific.

5.4 Pharmacological activators of AMPK

However, conflicting information has been demonstrated on the effects of the AMPK activator, 5-aminoimidazole-4-carboxyamide ribonucleoside (AICAR). On the one hand, fibrogenic processes following obstructive injury are inhibited by AICAR treatment [154]. Similarly, the AMPK activator metformin ameliorates the epithelial to mesenchymal transition in vitro [153]. On the other hand, treatment of AICAR causes scar formation and myofibroblast activation following myocardial infarction [204]. The described effects of AICAR and metformin are however not necessarily mediated by AMPK, as both may exert AMPK independent-cellular and metabolic effects [155]. Beyond that, two AMPK isoforms α1/ α2 might have different cellular targets and the AMPKα1 isoform may exert distinct effects from the AMPKα2 isoform [205]. Numerous studies have demonstrated distinct effects of the α2 and α1 containing AMPK complex. AMPKα1 has been shown to be less sensitive to AMP than AMPKα2, and is activated especially by cellular stress [206]. AMPKα2, but not AMPKα1 plays a major role in protecting heart from the adverse effects of pressure overload [207]. In human heart failure, an isoform shift from AMPKα2 to AMPKα1 was reported [183]. AMPKα2 isoform is able to prevent myofibroblast trans-differentiation [208]. Furthermore, AMPKα2 suppresses vascular inflammation and endothelial dysfunction [209]. On the other hand, constitutively active AMPKα1 expression in endothelial cells promotes vascular inflammation via induction of COX2 [161]. In consistence with this, we found that angiotensin II treatment upregulated renal COX2 expression, an effect significantly blunted by AMPKα1 deficiency. Taken together, the observed isoform shift of AMPKα2 towards AMPKα1 in obstructed kidney tissues may therefore contribute to the pro-fibrotic signaling events.

5.5 AMPK and Kv1.5

Further experiments revealed that AMP-activated protein kinase α1 (AMPKα1) regulates the voltage-gated K^+ channel Kv1.5 by reducing the protein abundance in the cell membrane. Therefore, AMPK might be a potential candidate to decrease K^+ conductance and repolarization in the cellular system. In addition, the inhibitory effect of AMPKα1on Kv1.5 channel could be involved in the pro-fibrotic signalling effects of AMPKα1: macrophages

express Kv1.5, which may contribute to the regulation of the immune response [210]. Kv1.5 is expressed in fibroblasts [113]. In the failing heart, Kv1.5 potassium current expression is reduced [113] . Inhibiting potassium current in fibroblasts triggers proliferation of these cells [113]. The downregulation of Kv1.5 by AMPKα1 may therefore at least in theory stimulate proliferation and fibrosis of renal tissue.

Interestingly, Nedd4-2 and AMPK similarly down-regulate the Kv1.5 channel mediated K^+ current. This result is consistent with other studies showing inhibitory effects of AMPK on the sodium channel protein ENaC through activation of ubiquitin ligase Nedd4-2 [211, 212]. In addition to ENaC, AMPK similarly reduced the activity of the inwardly rectifying K^+ channel Kir2.1 [73] and the outwardly rectifying K^+ channel KCNQ1/KCNE1 by stimulating Nedd42 dependent pathways [134]. Furthermore, AMPK stimulates several glucose transporters including GLUT1, GLUT2, GLUT3 and GLUT4 and thereby supply glucose, which could be used for ATP production in energy depleted cells [213, 214]. Beyond that, AMPK also stimulates cellular energy production by stimulating fatty acid oxidation and expression of enzymes required for ATP production [215].

This inhibitory effect of AMPK on K^+ channels may contribute to cell membrane depolarization. Depolarization of cell membrane decreases the driving force for electrogenic HCO_3^- exit across the basolateral cell membrane, which alkalinizes the cytosole and thus favours the glucose utilization by glycolysis [216]. The cytosolic alkalinization inhibits Na^+/H^+ exchanger activity [137] resulting in reduced Na^+ entry which further decreases the costly Na^+ extrusion by a Na^+/ K^+ ATPase. In contrast, AMPK can stimulate Na^+/H^+ exchanger activity and cause alkalinization of the cytosol [137]. Furthermore, inhibition of K^+ channels could limit cellular K^+ loss during the impaired function of Na^+/K^+ ATPase in energy-depleted cells. Previously it has been described that cellular K^+ loss triggers the suicidal cell death or apoptosis [217]. In addition to this, apoptosis is cytosolic pH sensitive and facilitated by cytosolic acidification [218]. Inhibition of Kv1.5 may therefore be a mechanism, how AMPK exerts anti-apoptotic functions

During hypoxic conditions the activity and expression of Kv1.5 is reduced [111]. Furthermore, AMPK is activated during hypoxic conditions in energy depleted cells [219]. In addition to conditions of energy depletion, AMPK activation could be facilitated by elevation of cytosolic Ca^{2+} activity [220], by a decrease of O_2 levels [221] and by exposure to nitric oxide [222]. The regulation of Kv1.5 may therefore contribute to increased fibrotic effects and inhibit apoptosis. The regulation of KV1.5 by AMPK may therefore be of relevance during these processes.

5.6 AMPK and apoptosis

The impaired α-SMA expression following obstructive injury in AMPKα1 deficient mice was surprisingly associated with an increased tubular dilation and an increased Bax/Bcl2. This effect may in theory be due to an increased cellular potassium loss by Kv1.5 [217]. These observations are consistent with other studies, which demonstrated that AMPKα1 deficient cells are highly sensitive to apoptosis [223]. The energy sensing kinase AMPK counteracts ATP depletion as a first line defense mechanism to restore cellular energy balance by stimulating cellular glucose uptake via up-regulation of glucose carriers GLUT1, GLUT2, GLUT3, GLUT4 and the Na^+ coupled glucose transporter SGLT1[214, 224-235]. Furthermore, AMPK may stimulate glycolysis, fatty acid oxidation and expression of several enzymes required for ATP production in energy depleted conditions [236, 237]. If, however, all those mechanisms are unable to restore cellular energy supply, cell death may occur. Therefore, AMPKα1 may well function to promote the replacement of functional tissues by less energy demanding fibrotic tissues, and thereby promotes the survival of parenchymal cells in an ischemic or otherwise strained condition. Thus, stimulation of tissue fibrosis could be an evolutionary protective mechanism to preserve organ structure and survival, but for the cost of long term function.

6. CONCLUSION

In conclusion, AMPKα1 is upregulated in models of renal fibrosis. AMPKα1 exerts complex pro-fibrotic signaling effects in the kidney and limits apoptosis during renal fibrosis. The effects of AMPKα1 may be due to a regulation of TAK1 induced inflammatory processes and myofibroblast accumulation and regulation of Kv1.5. Preventing the isoform shift of AMPK in renal fibrotic disease may harbor therapeutic potential.

7. REFERENCES

1. Bataller, R. and D.A. Brenner, *Liver fibrosis.* J Clin Invest, 2005. **115**(2): p. 209-18.
2. Tomasek, J.J., et al., *Myofibroblasts and mechano-regulation of connective tissue remodelling.* Nat Rev Mol Cell Biol, 2002. **3**(5): p. 349-63.
3. Grgic, I., J.S. Duffield, and B.D. Humphreys, *The origin of interstitial myofibroblasts in chronic kidney disease.* Pediatr Nephrol, 2012. **27**(2): p. 183-93.
4. Duffield, J.S., et al., *Host responses in tissue repair and fibrosis.* Annu Rev Pathol, 2013. **8**: p. 241-76.
5. Wynn, T.A., *Cellular and molecular mechanisms of fibrosis.* J Pathol, 2008. **214**(2): p. 199-210.
6. Gabbiani, G., *The myofibroblast in wound healing and fibrocontractive diseases.* J Pathol, 2003. **200**(4): p. 500-3.
7. Kriz, W., B. Kaissling, and M. Le Hir, *Epithelial-mesenchymal transition (EMT) in kidney fibrosis: fact or fantasy?* J Clin Invest, 2011. **121**(2): p. 468-74.
8. Eddy, A.A. and E.G. Neilson, *Chronic kidney disease progression.* J Am Soc Nephrol, 2006. **17**(11): p. 2964-6.
9. Liu, Y., *Cellular and molecular mechanisms of renal fibrosis.* Nat Rev Nephrol, 2011. **7**(12): p. 684-96.
10. Grande, M.T. and J.M. Lopez-Novoa, *Fibroblast activation and myofibroblast generation in obstructive nephropathy.* Nat Rev Nephrol, 2009. **5**(6): p. 319-28.
11. Samarakoon, R., et al., *TGF-beta1 --> SMAD/p53/USF2 --> PAI-1 transcriptional axis in ureteral obstruction-induced renal fibrosis.* Cell Tissue Res, 2012. **347**(1): p. 117-28.
12. Kisseleva, T. and D.A. Brenner, *Mechanisms of fibrogenesis.* Exp Biol Med (Maywood), 2008. **233**(2): p. 109-22.
13. Koo, J.W., *Renal interstitial fibrosis and Angiotensin inhibition.* Electrolyte Blood Press, 2006. **4**(1): p. 35-43.
14. Torres, I.B., et al., *The Interplay between inflammation and fibrosis in kidney transplantation.* Biomed Res Int, 2014. **2014**: p. 750602.
15. Kanasaki, K., G. Taduri, and D. Koya, *Diabetic nephropathy: the role of inflammation in fibroblast activation and kidney fibrosis.* Front Endocrinol (Lausanne), 2013. **4**: p. 7.
16. Kanasaki, K., G. Taduri, and D. Koya, *Diabetic Nephropathy: The Role of Inflammation in Fibroblasts Activation and Kidney Fibrosis.* Frontiers in Endocrinology, 2013. **4**.
17. Ariel, A. and O. Timor, *Hanging in the balance: endogenous anti-inflammatory mechanisms in tissue repair and fibrosis.* J Pathol, 2013. **229**(2): p. 250-63.
18. Nathan, C. and A. Ding, *Nonresolving inflammation.* Cell, 2010. **140**(6): p. 871-82.

19. Chung, A.C. and H.Y. Lan, *Chemokines in renal injury.* J Am Soc Nephrol, 2011. **22**(5): p. 802-9.
20. Ucero, A.C., et al., *Unilateral ureteral obstruction: beyond obstruction.* Int Urol Nephrol, 2014. **46**(4): p. 765-76.
21. Ricardo, S.D., et al., *Expression of adhesion molecules in rat renal cortex during experimental hydronephrosis.* Kidney Int, 1996. **50**(6): p. 2002-10.
22. Morrissey, J.J. and S. Klahr, *Differential effects of ACE and AT1 receptor inhibition on chemoattractant and adhesion molecule synthesis.* Am J Physiol, 1998. **274**(3 Pt 2): p. F580-6.
23. Ricardo, S.D., H. van Goor, and A.A. Eddy, *Macrophage diversity in renal injury and repair.* J Clin Invest, 2008. **118**(11): p. 3522-30.
24. Lin, S.L., et al., *Bone marrow Ly6Chigh monocytes are selectively recruited to injured kidney and differentiate into functionally distinct populations.* J Immunol, 2009. **183**(10): p. 6733-43.
25. Martinez, F.O. and S. Gordon, *The M1 and M2 paradigm of macrophage activation: time for reassessment.* F1000Prime Rep, 2014. **6**: p. 13.
26. Chevalier, R.L., M.S. Forbes, and B.A. Thornhill, *Ureteral obstruction as a model of renal interstitial fibrosis and obstructive nephropathy.* Kidney Int, 2009. **75**(11): p. 1145-1152.
27. Braga, T.T., et al., *MyD88 Signaling Pathway Is Involved in Renal Fibrosis by Favoring a T(H)2 Immune Response and Activating Alternative M2 Macrophages.* Molecular Medicine, 2012. **18**(1): p. 1231-1239.
28. Mounier, R., et al., *AMPKalpha1 regulates macrophage skewing at the time of resolution of inflammation during skeletal muscle regeneration.* Cell Metab, 2013. **18**(2): p. 251-64.
29. Meldrum, K.K., et al., *TNF-alpha neutralization decreases nuclear factor-kappaB activation and apoptosis during renal obstruction.* J Surg Res, 2006. **131**(2): p. 182-8.
30. Kanasaki, K., G. Taduri, and D. Koya, *Diabetic nephropathy: the role of inflammation in fibroblast activation and kidney fibrosis.* Frontiers in Endocrinology, 2013. **4**: p. 7.
31. Li, R.X., W.H. Yiu, and S.C.W. Tang, *Role of bone morphogenetic protein-7 in renal fibrosis.* Frontiers in Physiology, 2015. **6**: p. 114.
32. Yang, J., et al., *Adiponectin promotes monocyte-to-fibroblast transition in renal fibrosis.* J Am Soc Nephrol, 2013. **24**(10): p. 1644-59.
33. Linkermann, A., et al., *Rip1 (receptor-interacting protein kinase 1) mediates necroptosis and contributes to renal ischemia/reperfusion injury.* Kidney Int, 2012. **81**(8): p. 751-61.
34. Ortega, A., et al., *Role of parathyroid hormone-related protein in tubulointerstitial apoptosis and fibrosis after folic acid-induced nephrotoxicity.* J Am Soc Nephrol, 2006. **17**(6): p. 1594-603.
35. Sanz, A.B., et al., *Mechanisms of renal apoptosis in health and disease.* J Am Soc Nephrol, 2008. **19**(9): p. 1634-42.

36. Zeisberg, M. and J.S. Duffield, *Resolved: EMT produces fibroblasts in the kidney.* J Am Soc Nephrol, 2010. **21**(8): p. 1247-53.
37. Yang, L., et al., *Epithelial cell cycle arrest in G2/M mediates kidney fibrosis after injury.* Nat Med, 2010. **16**(5): p. 535-43, 1p following 143.
38. Jones, E.A., A. Shahed, and D.A. Shoskes, *Modulation of apoptotic and inflammatory genes by bioflavonoids and angiotensin II inhibition in ureteral obstruction.* Urology, 2000. **56**(2): p. 346-51.
39. Mezzano, S.A., M. Ruiz-Ortega, and J. Egido, *Angiotensin II and renal fibrosis.* Hypertension, 2001. **38**(3 Pt 2): p. 635-8.
40. Mann, C., et al., *Aberrant repair and fibrosis development in skeletal muscle.* Skeletal Muscle, 2011. **1**(1): p. 21.
41. Liu, Y., *Renal fibrosis: new insights into the pathogenesis and therapeutics.* Kidney Int, 2006. **69**(2): p. 213-7.
42. Chen, X., et al., *Integrin-mediated type II TGF-beta receptor tyrosine dephosphorylation controls SMAD-dependent profibrotic signaling.* J Clin Invest, 2014. **124**(8): p. 3295-310.
43. Lavoie, P., et al., *Neutralization of transforming growth factor-beta attenuates hypertension and prevents renal injury in uremic rats.* J Hypertens, 2005. **23**(10): p. 1895-903.
44. Chen, M.M., et al., *CTGF expression is induced by TGF- beta in cardiac fibroblasts and cardiac myocytes: a potential role in heart fibrosis.* J Mol Cell Cardiol, 2000. **32**(10): p. 1805-19.
45. Sheng, W., et al., *Versican mediates mesenchymal-epithelial transition.* Mol Biol Cell, 2006. **17**(4): p. 2009-20.
46. Guaita, S., et al., *Snail induction of epithelial to mesenchymal transition in tumor cells is accompanied by MUC1 repression and ZEB1 expression.* J Biol Chem, 2002. **277**(42): p. 39209-16.
47. Kokudo, T., et al., *Snail is required for TGFbeta-induced endothelial-mesenchymal transition of embryonic stem cell-derived endothelial cells.* J Cell Sci, 2008. **121**(Pt 20): p. 3317-24.
48. Wu, Y., et al., *Stabilization of snail by NF-kappaB is required for inflammation-induced cell migration and invasion.* Cancer Cell, 2009. **15**(5): p. 416-28.
49. Thiery, J.P., et al., *Epithelial-mesenchymal transitions in development and disease.* Cell, 2009. **139**(5): p. 871-90.
50. Leask, A. and D.J. Abraham, *TGF-beta signaling and the fibrotic response.* FASEB J, 2004. **18**(7): p. 816-27.
51. Zhang, Y. and R. Derynck, *Regulation of Smad signalling by protein associations and signalling crosstalk.* Trends Cell Biol, 1999. **9**(7): p. 274-9.
52. Bottinger, E.P. and M. Bitzer, *TGF-beta signaling in renal disease.* J Am Soc Nephrol, 2002. **13**(10): p. 2600-10.

53. Choi, M.E., Y. Ding, and S.I. Kim, *TGF-beta signaling via TAK1 pathway: role in kidney fibrosis.* Semin Nephrol, 2012. **32**(3): p. 244-52.
54. Sutaría, P.M., et al., *Transforming growth factor-β receptor types I and II are expressed in renal tubules and are increased after chronic unilateral ureteral obstruction.* Life Sciences, 1998. **62**(21): p. 1965-1972.
55. Hills, C.E. and P.E. Squires, *TGF-β1-Induced Epithelial-to-Mesenchymal Transition and Therapeutic Intervention in Diabetic Nephropathy.* American Journal of Nephrology, 2010. **31**(1): p. 68-74.
56. Yanagita, M., *Inhibitors/antagonists of TGF-beta system in kidney fibrosis.* Nephrol Dial Transplant, 2012. **27**(10): p. 3686-91.
57. Moustakas, A. and C.H. Heldin, *Non-Smad TGF-beta signals.* J Cell Sci, 2005. **118**(Pt 16): p. 3573-84.
58. Sakurai, H., et al., *Tumor necrosis factor-alpha-induced IKK phosphorylation of NF-kappaB p65 on serine 536 is mediated through the TRAF2, TRAF5, and TAK1 signaling pathway.* J Biol Chem, 2003. **278**(38): p. 36916-23.
59. Ninomiya-Tsuji, J., et al., *The kinase TAK1 can activate the NIK-I kappaB as well as the MAP kinase cascade in the IL-1 signalling pathway.* Nature, 1999. **398**(6724): p. 252-6.
60. Irie, T., T. Muta, and K. Takeshige, *TAK1 mediates an activation signal from toll-like receptor(s) to nuclear factor-kappaB in lipopolysaccharide-stimulated macrophages.* FEBS Lett, 2000. **467**(2-3): p. 160-4.
61. Ono, K., et al., *A dominant negative TAK1 inhibits cellular fibrotic responses induced by TGF-β.* Biochemical and Biophysical Research Communications, 2003. **307**(2): p. 332-337.
62. Choi, M.E., Y. Ding, and S.I. Kim, *TGF-β signaling via TAK1 pathway: Role in kidney fibrosis.* Seminars in nephrology, 2012. **32**(3): p. 244-252.
63. Inokuchi, S., et al., *Disruption of TAK1 in hepatocytes causes hepatic injury, inflammation, fibrosis, and carcinogenesis.* Proc Natl Acad Sci U S A, 2010. **107**(2): p. 844-9.
64. Zhang, D., et al., *TAK1 is activated in the myocardium after pressure overload and is sufficient to provoke heart failure in transgenic mice.* Nat Med, 2000. **6**(5): p. 556-63.
65. Euler, G., *Good and bad sides of TGFβ-signaling in myocardial infarction.* Frontiers in Physiology, 2015. **6**: p. 66.
66. Hall, J.E., *Historical perspective of the renin-angiotensin system.* Mol Biotechnol, 2003. **24**(1): p. 27-39.
67. Menard, J., et al., *Biochemistry and regulation of angiotensinogen.* Clin Exp Hypertens A, 1983. **5**(7-8): p. 1005-19.
68. Parsons, K.K. and T.M. Coffman, *The renin-angiotensin system: it's all in your head.* J Clin Invest, 2007. **117**(4): p. 873-6.
69. Giani, J.F., et al., *Renal Angiotensin-Converting Enzyme Is Essential for the Hypertension Induced by Nitric Oxide Synthesis Inhibition.* J Am Soc Nephrol, 2014.

70. Ng, K.K. and J.R. Vane, *Conversion of angiotensin I to angiotensin II.* Nature, 1967. **216**(5117): p. 762-6.
71. Quinn, S.J. and G.H. Williams, *Regulation of aldosterone secretion.* Annu Rev Physiol, 1988. **50**: p. 409-26.
72. Lv, L.L. and B.C. Liu, *Role of non-classical renin-angiotensin system axis in renal fibrosis.* Front Physiol, 2015. **6**: p. 117.
73. De Mello, W.C., *Chemical Communication between Heart Cells is Disrupted by Intracellular Renin and Angiotensin II: Implications for Heart Development and Disease.* Front Endocrinol (Lausanne), 2015. **6**: p. 72.
74. Marquez, E., et al., *Renin-angiotensin system within the diabetic podocyte.* Am J Physiol Renal Physiol, 2015. **308**(1): p. F1-10.
75. Ji, Y.Y., et al., *PPARalpha activator fenofibrate modulates angiotensin II-induced inflammatory responses in vascular smooth muscle cells via the TLR4-dependent signaling pathway.* Biochem Pharmacol, 2009. **78**(9): p. 1186-97.
76. Klahr, S., G. Schreiner, and I. Ichikawa, *The progression of renal disease.* N Engl J Med, 1988. **318**(25): p. 1657-66.
77. Cattell, V., *Macrophages in acute glomerular inflammation.* Kidney Int, 1994. **45**(4): p. 945-52.
78. Ruiz-Ortega, M., et al., *Angiotensin II: a key factor in the inflammatory and fibrotic response in kidney diseases.* Nephrol Dial Transplant, 2006. **21**(1): p. 16-20.
79. Ruiz-Ortega, M., et al., *Proinflammatory actions of angiotensins.* Curr Opin Nephrol Hypertens, 2001. **10**(3): p. 321-9.
80. Eddy, A.A., *Molecular basis of renal fibrosis.* Pediatr Nephrol, 2000. **15**(3-4): p. 290-301.
81. Johnson, R.J., et al., *Renal injury from angiotensin II-mediated hypertension.* Hypertension, 1992. **19**(5): p. 464-74.
82. Mezzano, S.A., M. Ruiz-Ortega, and J. Egido, *Angiotensin II and Renal Fibrosis.* Hypertension, 2001. **38**(3): p. 635-638.
83. Fukagawa, M., et al., *Chronic progressive interstitial fibrosis in renal disease--are there novel pharmacological approaches?* Nephrol Dial Transplant, 1999. **14**(12): p. 2793-5.
84. Lapinski, R., et al., *Angiotensin II modulates glomerular capillary permselectivity in rat isolated perfused kidney.* J Am Soc Nephrol, 1996. **7**(5): p. 653-60.
85. Muenter, K. and M.R. Dashwood, *Blockade of the renin-angiotensin and endothelin systems on progressive renal injury.* Hypertension, 2001. **37**(5): p. E13.
86. Ledbetter, S., et al., *Renal fibrosis in mice treated with human recombinant transforming growth factor-beta2.* Kidney Int, 2000. **58**(6): p. 2367-76.
87. Rodriguez-Vita, J., et al., *Angiotensin II activates the Smad pathway in vascular smooth muscle cells by a transforming growth factor-beta-independent mechanism.* Circulation, 2005. **111**(19): p. 2509-17.

88. Hao, J., et al., *Interaction between angiotensin II and Smad proteins in fibroblasts in failing heart and in vitro.* Am J Physiol Heart Circ Physiol, 2000. **279**(6): p. H3020-30.
89. Wamsley-Davis, A., et al., *AT1A-mediated activation of kidney JNK1 and SMAD2 in obstructive uropathy: preservation of kidney tissue mass using candesartan.* Am J Physiol Renal Physiol, 2004. **287**(3): p. F474-80.
90. Doyon, P. and M.J. Servant, *Tumor necrosis factor receptor-associated factor-6 and ribosomal S6 kinase intracellular pathways link the angiotensin II AT1 receptor to the phosphorylation and activation of the IkappaB kinase complex in vascular smooth muscle cells.* J Biol Chem, 2010. **285**(40): p. 30708-18.
91. Watkins, S.J., et al., *Angiotensin II-induced cardiomyocyte hypertrophy in vitro is TAK1-dependent and Smad2/3-independent.* Hypertens Res, 2012. **35**(4): p. 393-8.
92. Huang, C., et al., *KCa3.1 mediates activation of fibroblasts in diabetic renal interstitial fibrosis.* Nephrol Dial Transplant, 2014. **29**(2): p. 313-24.
93. Saliba, Y., et al., *Evidence of a Role for Fibroblast Transient Receptor Potential Canonical 3 Ca2+ Channel in Renal Fibrosis.* J Am Soc Nephrol, 2014.
94. Chen, W.L., et al., *Involvement of Kv1.5 protein in oxidative vascular endothelial cell injury.* PLoS One, 2012. **7**(11): p. e49758.
95. Hald, B.O., et al., *BKCa and KV channels limit conducted vasomotor responses in rat mesenteric terminal arterioles.* Pflugers Arch, 2012. **463**(2): p. 279-95.
96. Sutendra, G., et al., *Pyruvate dehydrogenase inhibition by the inflammatory cytokine TNFalpha contributes to the pathogenesis of pulmonary arterial hypertension.* J Mol Med (Berl), 2011. **89**(8): p. 771-83.
97. Feng, J., et al., *Antisense oligodeoxynucleotides directed against Kv1.5 mRNA specifically inhibit ultrarapid delayed rectifier K+ current in cultured adult human atrial myocytes.* Circ Res, 1997. **80**(4): p. 572-9.
98. Nattel, S., L. Yue, and Z. Wang, *Cardiac ultrarapid delayed rectifiers: a novel potassium current family o f functional similarity and molecular diversity.* Cell Physiol Biochem, 1999. **9**(4-5): p. 217-26.
99. Coma, M., et al., *Impaired voltage-gated K+ channel expression in brain during experimental cancer cachexia.* FEBS Lett, 2003. **536**(1-3): p. 45-50.
100. Vicente, R., et al., *Differential voltage-dependent K+ channel responses during proliferation and activation in macrophages.* J Biol Chem, 2003. **278**(47): p. 46307-20.
101. Villalonga, N., et al., *Cell cycle-dependent expression of Kv1.5 is involved in myoblast proliferation.* Biochim Biophys Acta, 2008. **1783**(5): p. 728-36.
102. Olson, T.M., et al., *Kv1.5 channelopathy due to KCNA5 loss-of-function mutation causes human atrial fibrillation.* Hum Mol Genet, 2006. **15**(14): p. 2185-91.
103. Yang, Q., et al., *Drug discoveries towards Kv1.5 potassium channel.* Curr Top Med Chem, 2009. **9**(4): p. 339-47.

104. Munoz, C., et al., *Activation of voltage gated K(+) channel Kv1.5 by beta-catenin.* Biochem Biophys Res Commun, 2012. **417**(2): p. 692-6.
105. Lu, G., et al., *Angiotensin II upregulates Kv1.5 expression through ROS-dependent transforming growth factor-beta1 and extracellular signal-regulated kinase 1/2 signalings in neonatal rat atrial myocytes.* Biochem Biophys Res Commun, 2014. **454**(3): p. 410-416.
106. Abdul, M. and N. Hoosein, *Expression and activity of potassium ion channels in human prostate cancer.* Cancer Lett, 2002. **186**(1): p. 99-105.
107. Abdul, M. and N. Hoosein, *Voltage-gated potassium ion channels in colon cancer.* Oncol Rep, 2002. **9**(5): p. 961-4.
108. Abdul, M., A. Santo, and N. Hoosein, *Activity of potassium channel-blockers in breast cancer.* Anticancer Res, 2003. **23**(4): p. 3347-51.
109. Wang, L., et al., *[Influence of 4-aminopyridine on voltage-activated K(+) current and cell proliferation in small cell lung cancer]*. Zhonghua Zhong Liu Za Zhi, 2002. **24**(3): p. 230-3.
110. Conti, M., *Targeting K+ channels for cancer therapy.* J Exp Ther Oncol, 2004. **4**(2): p. 161-6.
111. Chu, X., et al., *Hypoxia suppresses KV1.5 channel expression through endogenous 15-HETE in rat pulmonary artery.* Prostaglandins Other Lipid Mediat, 2009. **88**(1-2): p. 42-50.
112. Archer, S.L., et al., *Mitochondrial metabolism, redox signaling, and fusion: a mitochondria-ROS-HIF-1alpha-Kv1.5 O2-sensing pathway at the intersection of pulmonary hypertension and cancer.* Am J Physiol Heart Circ Physiol, 2008. **294**(2): p. H570-8.
113. Wu, C.T., et al., *Disease and region-related cardiac fibroblast potassium current variations and potential functional significance.* Cardiovasc Res, 2014. **102**(3): p. 487-96.
114. Bascands, J.L. and J.P. Schanstra, *Obstructive nephropathy: insights from genetically engineered animals.* Kidney Int, 2005. **68**(3): p. 925-37.
115. Ruster, C. and G. Wolf, *Angiotensin II as a morphogenic cytokine stimulating renal fibrogenesis.* J Am Soc Nephrol, 2011. **22**(7): p. 1189-99.
116. Stapleton, D., et al., *Mammalian 5'-AMP-activated protein kinase non-catalytic subunits are homologs of proteins that interact with yeast Snf1 protein kinase.* J Biol Chem, 1994. **269**(47): p. 29343-6.
117. Viollet, B., et al., *AMPK inhibition in health and disease.* Crit Rev Biochem Mol Biol, 2010. **45**(4): p. 276-95.
118. Cheung, P.C., et al., *Characterization of AMP-activated protein kinase gamma-subunit isoforms and their role in AMP binding.* Biochem J, 2000. **346 Pt 3**: p. 659-69.

119. Santidrian, A.F., et al., *AICAR induces apoptosis independently of AMPK and p53 through up-regulation of the BH3-only proteins BIM and NOXA in chronic lymphocytic leukemia cells.* Blood, 2010. **116**(16): p. 3023-32.
120. Zaha, V.G. and L.H. Young, *AMP-activated protein kinase regulation and biological actions in the heart.* Circ Res, 2012. **111**(6): p. 800-14.
121. Qin, S. and G.W. De Vries, *alpha2 But not alpha1 AMP-activated protein kinase mediates oxidative stress-induced inhibition of retinal pigment epithelium cell phagocytosis of photoreceptor outer segments.* J Biol Chem, 2008. **283**(11): p. 6744-51.
122. Viollet, B., et al., *AMPK: Lessons from transgenic and knockout animals.* Front Biosci (Landmark Ed), 2009. **14**: p. 19-44.
123. Viollet, B., et al., *Activation of AMP-activated protein kinase in the liver: a new strategy for the management of metabolic hepatic disorders.* J Physiol, 2006. **574**(Pt 1): p. 41-53.
124. Jager, S., et al., *AMP-activated protein kinase (AMPK) action in skeletal muscle via direct phosphorylation of PGC-1alpha.* Proc Natl Acad Sci U S A, 2007. **104**(29): p. 12017-22.
125. Viollet, B., et al., *AMP-activated protein kinase in the regulation of hepatic energy metabolism: from physiology to therapeutic perspectives.* Acta Physiol (Oxf), 2009. **196**(1): p. 81-98.
126. Xu, Q. and L.Y. Si, *Protective effects of AMP-activated protein kinase in the cardiovascular system.* J Cell Mol Med, 2010. **14**(11): p. 2604-13.
127. Hardie, D.G. and D. Carling, *The AMP-activated protein kinase--fuel gauge of the mammalian cell?* Eur J Biochem, 1997. **246**(2): p. 259-73.
128. Dridi, S. and M. Taouis, *Adiponectin and energy homeostasis: consensus and controversy.* J Nutr Biochem, 2009. **20**(11): p. 831-9.
129. Lang, F. and M. Foller, *Regulation of ion channels and transporters by AMP-activated kinase (AMPK).* Channels (Austin), 2014. **8**(1): p. 20-8.
130. Andersen, M.N. and H.B. Rasmussen, *AMPK.* Communicative & Integrative Biology, 2012. **5**(5): p. 480-484.
131. Wyatt, C.N., et al., *AMP-activated protein kinase mediates carotid body excitation by hypoxia.* J Biol Chem, 2007. **282**(11): p. 8092-8.
132. Bhalla, V., et al., *AMP-activated kinase inhibits the epithelial Na+ channel through functional regulation of the ubiquitin ligase Nedd4-2.* J Biol Chem, 2006. **281**(36): p. 26159-69.
133. Klein, H., et al., *Inhibition of the KCa3.1 channels by AMP-activated protein kinase in human airway epithelial cells.* Am J Physiol Cell Physiol, 2009. **296**(2): p. C285-95.
134. Alesutan, I., et al., *Inhibition of the heterotetrameric K+ channel KCNQ1/KCNE1 by the AMP-activated protein kinase.* Mol Membr Biol, 2011. **28**(2): p. 79-89.
135. Andersen, M.N., et al., *AMP-activated protein kinase downregulates Kv7.1 cell surface expression.* Traffic, 2012. **13**(1): p. 143-56.

136. Light, P.E., C.H. Wallace, and J.R. Dyck, *Constitutively active adenosine monophosphate-activated protein kinase regulates voltage-gated sodium channels in ventricular myocytes.* Circulation, 2003. **107**(15): p. 1962-5.
137. Rotte, A., et al., *Upregulation of Na+/H+ exchanger by the AMP-activated protein kinase.* Biochem Biophys Res Commun, 2010. **398**(4): p. 677-82.
138. Hardie, D.G., *AMP-activated protein kinase: an energy sensor that regulates all aspects of cell function.* Genes Dev, 2011. **25**(18): p. 1895-908.
139. Carling, D., M.J. Sanders, and A. Woods, *The regulation of AMP-activated protein kinase by upstream kinases.* Int J Obes (Lond), 2008. **32 Suppl 4**: p. S55-9.
140. Hawley, S.A., et al., *Characterization of the AMP-activated protein kinase kinase from rat liver and identification of threonine 172 as the major site at which it phosphorylates AMP-activated protein kinase.* J Biol Chem, 1996. **271**(44): p. 27879-87.
141. Alexander, A. and C.L. Walker, *The role of LKB1 and AMPK in cellular responses to stress and damage.* FEBS Letters, 2011. **585**(7): p. 952-957.
142. Shaw, R.J., et al., *The tumor suppressor LKB1 kinase directly activates AMP-activated kinase and regulates apoptosis in response to energy stress.* Proc Natl Acad Sci U S A, 2004. **101**(10): p. 3329-35.
143. Mungai, P.T., et al., *Hypoxia triggers AMPK activation through reactive oxygen species-mediated activation of calcium release-activated calcium channels.* Mol Cell Biol, 2011. **31**(17): p. 3531-45.
144. Xie, M., et al., *A pivotal role for endogenous TGF-beta-activated kinase-1 in the LKB1/AMP-activated protein kinase energy-sensor pathway.* Proc Natl Acad Sci U S A, 2006. **103**(46): p. 17378-83.
145. Wang, S., P. Song, and M.H. Zou, *AMP-activated protein kinase, stress responses and cardiovascular diseases.* Clin Sci (Lond), 2012. **122**(12): p. 555-73.
146. Mount, P.F., et al., *Acute renal ischemia rapidly activates the energy sensor AMPK but does not increase phosphorylation of eNOS-Ser1177.* Am J Physiol Renal Physiol, 2005. **289**(5): p. F1103-15.
147. Kitani, T., S. Okuno, and H. Fujisawa, *Molecular cloning of Ca2+/calmodulin-dependent protein kinase kinase beta.* J Biochem, 1997. **122**(1): p. 243-50.
148. Hallows, K.R., *Emerging role of AMP-activated protein kinase in coupling membrane transport to cellular metabolism.* Curr Opin Nephrol Hypertens, 2005. **14**(5): p. 464-71.
149. Hallows, K.R., et al., *Role of the energy sensor AMP-activated protein kinase in renal physiology and disease.* Am J Physiol Renal Physiol, 2010. **298**(5): p. F1067-77.
150. Fraser, S., et al., *Regulation of the energy sensor AMP-activated protein kinase in the kidney by dietary salt intake and osmolality.* Am J Physiol Renal Physiol, 2005. **288**(3): p. F578-86.
151. Sharma, K., et al., *Adiponectin regulates albuminuria and podocyte function in mice.* J Clin Invest, 2008. **118**(5): p. 1645-56.

152. Cammisotto, P.G., et al., *Control of glycogen synthase through ADIPOR1-AMPK pathway in renal distal tubules of normal and diabetic rats.* Am J Physiol Renal Physiol, 2008. **294**(4): p. F881-9.
153. Lee, J.H., et al., *AMP-activated protein kinase inhibits TGF-beta-, angiotensin II-, aldosterone-, high glucose-, and albumin-induced epithelial-mesenchymal transition.* Am J Physiol Renal Physiol, 2013. **304**(6): p. F686-97.
154. Chen, K.H., et al., *The AMPK agonist AICAR inhibits TGF-beta1 induced activation of kidney myofibroblasts.* PLoS One, 2014. **9**(9): p. e106554.
155. Liu, X., et al., *Discrete mechanisms of mTOR and cell cycle regulation by AMPK agonists independent of AMPK.* Proc Natl Acad Sci U S A, 2014. **111**(4): p. E435-44.
156. Russell, R.R., 3rd, et al., *AMP-activated protein kinase mediates ischemic glucose uptake and prevents postischemic cardiac dysfunction, apoptosis, and injury.* J Clin Invest, 2004. **114**(4): p. 495-503.
157. Lempiäinen, J., et al., *AMPK activator AICAR ameliorates ischaemia reperfusion injury in the rat kidney.* British Journal of Pharmacology, 2012. **166**(6): p. 1905-1915.
158. Pan, J.S., et al., *Stanniocalcin-1 inhibits renal ischemia/reperfusion injury via an AMP-activated protein kinase-dependent pathway.* J Am Soc Nephrol, 2015. **26**(2): p. 364-78.
159. Viollet, B., et al., *AMPK inhibition in health and disease.* Critical Reviews in Biochemistry and Molecular Biology, 2010. **45**(4): p. 276-295.
160. Decleves, A.E., et al., *AMPK mediates the initiation of kidney disease induced by a high-fat diet.* J Am Soc Nephrol, 2011. **22**(10): p. 1846-55.
161. Liang, Y., et al., *Constitutive activation of AMPK alpha1 in vascular endothelium promotes high-fat diet-induced fatty liver injury: role of COX-2 induction.* Br J Pharmacol, 2014. **171**(2): p. 498-508.
162. Kim, S.Y., et al., *AMP-activated protein kinase-alpha1 as an activating kinase of TGF-beta-activated kinase 1 has a key role in inflammatory signals.* Cell Death Dis, 2012. **3**: p. e357.
163. Sag, D., et al., *Adenosine 5'-monophosphate-activated protein kinase promotes macrophage polarization to an anti-inflammatory functional phenotype.* J Immunol, 2008. **181**(12): p. 8633-41.
164. Cacicedo, J.M., et al., *AMPK inhibits fatty acid-induced increases in NF-kappaB transactivation in cultured human umbilical vein endothelial cells.* Biochem Biophys Res Commun, 2004. **324**(4): p. 1204-9.
165. Dey, A., et al., *Altered kidney CYP2C and cyclooxygenase-2 levels are associated with obesity-related albuminuria.* Obes Res, 2004. **12**(8): p. 1278-89.
166. Cao, J., et al., *High fat diet enhances cardiac abnormalities in SHR rats: Protective role of heme oxygenase-adiponectin axis.* Diabetol Metab Syndr, 2011. **3**(1): p. 37.
167. Ruderman, N. and M. Prentki, *AMP kinase and malonyl-CoA: targets for therapy of the metabolic syndrome.* Nat Rev Drug Discov, 2004. **3**(4): p. 340-51.

168. Cavaglieri, R.C., et al., *Metformin prevents renal interstitial fibrosis in mice with unilateral ureteral obstruction.* Mol Cell Endocrinol, 2015.
169. Tilg, H. and A.R. Moschen, *Adipocytokines: mediators linking adipose tissue, inflammation and immunity.* Nat Rev Immunol, 2006. **6**(10): p. 772-83.
170. Hattori, Y., et al., *Activation of AMP-activated protein kinase enhances angiotensin ii-induced proliferation in cardiac fibroblasts.* Hypertension, 2006. **47**(2): p. 265-70.
171. Jorgensen, S.B., et al., *Knockout of the alpha2 but not alpha1 5'-AMP-activated protein kinase isoform abolishes 5-aminoimidazole-4-carboxamide-1-beta-4-ribofuranosidebut not contraction-induced glucose uptake in skeletal muscle.* J Biol Chem, 2004. **279**(2): p. 1070-9.
172. Voelkl, J., et al., *Sgk1 sensitivity of Na(+)/H(+) exchanger activity and cardiac remodeling following pressure overload.* Basic Res Cardiol, 2012. **107**(2): p. 236.
173. Viollet, B., et al., *Physiological role of AMP-activated protein kinase (AMPK): insights from knockout mouse models.* Biochem Soc Trans, 2003. **31**(Pt 1): p. 216-9.
174. Chevalier, R.L., M.S. Forbes, and B.A. Thornhill, *Ureteral obstruction as a model of renal interstitial fibrosis and obstructive nephropathy.* Kidney Int, 2009. **75**(11): p. 1145-52.
175. Xiong, M., et al., *Loss of vitamin D receptor in chronic kidney disease: a potential mechanism linking inflammation to epithelial-to-mesenchymal transition.* Am J Physiol Renal Physiol, 2012. **303**(7): p. F1107-15.
176. Voelkl, J., et al., *PKB/SGK-resistant GSK-3 signaling following unilateral ureteral obstruction.* Kidney Blood Press Res, 2013. **38**(1): p. 156-64.
177. Mohamed, M.R., et al., *Functional analysis of a novel I71N mutation in the GJB2 gene among Southern Egyptians causing autosomal recessive hearing loss.* Cell Physiol Biochem, 2010. **26**(6): p. 959-66.
178. Koutsouki, E., et al., *Modulation of human Kv1.5 channel kinetics by N-cadherin.* Biochem Biophys Res Commun, 2007. **363**(1): p. 18-23.
179. Fraser, S.A., et al., *Regulation of the renal-specific Na+-K+-2Cl- co-transporter NKCC2 by AMP-activated protein kinase (AMPK).* Biochem J, 2007. **405**(1): p. 85-93.
180. Hamilton, S.R., et al., *Subcellular distribution and membrane topology of the mammalian concentrative Na+-nucleoside cotransporter rCNT1.* J Biol Chem, 2001. **276**(30): p. 27981-8.
181. Hallows, K.R., et al., *Physiological modulation of CFTR activity by AMP-activated protein kinase in polarized T84 cells.* Am J Physiol Cell Physiol, 2003. **284**(5): p. C1297-308.
182. Boehmer, C., et al., *Modulation of the voltage-gated potassium channel Kv1.5 by the SGK1 protein kinase involves inhibition of channel ubiquitination.* Cell Physiol Biochem, 2008. **22**(5-6): p. 591-600.
183. Kim, M., et al., *AMPK isoform expression in the normal and failing hearts.* J Mol Cell Cardiol, 2012. **52**(5): p. 1066-73.

184. Noppe, G., et al., *Reduced scar maturation and contractility lead to exaggerated left ventricular dilation after myocardial infarction in mice lacking AMPKalpha1*. J Mol Cell Cardiol, 2014. **74**: p. 32-43.
185. Yang, J., et al., *Adiponectin Promotes Monocyte-to-Fibroblast Transition in Renal Fibrosis.* Journal of the American Society of Nephrology, 2013. **24**(10): p. 1644-1659.
186. Yanagita, M., *Inhibitors/antagonists of TGF-β system in kidney fibrosis.* Nephrology Dialysis Transplantation, 2012. **27**(10): p. 3686-3691.
187. Ma, F.Y., et al., *TGF-beta1-activated kinase-1 regulates inflammation and fibrosis in the obstructed kidney.* Am J Physiol Renal Physiol, 2011. **300**(6): p. F1410-21.
188. Li, J., et al., *AMP-activated protein kinase activates p38 mitogen-activated protein kinase by increasing recruitment of p38 MAPK to TAB1 in the ischemic heart.* Circ Res, 2005. **97**(9): p. 872-9.
189. Sasaki, Y. and K. Sugamura, *Involvement of Hgs/Hrs in signaling for cytokine-mediated c-fos induction through interaction with TAK1 and Pak1*. J Biol Chem, 2001. **276**(32): p. 29943-52.
190. Yu, Y., et al., *Phosphorylation of Thr-178 and Thr-184 in the TAK1 T-loop is required for interleukin (IL)-1-mediated optimal NFkappaB and AP-1 activation as well as IL-6 gene expression.* J Biol Chem, 2008. **283**(36): p. 24497-505.
191. Strippoli, R., et al., *Inhibition of transforming growth factor-activated kinase 1 (TAK1) blocks and reverses epithelial to mesenchymal transition of mesothelial cells.* PLoS One, 2012. **7**(2): p. e31492.
192. Cheng, J., et al., *Serum- and glucocorticoid-regulated kinase 1 is upregulated following unilateral ureteral obstruction causing epithelial-mesenchymal transition.* Kidney Int, 2010. **78**(7): p. 668-78.
193. Dai, Y., et al., *A2B adenosine receptor-mediated induction of IL-6 promotes CKD.* J Am Soc Nephrol, 2011. **22**(5): p. 890-901.
194. Silverstein, D.M., et al., *Altered expression of immune modulator and structural genes in neonatal unilateral ureteral obstruction.* Kidney Int, 2003. **64**(1): p. 25-35.
195. Cieslik, K.A., J. Trial, and M.L. Entman, *Defective myofibroblast formation from mesenchymal stem cells in the aging murine heart rescue by activation of the AMPK pathway.* Am J Pathol, 2011. **179**(4): p. 1792-806.
196. Mutsaers, S.E., et al., *Mechanisms of tissue repair: from wound healing to fibrosis.* Int J Biochem Cell Biol, 1997. **29**(1): p. 5-17.
197. Wynn, T.A., *Common and unique mechanisms regulate fibrosis in various fibroproliferative diseases.* J Clin Invest, 2007. **117**(3): p. 524-9.
198. Fielding, C.A., et al., *Interleukin-6 signaling drives fibrosis in unresolved inflammation.* Immunity, 2014. **40**(1): p. 40-50.
199. Roca, H., et al., *CCL2 and interleukin-6 promote survival of human CD11b+ peripheral blood mononuclear cells and induce M2-type macrophage polarization.* J Biol Chem, 2009. **284**(49): p. 34342-54.

200. Pan, B., et al., *Regulation of renal fibrosis by macrophage polarization.* Cell Physiol Biochem, 2015. **35**(3): p. 1062-9.
201. Shen, Y.Y., et al., *Up-regulation of adiponectin, its isoforms and receptors in end-stage kidney disease.* Nephrol Dial Transplant, 2007. **22**(1): p. 171-8.
202. He, J., et al., *Role of the endothelial-to-mesenchymal transition in renal fibrosis of chronic kidney disease.* Clin Exp Nephrol, 2013. **17**(4): p. 488-97.
203. Foller, M., et al., *Regulation of erythrocyte survival by AMP-activated protein kinase.* Faseb j, 2009. **23**(4): p. 1072-80.
204. Cieslik, K.A., et al., *AICAR-dependent AMPK activation improves scar formation in the aged heart in a murine model of reperfused myocardial infarction.* J Mol Cell Cardiol, 2013. **63**: p. 26-36.
205. Gusarova, G.A., et al., *Alpha1-AMP-activated protein kinase regulates hypoxia-induced Na,K-ATPase endocytosis via direct phosphorylation of protein kinase C zeta.* Mol Cell Biol, 2009. **29**(13): p. 3455-64.
206. Salt, I., et al., *AMP-activated protein kinase: greater AMP dependence, and preferential nuclear localization, of complexes containing the alpha2 isoform.* Biochem J, 1998. **334 (Pt 1)**: p. 177-87.
207. Xu, X., et al., *Metformin protects against systolic overload-induced heart failure independent of AMP-activated protein kinase alpha2.* Hypertension, 2014. **63**(4): p. 723-8.
208. Mishra, R., et al., *AMP-activated protein kinase inhibits transforming growth factor-beta-induced Smad3-dependent transcription and myofibroblast transdifferentiation.* J Biol Chem, 2008. **283**(16): p. 10461-9.
209. Wang, S., et al., *AMPKalpha2 deletion causes aberrant expression and activation of NAD(P)H oxidase and consequent endothelial dysfunction in vivo: role of 26S proteasomes.* Circ Res, 2010. **106**(6): p. 1117-28.
210. Vicente, R., et al., *Association of Kv1.5 and Kv1.3 contributes to the major voltage-dependent K+ channel in macrophages.* J Biol Chem, 2006. **281**(49): p. 37675-85.
211. Almaca, J., et al., *AMPK controls epithelial Na(+) channels through Nedd4-2 and causes an epithelial phenotype when mutated.* Pflugers Arch, 2009. **458**(4): p. 713-21.
212. Carattino, M.D., et al., *Epithelial sodium channel inhibition by AMP-activated protein kinase in oocytes and polarized renal epithelial cells.* J Biol Chem, 2005. **280**(18): p. 17608-16.
213. Lei, B., et al., *Exogenous nitric oxide reduces glucose transporters translocation and lactate production in ischemic myocardium in vivo.* Proc Natl Acad Sci U S A, 2005. **102**(19): p. 6966-71.
214. Guan, F., et al., *Chemical hypoxia-induced glucose transporter-4 translocation in neonatal rat cardiomyocytes.* Arch Med Res, 2008. **39**(1): p. 52-60.
215. Winder, W.W. and D.M. Thomson, *Cellular energy sensing and signaling by AMP-activated protein kinase.* Cell Biochem Biophys, 2007. **47**(3): p. 332-47.

216. Boiteux, A. and B. Hess, *Design of glycolysis.* Philos Trans R Soc Lond B Biol Sci, 1981. **293**(1063): p. 5-22.
217. Schneider, J., et al., *Suicidal erythrocyte death following cellular K+ loss.* Cell Physiol Biochem, 2007. **20**(1-4): p. 35-44.
218. Lupescu, A., et al., *Inhibition of Na+/H+ exchanger activity by parvovirus B19 protein NS1.* Cell Physiol Biochem, 2009. **23**(1-3): p. 211-20.
219. Lee, M., et al., *AMP-activated protein kinase activity is critical for hypoxia-inducible factor-1 transcriptional activity and its target gene expression under hypoxic conditions in DU145 cells.* J Biol Chem, 2003. **278**(41): p. 39653-61.
220. Towler, M.C. and D.G. Hardie, *AMP-activated protein kinase in metabolic control and insulin signaling.* Circ Res, 2007. **100**(3): p. 328-41.
221. Evans, A.M., et al., *Does AMP-activated protein kinase couple inhibition of mitochondrial oxidative phosphorylation by hypoxia to calcium signaling in O2-sensing cells?* J Biol Chem, 2005. **280**(50): p. 41504-11.
222. Lira, V.A., et al., *Nitric oxide increases GLUT4 expression and regulates AMPK signaling in skeletal muscle.* Am J Physiol Endocrinol Metab, 2007. **293**(4): p. E1062-8.
223. Kim, S.Y., et al., *AMP-activated protein kinase-α1 as an activating kinase of TGF-β-activated kinase 1 has a key role in inflammatory signals.* Cell Death & Disease, 2012. **3**(7): p. e357.
224. Sopjani, M., et al., *Regulation of Na+ -coupled glucose carrier SGLT1 by AMP-activated protein kinase.* Mol Membr Biol., 2010. **27**(2-3): p. 137-144.
225. Jessen, N., et al., *Effects of AICAR and exercise on insulin-stimulated glucose uptake, signaling, and GLUT-4 content in rat muscles.* J Appl Physiol, 2003. **94**(4): p. 1373-1379.
226. Lei, B., et al., *Exogenous nitric oxide reduces glucose transporters translocation and lactate production in ischemic myocardium in vivo.* Proc Natl Acad Sci U.S.A, 2005. **102**(19): p. 6966-6971.
227. Li, J., et al., *Role of the nitric oxide pathway in AMPK-mediated glucose uptake and GLUT4 translocation in heart muscle.* Am J Physiol Endocrinol.Metab, 2004. **287**(5): p. E834-E841.
228. Luiken, J.J., et al., *Regulation of cardiac long-chain fatty acid and glucose uptake by translocation of substrate transporters.* Pflugers Arch, 2004. **448**(1): p. 1-15.
229. MacLean, P.S., et al., *Exercise-induced transcription of the muscle glucose transporter (GLUT 4) gene.* Biochem Biophys.Res Commun., 2002. **292**(2): p. 409-414.
230. Natsuizaka, M., et al., *Synergistic up-regulation of Hexokinase-2, glucose transporters and angiogenic factors in pancreatic cancer cells by glucose deprivation and hypoxia.* Exp.Cell Res, 2007. **313**(15): p. 3337-3348.

231. Ojuka, E.O., L.A. Nolte, and J.O. Holloszy, *Increased expression of GLUT-4 and hexokinase in rat epitrochlearis muscles exposed to AICAR in vitro.* J Appl Physiol, 2000. **88**(3): p. 1072-1075.
232. Park, S., et al., *Chronic elevated calcium blocks AMPK-induced GLUT-4 expression in skeletal muscle.* Am J Physiol Cell Physiol, 2009. **296**(1): p. C106-C115.
233. Walker, J., et al., *5-aminoimidazole-4-carboxamide riboside (AICAR) enhances GLUT2-dependent jejunal glucose transport: a possible role for AMPK.* Biochem J, 2005. **385**(Pt 2): p. 485-491.
234. Winder, W.W., et al., *Activation of AMP-activated protein kinase increases mitochondrial enzymes in skeletal muscle.* J Appl Physiol, 2000. **88**(6): p. 2219-2226.
235. Zheng, D., et al., *Regulation of muscle GLUT-4 transcription by AMP-activated protein kinase.* J Appl Physiol, 2001. **91**(3): p. 1073-1083.
236. Carling, D., *The role of the AMP-activated protein kinase in the regulation of energy homeostasis.* Novartis.Found.Symp., 2007. **286**: p. 72-81.
237. Winder, W.W. and D.M. Thomson, *Cellular energy sensing and signaling by AMP-activated protein kinase.* Cell Biochem Biophys., 2007. **47**(3): p. 332-347.

CURRICULUM VITAE

Personal information

Name	Md. Sobuj Mia
Date of Birth	1st January 1985
Nationality	Bangladeshi
Address	Zeppelinstr. 05, 72770, Reutlingen, Germany
Email	Sobujbcmb123@gmail.com

Education

2011-2015:	**Ph.D.** Institute of Physiology I, University of Tübingen, Germany. *Thesis*: AMP-Activated Protein Kinase α1 Dependent Signaling in Renal Tissue Fibrosis. *Supervisor*: Prof. Dr. Med. Florian Lang
2009-2010:	**M.Sc**. Molecular Biology, University of Skövde, Sweden. *Thesis*: Identification and Molecular Characterization of *Salmonella* Effectors Suppressing PAMP Triggered Immunity in *Arabidopsis.* *Supervisor*: Dr. Frédéric Brunner
2003-2008:	**B.Sc.** (**Honors**) (*secured **1st class 1st position** according to the merit*). Department of Biochemistry and Molecular Biology, University of Rajshahi, Bangladesh.

Publications

1. **Mia, S**., Munoz, C., Pakladok, T., Siraskar, G., Voelkl, J., Alesutan, I., and Lang, F. (2012). Downregulation of Kv1.5 K channels by the AMP-activated protein kinase. *Cell. Physiol. Biochem.* 30(4):1039-50.
2. **Mia, S**., Giuseppina, F., Feger, M., Pakladok, T., Meissner, A., Voelkl, J., Groene, J. H., Alesutan, I., and Lang, F. (2015). AMP-activated protein kinase α1 deficiency blunts tissue fibrosis following unilateral ureteral obstruction. *Plos One*. (pending in acceptance).
3. **Mia, S.**, Feger, M., Pakladok, T., Meissner, A., Voelkl, J., Groene, J. H., Alesutan, I., and Lang, F. (2015). Role of AMP-activated protein kinase α1 in angiotensin II induced renal inflammation. (Manuscript in prep.).
4. Alesutan, I., Voelkl, J., Stockigt, F., **Mia**, **S**., Feger, M., Primessing, U, Sopjani, M., Munoz, C., Borst, B., Gawaz, M., Pieske, B., Metzler, B., Heinzel, F., Schrickel, J. W., and Lang, F. (2014). Ampk α1 regulates cardiac

gap junction protein connexin43 and electrical remodeling following pressure overload. *Cell Physiol Biochem (accepted).*

5. Feger, M., **Mia, S.,** Pakladok, T., Nicolay J. P., Alesutan, I., Schneider, S. W., Voelk, J., and Lang, F. (2014). Down-regulation of renal klotho expression by shiga toxin 2. *Kidney Blood Press Res*. 39:441-44.
6. Voelkl, J., Alesutan, I., Pakladok, T., Viereck, R., Feger, M., **Mia, S**., Schonberger, T., Noegel, A. A., Gawaz, M., and Lang, F. (2014). Annexin A7 deficiency potentiates cardiac NFAT activity promoting hypertrophic signaling. *Biochem Biophys Res Commun*. 445 (1):244-9.
7. Schmidt, S., Schneider, S., Yang, W., Liu, G., Schmidt, E. M., Schmid, E., **Mia, S.**, Brucker, S., Stournaras, C., Wallwiener, D., Brosens, J. J., and Lang, F. (2014). TGFβ1 and SGK1-sensitive store-operated Ca2+ entry and Orai1 expression in endometrial Ishikawa Cells. *Mol Hum Reprod*. 20(2):139-47
8. Voelkl, J., Alesutan, I., Leibrock, C. B., Quintanilla-Martinez, L., Kuhn, V., Feger, M., **Mia, S.**, Ahmed, M. S., Rosenblatt, K. P., Kuro-O, M., and Lang, F. (2013). Spironolactone ameliorates PIT1-dependent vascular osteoinduction in klotho-hypomorphic mice. *J Clin Invest*. 123 (2):812-22.
9. Voelkl, J., **Mia, S.**, Meissner, A., Ahmed, M. S., Feger, M., Elvira, B., Walker, B., Alessi, D. R., Alesutan, I., and Lang, F. (2013). PKB/SGK-resistant GSK-3 signaling following unilateral ureteral obstruction. *Kidney Blood Press Res*. 38(1):1546-64.
10. Alesutan, I., Feger, M., Pakladok, T., **Mia, S.**, Ahmed, M. S., Voelkl, J., and Lang, F. (2013). 25-Hydroxyvitamin D3 1-α-hydroxylase-dependent stimulation of renal klotho expression by spironolactone. *Kidney Blood Press Res*. 37(4-5):475-87.
11. Pasham, V., Rotte, A., **Mia, S.**, Alesutan, I., Chatterjee, S., Hosseinzade, Z., Bhandaru, M., Noegel, A. A., and Lang, F. (2013). Annexin 7 in the regulation of gastric acid secretion. *Cell Physiol Biochem*. 32(6):1643-54
12. Abed, M., Towhid, S. T., **Mia, S**. Pakladok, T., Alesutan, I., Borst, O., Gawaz, M., Gulbins, E., and Lang, F. (2012) Sphingomyelinase-induced adhesion of eryptotic erythrocytes to endothelial cells**.** *Am J Physiol Cell Physiol*. 303 (9): C991-9.
13. Voelkl, J., Lin, Y., Alesutan, I., Ahmed, M. S., Pasham, V., **Mia, S.**, Gu, S., Feger, M., Saxena, A., Metzler, B., Kuhl, D., Picer, B., and Lang, F. (2012). Sgk1 sensitivity of Na(+)/(H+) exchanger activity and cardiac remodeling following pressure overload. *Basic Res Cardiol*. 107(2):236.

DECLARATION OF CONTRIBUTIONS

The experiments, planning of the study and interpretation was performed by Sobuj Mia. Unilateral ureteral obstruction and Angiotensin II infusion were performed with the help of Jakob Voelkl and Martina Feger. Q-PCR, confocal microscopy and Western blotting was performed by Sobuj Mia and Ioana Alesutan with technical assistance from Tatsiana Pakladok, Katherina Musculus, Jakob Voelkl and Adrian Meissner. Immunohistochemsitry and histological analysis was performed by Giuseppina Federico and Hermann Groene. Electrophysiological measurements were performed by Carlos Munoz and Gulab Siraskar. Florian Lang supervised the study.